# From Recurrent Adaptation to Hebbian Plasticity: Biologically Plausible Networks of Typical and Atypical Sensory Processing

Vishnu Mohan

A thesis submitted in fulfilment of the requirements for the degree of Master of Philosophy (Science)

2025

School of Psychology

The University of Sydney

## Statement of originality

This is to certify that the content of this thesis is my own work. This thesis has not been submitted for any other degree or purpose.

I certify that the intellectual content of this thesis is the product of my own work, and that all assistance received in preparing this thesis and all sources have been acknowledged.

## Author Attribution Statement

Chapter 2 of this thesis has been published as Mohan, V., & Rideaux, R. (2025). *Energy efficiency and sensitivity benefits in a motion processing adaptive recurrent neural network*. *Neural Networks, 191*, 107834. https://doi.org/10.1016/j.neunet.2025.107834. I co-designed the study with Reuben Rideaux, analysed the data and wrote the drafts of the manuscript.

In addition to the authorship attribution statements above, in cases where I am not the corresponding author of a published item, permission to include the published material has been granted by the corresponding author.

Vishnu Mohan

As supervisor for the candidature upon which this thesis is based, I can confirm that the authorship attribution statements above are correct.

Reuben Rideaux

## Artificial intelligence statement

No content produced by generative AI tools has been used in the preparation of this thesis.

## Table of Contents


1. Abstract 6
2. Introduction
    i. Introduction 7
    ii. Biologically inspired neural network models 13
    iii. Healthy study: motion processing in the visual cortex 20
    iv. Studying neural dysfunction: multisensory integration 25
    v. Thesis overview 31
3. Energy efficiency and sensitivity benefits in a motion processing adaptive recurrent neural network 33
    i. Abstract 34
    ii. Introduction 35
    iii. Methods 39
    iv. Results 45
    v. Discussion 57
4. From Spikes to Symptoms: Simulating SC-Driven Multisensory Deficits in Autism Spectrum Disorder 61
    i. Abstract 62
    ii. Introduction 63
    iii. Methods 67
    iv. Results 78
    v. Discussion 90
5. Discussion 97
6. Appendix 113
7. Bibliography 115

## ABSTRACT

Most computational approaches utilized to study the brain today avoid explicit incorporation of biologically plausible mechanisms, instead prioritizing performance benchmarks. While these networks might display responses similar to those exhibited by animals, it is often by converging on mechanistic solutions that lack biological correlates. In doing so, findings derived from such models cannot be directly validated against physiological or neural recordings, and inferences drawn from such a network might thereby not hold true mechanistic value. For instance, deep neural networks (DNN) have been utilized to model a wide variety of biological neural systems, but they cannot typically be employed to explore neurotransmission dynamics or spike timing patterns, as is. Recognizing this hurdle, a growing number of recent studies have adopted biophysical mechanisms into their computational simulations, resulting in findings that account for perceptual phenomena that cannot be studied by traditional computational approaches alone. Following a similar strategy, this thesis explores two studies designed with enough resolution to reproduce specific biological phenomena while at the same time remaining computationally tractable. The first study introduces AdaptNet, a motion processing network that learns from natural sequences while implementing neuronal adaptation — a mechanism long implicated in efficient coding and perceptual aftereffects. While this study validates the effects of adaptation against classical theories of metabolism and perception, the subsequent work demonstrates how the same computational approach could be utilized to investigate neurodevelopmental dysfunction. The second project builds a spiking model of the superior colliculus (SC) with explicit α-amino-3-hydroxy-5-methyl-4-isoxazolepropionic acid (AMPA)/N-methyl-D-aspartate (NMDA) conductances, gamma-aminobutyric (GABA) inhibition, and spike timing dependent plasticity (STDP). The study initially validates the network's responses against established metrics of multisensory integration and then analyses how perturbations in the model's mechanics lead to the altered responses observed in conditions like autism spectrum disorder (ASD). Taken together, these models advocate for 'minimal realism' — careful adherence to key biologically grounded mechanisms, when balanced alongside planned abstraction of secondary mechanisms, can produce network architectures that can be used to derive useful insights about neural activity as well as behavioural responses, in both health and dysfunction.

# INTRODUCTION

THESIS

"*Experiments will yield theoretical insight only when used to test brain-computational models*" - Kriegeskorte & Douglas (2018)

One of the hardest, yet key, challenges in studying the brain, both in health and disease, is linking neural mechanisms to behaviour. This difficulty mainly derives from the scale and complexity of neural systems. The human brain contains approximately 86 billion neurons, which are arranged in vast, recurrent networks operating across various timescales and organisational levels (Azevedo et al., 2009; Herculano-Houzel, 2009). The main issue associated with this scale is that observing correlations between neural activity and behaviour no longer gives a complete picture of how the brain computes. Large scale efforts like the BRAIN initiative have generated massive volumes of data (Schneider-Mizell et al., 2025; Wang et al., 2025) yet as Jazayeri & Afraz (2017) argue, we still lack frameworks that can derive a mechanistic understanding from these observations. There is a need for explanations that specify, for example, how altering a synapse's strength, a circuit's connectivity pattern, or a population's temporal dynamics affects perception. These links matter because in order to develop intervention strategies, the causal factors involved have to first be understood. This could take the form of identifying neural parameters that drugs or training paradigms should target to achieve therapeutic effects (Ross & Bassett, 2024). The focus should be on using empirical data to validate specific mechanistic hypotheses, instead of just cataloguing neural phenomena.

Understanding the causal mechanisms that lead to neural phenomena offers advantages to researchers from all areas of neuroscience (Ross & Bassett, 2024). For experimental neuroscientists, causal links enable them to extract canonical mechanisms that recur across circuits and treat them like building blocks when designing new simulations. This is especially true when a computational principle is so fundamental that it is repeatedly seen across brain areas (such as divisive normalization, which Carandini & Heeger (2012) identified as a "canonical neural computation" appearing across sensory modalities). For clinicians, these mechanistic links can be used to construct translational models that connect symptoms to modifiable circuit parameters. For example, in computational psychiatry, as Huys et al. (2016) describe, there is an active attempt to link behavioural phenotypes like those observed in autism and schizophrenia to variances in neural parameters. Following such linking, the clinical correlates of these parameters could be therapeutically

modulated. On a similar note, the excitation-inhibition (E/I) balance hypothesis in ASD (reviewed by Sohal & Rubenstein (2019)) shows how studying mechanistic pathways could aid biomarker development, along with strategies for intervention. Within the field of computational engineering, adopting biological constraints could support development of more efficient artificial systems. For example, spiking neural networks (SNN) running on neuromorphic hardware achieve competitive performance while consuming markedly lower power. When Idrees et al. (2024) similarly added biologically rooted adaptation mechanisms to artificial networks, they found that the networks could be used to predict retinal responses with better accuracy, especially when the visual stimulus varied dynamically. These examples demonstrate the multifaceted benefits of linking neural mechanisms to behavioural responses.

Classical neuroscience tools have long been used to link observed responses to neural correlates, but each method comes with its own strengths and limitations. For example, some large-scale recording techniques are effective for investigating the timing of brain activity; methods like electroencephalography (EEG) and magnetoencephalography (MEG) do this by recording the brain's activity with millisecond resolution. Other techniques focus on investigating the regional correlates of behaviour, such as functional magnetic resonance imaging (fMRI), where the blood oxygen levels at specific neural regions are measured in response to stimuli. As a complementary approach, electrophysiology can simultaneously track hundreds to thousands of neurons (Stevenson & Kording, 2011). Despite this wealth of data, there remains a logical issue. There are infinite different computational paths by which the same behavioural response could be produced (Siddiqi et al., 2022). This equifinality persists across methodologies. Techniques with higher temporal resolution like MEG also cannot identify which computational model is closest to what is seen in biology, without explicitly specifying underlying mechanisms first (Baillet, 2017). Perturbation approaches such as ablation and lesion studies have been used to close this gap, by inferring the functionality of a mechanism from the consequences its disruptions make on the system (Paus, 2005). While techniques like lesioning and optogenetics can narrow down which neural elements are necessary, specific issues limit their usage. Lesions and drugs affect multiple processes at once, making it difficult to isolate the contribution of a specific mechanism (Otchy et al., 2015). Even optogenetic manipulations, with their high precision, need accompanying theoretical frameworks to back up findings (Deisseroth, 2015). This recurring theme, that experimental data

alone cannot determine mechanism, motivates the adoption of computational modelling approaches.

Under computational modelling, there are several different approaches that explain different aspects of the brain-behaviour relationship while forming mechanistic accounts (Kriegeskorte & Douglas, 2018). At the most abstract level, Bayesian models ask not how the brain works but what it should do (Pouget et al., 2013). That is, given uncertainty and resource constraints, what would optimal behaviour look like? This approach has resulted in some useful insights, like Ernst & Banks (2002) demonstration that humans combine cues in a near optimal fashion, by weighing different input signals by their reliability. Moving closer to neural implementation, statistical encoding and decoding models attempt to define what information is carried by neural signals, which provides bidirectional maps between stimuli and responses (Naselaris et al., 2010). This framework reached a milestone when Kay et al (2008) showed that voxel-wise encoding (using fMRI patterns alone) could be employed to resolve which natural image a subject was viewing. When decoded, even representations that at first may seem coarse carried significant information about visual processing in the brain. To understand how such representations would interact with each other, dynamical systems approaches model neural populations as coupled differential equations. Dynamic causal modelling exemplifies this by estimating the coupling strength between neural populations using such equations (Friston et al., 2003), but these frameworks fall short of describing the neural machinery that makes this activity possible (Breakspear, 2017). This is where mechanistic circuit models may provide a solution. Neural network models stand out in this class, mainly because they can both be trained on real world goals, while maintaining sufficient neural structure from which to draw inferences (Kell et al., 2018; Yamins & DiCarlo, 2016). This dual nature positions them as valuable tools to define abstract computational principles (Schrimpf et al., 2020). A noticeable trend from these types of studies is that approaching a biological problem by incorporating multiple physiologically plausible mechanisms instead of viewing it through any particular computational lens results in findings that converge more closely with biology across various metrics; this in turn raises the question of how closely our models should mirror biology, to yield valuable inferences.

Adopting biologically motivated mechanisms can result in better inferential quality, and this holds especially true for neural networks. This realization was first

made clear in vision, where DNNs trained to perform object recognition developed internal features that resembled simple and complex edge detectors found in visual area V1 (V1). Even the hierarchical order of processing emerges in these networks (Yamins et al., 2014). Similarly artificial neural networks (ANNs) trained solely to perform naturalistic tasks can form representations that match biology (Khaligh-Razavi & Kriegeskorte, 2014; Lindsay, 2021). When such deep networks are given a basic architecture resembling a biological neural system to start with, they are also capable of predicting neural activity in later visual areas such as V4 and inferotemporal (IT) cortex. Beyond neural activity, deep networks can also capture aspects of human behavioural performance. This could potentially suggest that these networks have converged on computational solutions similar to those shaped by evolution (Yamins & DiCarlo, 2016). This convergence also extends to the temporal domain (Lotter et al., 2020), and by adding biologically motivated mechanisms like adaptation, networks can begin to exhibit even illusory precepts. Visual aftereffects emerge from adapted units in such models, which provides insights into existing accounts of illusory phenomena (Vinken et al., 2020). This approach proves similarly advantageous for studying motion processing. When Rideaux & Welchman (2020, 2021) trained a convolutional network to estimate the velocity of natural image sequences, they could then reproduce neural tuning and human misperceptions driven by natural-image statistics. These successes show that biologically inspired networks are more than just performance benchmarking tools and position these models as scientific instruments that can be utilized to generate testable hypotheses about how the brain works.

This utility of computational networks in deriving mechanistic inferences calls for a deeper understanding of such artificially constructed networks (Kriegeskorte & Douglas, 2018). If networks that bear only passing resemblance to real neurons can predict brain activity, what aspects of biological detail matter for understanding neural computation? The answer becomes clear upon examining where these models diverge from biology (Richards et al., 2019). Perhaps the most glaring divergence lies in how learning occurs. Backpropagation, which is used by most deep learning networks today, requires error signals to flow backward through the network with mathematical precision. Additionally, identical weights are used in both forward and backward passes, a symmetry that biological circuits with their local information constraints simply cannot implement (Lillicrap et al., 2020). Apart from being a theoretical concern, this means that the learning dynamics in artificial networks may

give an incomplete picture of how biological circuits reorganize. The temporal dimension presents an equally fundamental challenge. Biological neurons do not compute in synchronized steps like most artificial networks but instead operate in continuous time. They communicate through discrete spikes whose precise timing carries crucial information about stimulus features (Bellec et al., 2020; Gollisch & Meister, 2008). This event-based communication scheme, which Maass (1997) identified as the defining feature of "third generation" neural networks, enables computations like coincidence detection that underlie everything from sound localization to motor control (Franken et al., 2015; Srivastava et al., 2017). These differences compound when considered alongside the brain's strict energy budget. Each spike consumes precious metabolic resources, forcing neural circuits to evolve sparse, adaptive coding strategies that extract maximum information from minimum activity (Harris et al., 2012; Lennie, 2003). Unlike brains under tight energy budgets, standard ANN objectives typically omit explicit metabolic costs. Most critically for those hoping to translate computational insights into treatments, predictive accuracy alone cannot identify the mechanistic levers like the specific receptors that represent intervention targets in neurological conditions (Danks & Davis, 2023). These limitations have catalysed a new movement toward biologically grounded models that incorporate spikes, local learning rules, and metabolic constraints, moving the field closer to networks that go beyond predicting neural responses to those that behave like brains.

The quest to design networks that are more directly comparable with biological recordings motivated computational neuroscientists to redesign artificial networks around how neurons communicate. While ANNs primarily pass continuous activation values between their units, biological neurons utilize spikes, which are brief electrical pulses that propagate through circuits with millisecond precision (Fiorillo et al., 2014; Mainen & Sejnowski, 1995). This distinction is what allows biological neural circuits to capture computations that depend on precise timing, rather than just average activity levels (Gollisch & Meister, 2008; Stöckl & Maass, 2021). For example, the auditory system localizes sounds by detecting microsecond differences in arrival timing between ears. Working with a similar temporal scale, the visual system uses the relative timing of spikes to encode rapidly changing stimuli (Brand et al., 2002; Gollisch & Meister, 2008). These temporal codes simply cannot be captured by networks that abstract away spike timing, and implementing this level of biological detail offers

computational advantages beyond just theoretical accuracy. For example, researchers utilizing spiking networks can achieve competitive performance while using remarkably few spikes (Esser et al., 2016; Stanojevic et al., 2024). Such efficiency naturally aligns with the brain's need to minimize metabolic costs (Attwell & Laughlin, 2001), a convergence that has sparked renewed interest in energy-efficient neuromorphic hardware.

**Biologically inspired neural network models**

Neural computation is typically studied at various levels of abstraction, each revealing certain mechanisms while obscuring others (Krakauer et al., 2017; Lengyel, 2024). Early work explored biophysical foundations; Hodgkin and Huxley demonstrated how voltage-gated sodium and potassium currents generate action potentials, while cable theory explained how dendritic geometry shapes signal integration (Bean, 2007; Catterall et al., 2012; Rall, 2011). Network scale analysis aimed to simplify these complex representations, by describing populations of neurons using firing rates rather than discrete spikes (Abbott, 1994). This simplification produced computational insights, particularly the finding that balanced excitation and inhibition produces the irregular yet stable activity characteristic of cortical dynamics (van Vreeswijk & Sompolinsky, 1996). Modern deep learning pushed abstraction further, creating hierarchical networks that capture sensory representations with unprecedented accuracy, yet these systems sacrifice the very features (spike timing, synaptic dynamics, metabolic constraints) that determine how biological circuits compute (Lillicrap et al., 2020; Yamins et al., 2014). Recognizing this gap, contemporary approaches seek a middle ground through compact spiking models like Izhikevich neurons that reproduce diverse firing patterns while remaining computationally tractable (the training time for SNNs are comparable to similar ANN solutions, utilizing reasonable computational requirements), enabling network-scale investigations where timing, adaptation, and excitation-inhibition balance serve as explicit, manipulable parameters that link circuit mechanisms to behavioural outcomes (Izhikevich, 2003).

Biological neurons exploit spike timing to enable key mechanisms like learning and temporal integration (**Fig. 1**), and this realisation serves as a primary motivation for spiking neural networks (Gollisch & Meister, 2008; Maass, 1997). Pure rate based models cannot capture computations of this nature (Johansson & Birznieks, 2004; Mainen & Sejnowski, 1995), which has motivated event driven neuromorphic systems

that utilize spikes to compute in real time, while using up less power than conventional hardware, like graphics processing units (GPUs) (Esser et al., 2016; Merolla et al., 2014). While one of the key factors limiting their adoption in the past was their training, innovative solutions like e-prop have been developed by utilizing locally available signals (Bellec et al., 2020). In terms of biological realism, local learning also helps to avoid the implausibility associated with backpropagation. Unlike deep learning which is typically used to derive rich structural relationships in the data, these localised learning algorithms are one step closer towards implementing biologically rooted computations (Denève & Machens, 2016; Yamins & DiCarlo, 2016). The practical value of using a spiking neural network (SNN) architecture depends on the type of neuron used in the network, most often leaky integrate -and fire or Izhikevich- cells.

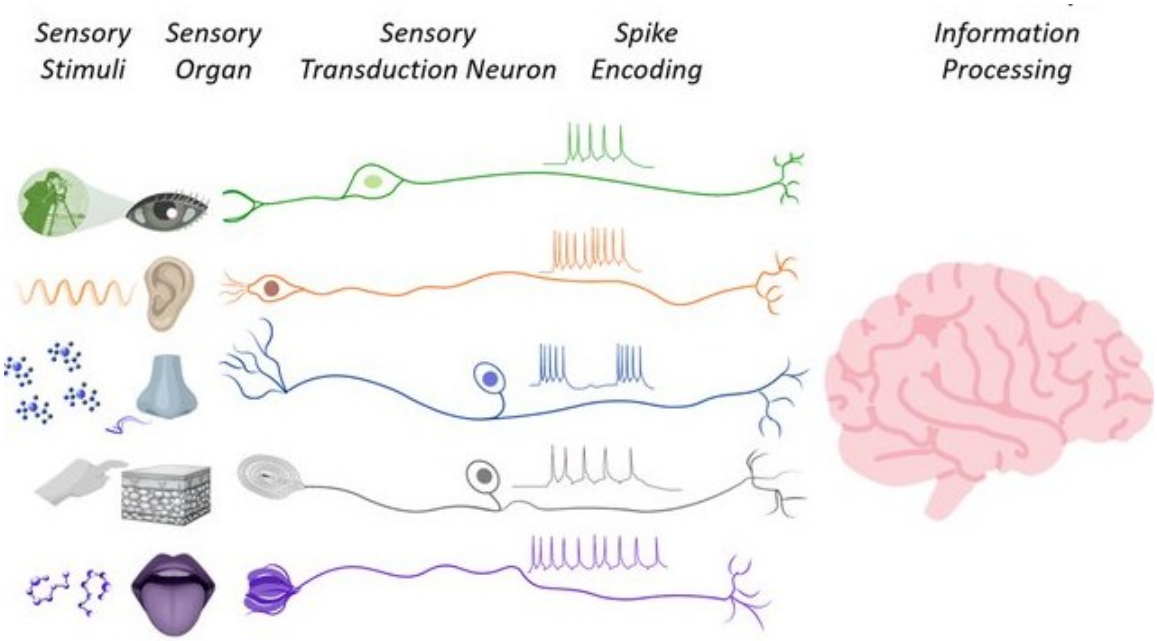


**Figure 1. Spike based communication.** External stimuli are detected by specialized neural groups, which represent them as electrical signals. These electrical signals are then converted into action potential spike trains that form the basis of communication across the brain. Spiking neural networks explicitly model such dynamics instead of abstracting neural responses as point values. Reproduced from Radhakrishnan et al. (2021)

The choice of neuronal unit shapes what a spiking network can reveal about brain computation (Gerstner & Naud, 2009). At the simplest level, leaky integrate-and-fire models capture the basic cycle of integration and discharge (neurons accumulate input until threshold, fire, then reset). The main advantage of this type of neuron lies in its computational simplicity, which enables it to power large scale simulations involving thousands of units. But the cost of this simplicity is a lack of adherence to realistic spiking dynamics, with spikes being represented as discrete events followed

by a programmed reset. Izhikevich neurons extend this model by adding a recovery variable post spiking and differentiating between various neuron types (Izhikevich, 2003). For example, by varying the basic parameters of this neuron, you can implement both regular spiking pyramidal cells as well as fast spiking interneurons, within the same network. These point neuron abstractions work remarkably well at a whole brain scale, as demonstrated by recent whole-brain models that predict sensorimotor transformations in Drosophila connectomes using only point neurons (Shiu et al., 2024). Once these unit level details are identified, the subsequent focus becomes network level implementation factors, such as recurrence.

Recurrence in connection impacts how neural networks process information, by creating feedback loops (**Fig. 2**) that persist even after external inputs cease (Oldenburg et al., 2024). This seemingly simple principle has been implicated in some of the brain's most sophisticated computations. When Hopfield showed how recurrence enabled content addressable memory (via attractor dynamics), he found that networks could store/retrieve patterns through their connectivity alone. This is a principle that cortical circuits exploit to sustain working memory (Hopfield, 1982; Wang, 2001). The amplificative effect of recurrence could be further exploited by the brain in multiple ways — recurrent feedback could both amplify weak signals by passing it through neighbouring nodes, as well as prolong integration to link events that are separated in time (Buzsáki & Draguhn, 2004; Wong & Wang, 2006). Recurrent loops are carefully balanced, to the point where disruptions in their activity could alter the computational mode of the network. Too much excitation could lead to runaway activity, and too much inhibition could silence the network. At the critical point of balance, recurrence can lead to rich network dynamics, like irregular spiking and network oscillations (Brunel, 2000; Turrigiano & Nelson, 2004; van Vreeswijk & Sompolinsky, 1996). Alongside recurrent dynamics, synaptic kinetics and inhibitory gating play an equally important role in determining when and how inputs combine.

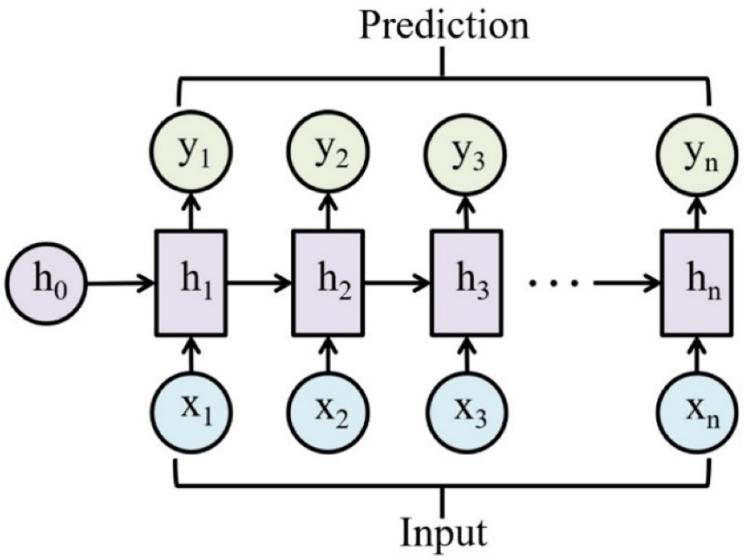


**Figure 2. Time-unrolled recurrent neural network. At each computational step, the current input is combined with a hidden state that represents the previous computational step, to produce an output and a hidden state corresponding to the current computational step. This hidden state is then combined with the next step and so on.** The outputs can be aggregated for a sequence-level prediction. Reproduced from Mienye et al. (2024).

Computation at a neural level emerges as a result of diverse synaptic currents whose timescales determine how an input signal is to be treated. For multisensory integration, this could be deciding what information gets integrated and what gets segregated (Abbott & Regehr, 2004; Silver, 2010). To achieve a computation even this seemingly basic, the brain utilizes various synaptic types. AMPA receptors are fast acting in nature, and they enable precise temporal transmission of sensory events. NMDA receptors on the other hand operate more slowly and generate prolonged currents, which enables them to integrate inputs farther apart in time (**Fig. 3**). Their unique voltage dependent magnesium block also ensures that they activate under sufficient depolarization, which typically occurs as multiple signals converge in time (Abbott & Regehr, 2004; Paoletti et al., 2013). To balance these excitatory currents, GABAergic inhibition is expressed through multiple pathways — feedforward inhibition from interneurons, feedback inhibition to prevent runaway excitation and surround inhibition to strengthen population responses (Isaacson & Scanziani, 2011; Pouille & Scanziani, 2001). The interactions between these opposing forces (what is often referred to as E/I balance) affects multiple aspects of network function, from basic stability to complex computations like gain control and normalization (Atallah et al., 2012; Denève & Machens, 2016). But beyond the properties of any individual synapse, it is their tuning within the interconnected network that gives them value, with their relative strengths being determined by local learning algorithms that continuously

change in response to the environment (Clopath et al., 2010; Urbanczik & Senn, 2014).

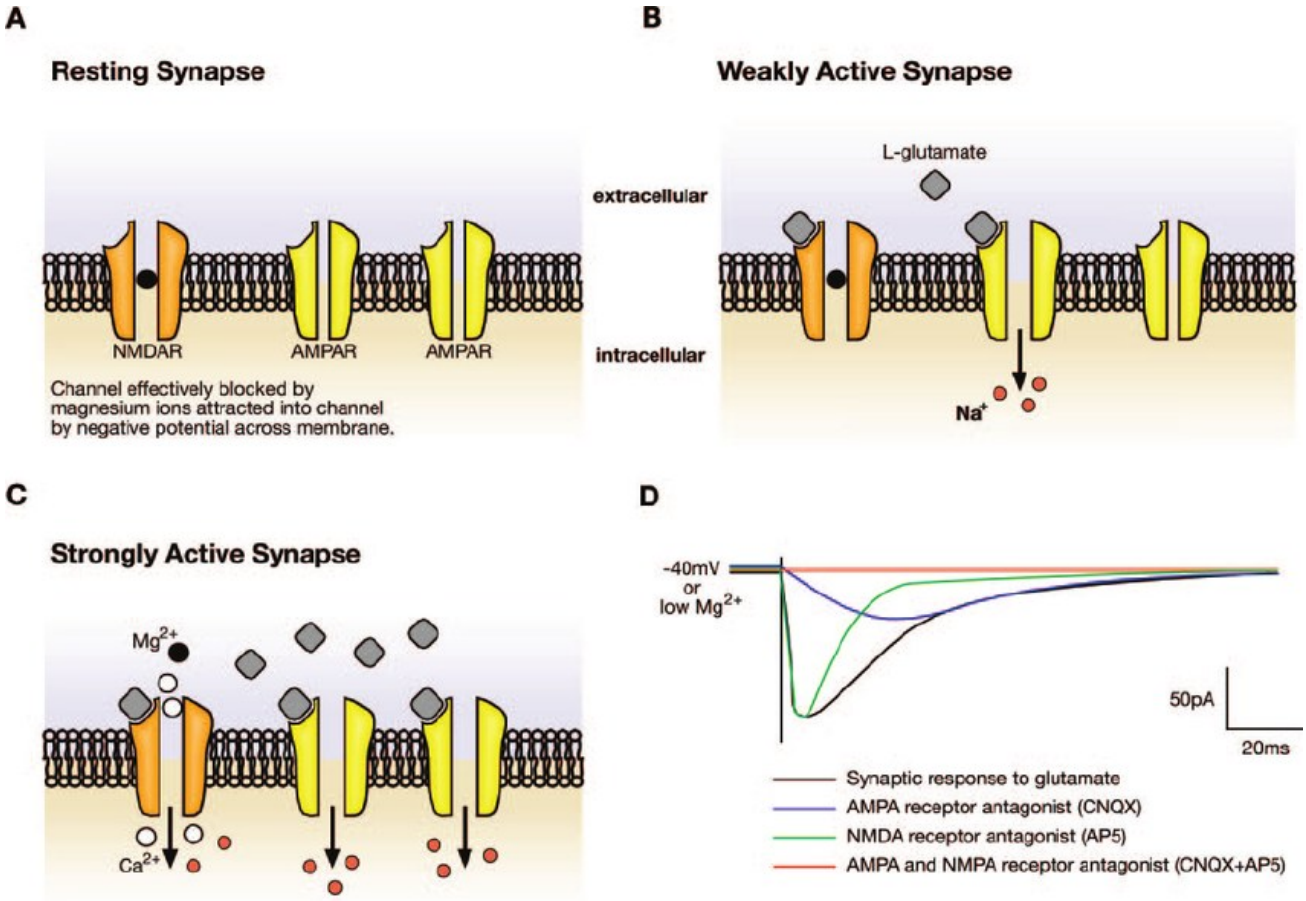


**Figure 3. NMDA-AMPA contributions to coincidence detection. (A) Resting:** NMDA receptors (NMDARs) are blocked by $Mg^{2+}$ at negative potentials. **(B) Weak Activation:** glutamate opens AMPA receptors (AMPARs), but the depolarization is not strong enough to relieve the $Mg^{2+}$ block. **(C) Strong activation:** AMPAR-mediated depolarization expels $Mg^{2+}$, opening NMDARs and allowing $Ca^{2+}$ influx, which enables them to detect coincident signals. **(D) Time course:** EPSPs comprise a fast AMPAR and slow NMDAR component; selective antagonists CNQX (AMPA) or AP5/APV (NMDA) isolate these components. Reproduced from Cooke & Bliss (2006).

Learning in the brain occurs primarily via local STDP mechanisms, where the network only has access to localised information instead of a global error signal (Lillicrap et al., 2020; Roelfsema & Holtmaat, 2018). This locality constraint has shaped the brain's learning mechanisms profoundly (Abbott & Nelson, 2000). On studying STDP mechanisms, Markram and colleagues revealed that synapses reliably strengthen when the presynaptic spikes precede postsynaptic spikes (**Fig. 4**) (Feldman, 2012; Markram et al., 1997). This results in a causal learning rule that only utilizes the local information available within a narrow temporal window. Because such Hebbian based learning is unstable by itself and would grow into a state of runaway excitation, complementary rules involving inhibition and synaptic depression keep STDP in check (Turrigiano, 2012; Vogels et al., 2011). Since

homeostatic scaling affects firing rates globally rather than modifying specific synapses, the learned structure is retained. Taken together, local plasticity when stabilised by inhibition and homeostasis serves as a mechanistic platform whose parameters can be controlled to tune circuit models.

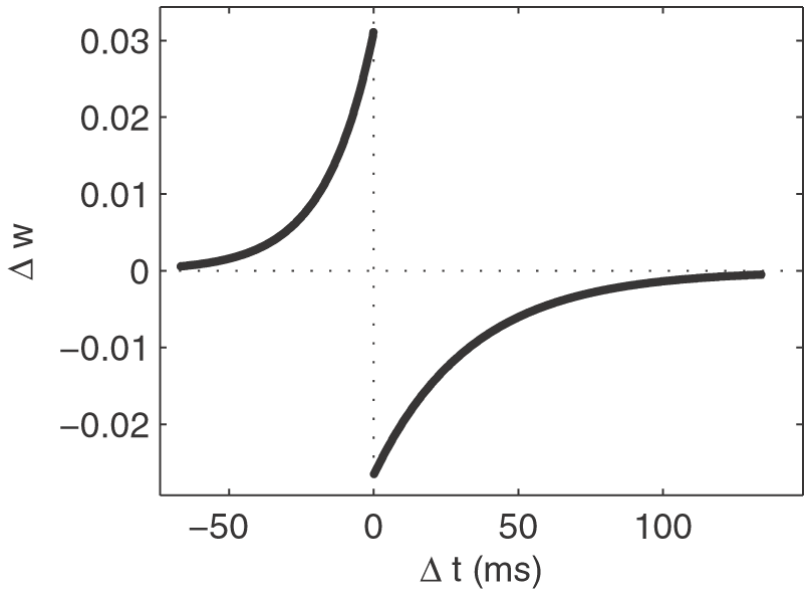


**Figure 4. STDP modification function.** Additive synaptic change $(\Delta w)$ as a function of spike-timing difference $(\Delta t)$. Negative $\Delta t$ leads to LTP; positive $\Delta t$ yields LTP. Curves follow single exponential values. Reproduced from Masquelier et al. (2008).

The true test of biologically grounded models lies in their ability to explain how specific circuit mechanisms lead to complex neural phenomena. Previous work has demonstrated this time and again. For example, sparse coding networks to predict natural image classes led to the emergence of Gabor-like filters that resembled simple cell types found in area V1 (Olshausen & Field, 1996). The same paradigm, if trained with autoencoder models (like principal component analysis (PCA)), would not produce V1-like structures, even though they might provide other useful insights. Another example is work by Carandini & Heeger (2012), where specifically incorporated divisive normalisation is used to explain gain control in sensory systems. Divisive normalisation has since been recognised as a canonical computation, predicting the effects of context across various cortical areas. When this same normalisation mechanism was applied to a multisensory integration framework, it provided explanations for the inverse effectiveness phenomena seen in the superior colliculus (Ohshiro et al., 2011). In line with work explored in this thesis, recurrent networks have been shown to spontaneously generate network oscillations like those observed in the cortex (Buzsáki & Draguhn, 2004; Buzsáki & Wang, 2012). Each of these successes followed the same strategy — construct a circuit with biologically

rooted mechanisms, validate its responses against what is observed in biology, then vary the parameters of the network and compare the changes in response with physiology (Marder & Bucher, 2007; Prinz et al., 2004). With this process, it is possible to both realize the mechanistic value of network parameters as well as generate testable hypotheses of how neurons process information.

The mechanistic insights derived from these models could gain clinical traction, if the networks' parameters align with quantities that clinicians can test. An example of this is the Virtual Epileptic Patient — personalized brain models which combine each patient's connectome with neural dynamics to predict how seizures may propagate (Wang et al., 2023). This information is also subsequently used to simulate surgical trials, and this approach has now been validated in prospective trials. Similarly, in psychiatry, an investigation utilizing dynamic causal modelling of EEG signatures has shown that the severity of psychosis in certain patients correlates with reduced neural gain and an altered E/I balance, a finding which implicates NMDA modulation drugs as intervention targets (Adams et al., 2022). In the case of movement disorders, the neural pathways that are most suitable for deep brain simulation were highlighted by biophysical models (Al-Fatly et al., 2019; Johnson & McIntyre, 2008; Miocinovic et al., 2006). Adding to this list, circuit models have been employed to show how dopamine suppresses pathological beta oscillations (Marreiros et al., 2013; Ortone et al., 2023). In all these cases, computational parameters were used to inform clinical decisions about patients. Each identified circuit parameters were linked with symptoms, then real-world estimates were computed from measurable signals, after which candidate interventions were chosen based on their values. Mapping from parameters to interventions in this way is perhaps the most immediate clinical promise of computational neuroscience.

The principles stated here require thorough explanation, and the two studies described in this thesis provide further support for them. Motion adaptation is supported by decades of research demonstrating a trade-off between metabolic efficiency and perceptual accuracy (Adibi, McDonald, et al., 2013; Fairhall et al., 2001; Kohn, 2007). This richness in empirical data makes adaptation a perfect avenue to test whether biologically grounded models can capture the link between network parameters and behavioural responses. Yet healthy computation represents only one aspect of circuit operation. To truly validate this mechanistic framework, it is crucial to investigate a model of dysfunction and observe whether altered neural parameters

could lead to the perceptual difficulties seen in neurodevelopmental conditions. In collicular neural populations, segregation or fusion of the incoming audiovisual signals are determined by an interplay between various synaptic groups which work together with millisecond precision to uphold a delicate E/I balance, which can be systematically manipulated (Stein & Stanford, 2008). The precision of these metrics becomes diagnostically relevant when considering how individuals with ASD often show enlarged binding windows and struggle with audiovisual speech perception, because such perceptive differences implicate parameters like NMDA conductance or inhibitory gain, that these models can isolate and test (Stevenson et al., 2014). So though motion and multisensory integration can appear distinct, both of these processes share network mechanisms like temporal dynamics, synaptic kinetics, and adaptive mechanisms. The first study is based on motion adaptation, which establishes these principles in their base form before confronting the additional complexity of cross-modal integration.

**Healthy study: motion processing in the visual cortex**

One of the core constraints that the brain operates under, is the need to maximize information extracted from the sensory signals in the environment, while minimizing overall energy consumption (Attwell & Laughlin, 2001). This information-energy balance is at the heart of the efficient encoding hypothesis (Barlow, 2012), which postulates that neural circuits encode maximal information, but subject to internal constraints like metabolic costs and noise (Ganguli & Simoncelli, 2014; Laughlin, 2001). The beauty of this principle is that it implies that diverse neural units and populations all converge on predictable computational solutions, due to the similarity in their constraints. Take the visual system for example, where millions of neurons are tasked with capturing the complexity of natural scenes. Through training, the population responses in the visual cortex are optimized for natural image statistics (Simoncelli & Olshausen, 2001). One example of this is the sparsity of responses in the primary visual area, reflecting the statistics of natural environments (Vinje & Gallant, 2000). ANN's with similar sparse mechanisms implemented also form analogous receptive fields, when trained on natural images (Olshausen & Field, 1996). Yet sensory systems are optimized to conserve energy as well, even in the face of constantly changing stimuli, which is not a feature that can be explained by static optimization alone. Biological neural networks rely on neural adaptation to maintain a

reasonable perceptual accuracy while minimizing metabolic energy expenditure (Adibi, Clifford, et al., 2013; Padamsey et al., 2022). In addition to this, adaptation prevents response saturation during sustained stimulation, allowing even smaller inputs to make an impact on perception (Brenner et al., 2000). Because it continuously reallocates sensitivity to signals in this fashion, adaptation effectively turns efficient coding into a computational reality. The net result of this is that information transmission across neural systems becomes maximised per spike, under a dynamic, changing stimuli.

This adaptive strategy for efficient coding reduces the metabolic burden on the brain by reducing unnecessary or redundant activity representations. Each action potential consumes approximately one billion adenosine triphosphate (ATP) molecules, and when considered alongside the energy being expended on ion transport in non-spiking neural tissue like the outer retina, the energy consumption of biological systems can accumulate exponentially (Hallermann et al., 2012). Any energy saved here translates into enhanced computational capabilities, especially when in detecting rapid changes in environmental stimuli. For example, the energy attributed to the spiking activity required to continuously process high contrast stimuli could cumulatively be a large energy burden on the brain, but the gain reduction that adaptation implements ensures that the responses are no longer consistent with the linear sums of the individual components. This reallocation of coding resources produces noticeable behavioural advantages, and translates to reduced resource consumption during neural activity (**Fig. 5**). For example, adaptation maintains a reasonable perceptual accuracy while utilizing substantially fewer spikes, while enhancing the sensitivity of the system to transient stimuli (Fairhall et al., 2001). Similarly, in the auditory cortex, a reduction in variance in the input stimulus leads to an increase in perceptual sensitivity, which allows for the correct lateralization of even smaller interaural differences (Lohse et al., 2020; Rabinowitz et al., 2011; Tollin et al., 2008). However, these benefits come at a cost — a reduction in reliability in representing constant or repeated stimuli (Avissar et al., 2007). The motion processing network developed in this thesis investigates this fundamental trade-off. Additionally, adaptive mechanisms set up certain neural ensembles for transient alterations in response post stimulus onset, which manifests as perceptual aftereffects. One such example is that of the waterfall illusion, which is a motion aftereffect induced by sustained viewing of a motion sequence, such as a waterfall. Upon cessation of the

motion stimulus, the observer perceives motion in the opposite direction to that of the original stimulus. The aim is to test if incrementally implementing adaptation in an ANN would lead to greater efficiency and enhanced change detection and to investigate if the same adaptation mechanism could be used to investigate perceptual aftereffect phenomena like the waterfall illusion. This could validate the role of adaptation as a mechanism that navigates the competing demands of representing event information across various sensory modalities.

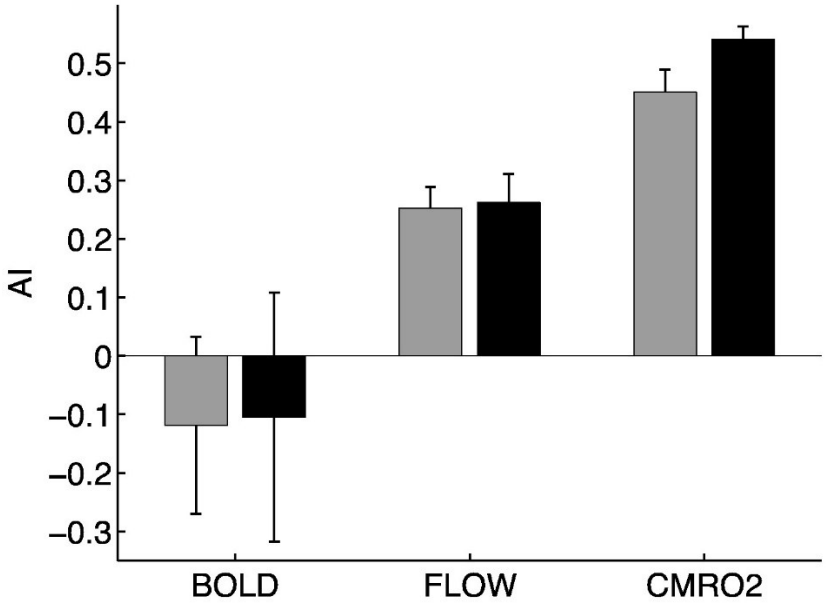


**Figure 5.** Adaptation index (AI) for the blood oxygenation level dependent signal (BOLD), cerebral blood flow (FLOW), and the cerebral metabolic rate of oxygen (CMRO2) for low-contrast (grey) and high-contrast (black) visual stimuli; positive values indicate adaptation, and error bars show the standard error of the mean across observers. Reproduced from Moradi (2013).

The trade-off associated with neural adaptation is utilized by the brain in a universal fashion across different sensory modalities. Each sensory cortex implements the same mechanism through distinct neural circuits. In the visual cortex, neurons modify their contrast response rapidly in response to changes in lighting (Kohn, 2007). This enables those neurons to shift their operating points to prevailing luminance levels, within seconds of exposure. This is a process that has been recorded all the way from retinal ganglion cells to cortical layers. The main theme here is the reduction of redundant representations which manifests as a decrease in the spiking rate with continuous stimulation (**Fig. 6**), an advantage which is further exemplified in the auditory cortex. Stimulus specific adaptation in the auditory realm is responsible for suppressing responses to predictable sounds, while amplifying responses to outlier signals (Taaseh et al., 2011). This transforms that base neural network into a novelty detector. Even our sense of touch exhibits these dynamics, which was recently shown

by two-photon imaging (Dobler et al., 2024). A study of the somatosensory cortex revealed that neurons in this area adjust their gain according to power-law relationships, which match the statistics of recent tactile input (Pozzorini et al., 2013). A recurring theme with these studies seems to be that incorporation of adaptive mechanisms enable the network to react strongly to novel stimuli/changes in stimuli while maintaining low yet stable spiking activity in response to sustained input, thus enhancing sensitivity to novel trends in the stimulus. These parallel implementations of adaptation share the same algorithmic backbone — by matching neural responses to the statistics of input signals, adaptation can attain near optimal information transmission, while managing energy demands. Among these modalities, the reason motion processing is chosen as a target to study this mechanism is due to its well-studied circuitry for encoding direction and speed, which yields measurable perceptual phenomena. Once implemented, this circuitry could be explored to study the underlying adaptive computations.

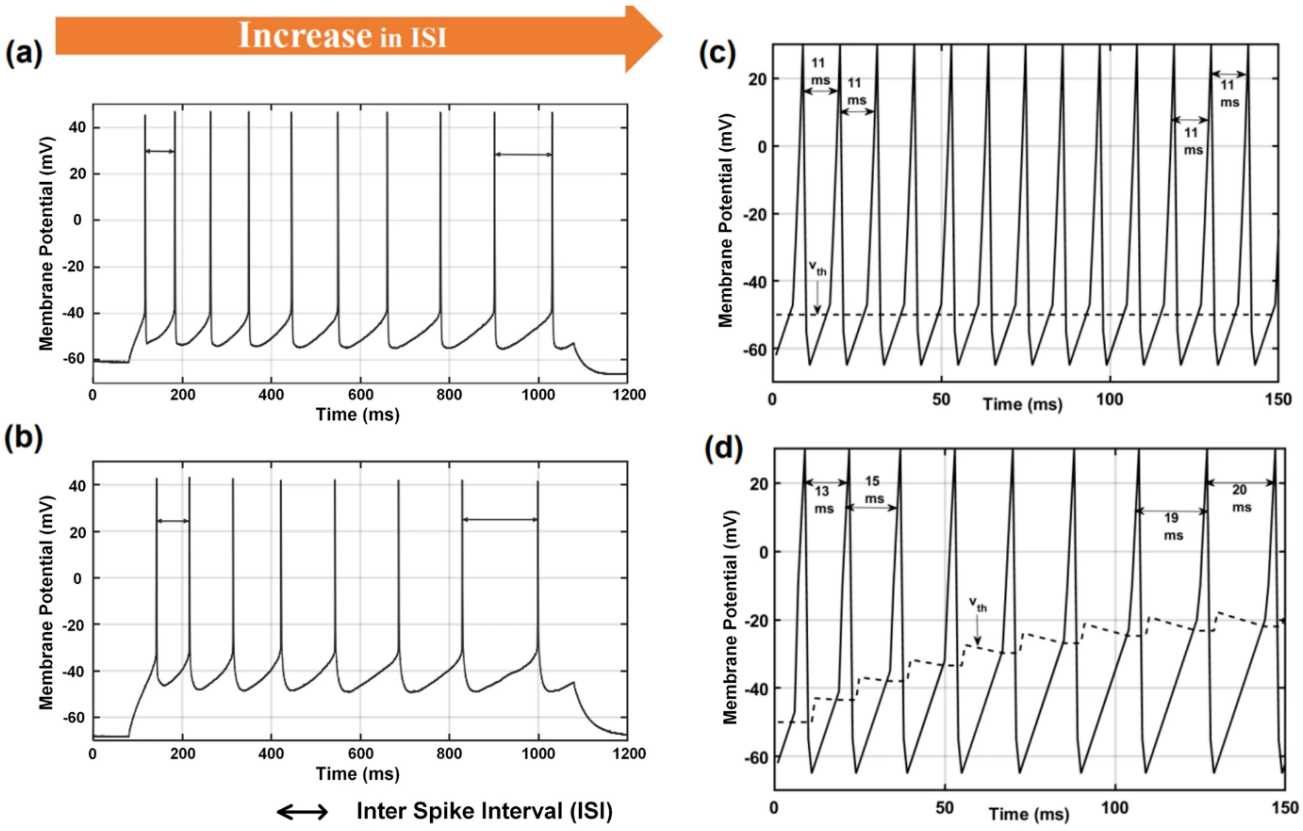


**Figure 6. Spike-frequency adaptation shown in data and simulations. (a)** Human temporal lobe neuron; interspike intervals lengthen during a one-second current step. **(b)** Mouse visual cortex neuron; same pattern. **(c)** Leaky integrate-and-fire model with a fixed threshold shows nearly constant intervals. **(d)** Adaptive leaky integrate-and-fire model with a rising threshold reproduces the

lengthening intervals (solid: membrane potential; dashed: threshold voltage). Reproduced from Ganguly et al. (2024).

The physiological mechanisms that make neural adaptation a reality operate across nested timescales. At the most rapid scale, short term depression (STD) at cortical synapses act like a dynamic gain control mechanism that begins within a few milliseconds after the onset of simulation (Abbott et al., 1997). Unlike blanket inhibition, STD scales down only the synapses involved in active firing over a period and leaves the inactive synapses ready to respond. This drop in synaptic efficacy following sustained periods of activity renders the network as a whole sensitive to changes in stimuli (that would typically recruit different synaptic channels) (Abbott et al., 1997; Fortune & Rose, 2001). Rapid adaptation mechanisms like these are accompanied by slower processes that occur over hundreds of milliseconds to seconds. For example, calcium-activated potassium channels such as big-conductance calcium activated potassium channels (BKCa) and small-conductance calcium activated potassium channels (SKCa) open during spike trains, where big-conductance channels provide rapid repolarization and small-conductance channels generate slow afterhyperpolarization currents (Bean, 2007; Faber & Sah, 2007). Further layers of adaptation are added by M-type potassium conductance and calcium-dependent chloride channels, each having their own time constants (Delmas & Brown, 2005; Ha et al., 2016). The consequences of multiple different adaptation mechanisms being simultaneously implemented are faster response latencies to novel stimuli, across multiple timescales (Antunes et al., 2010). This is also seen in the biphasic adaptation curves recorded in biological neural networks (Ghodrati et al., 2019). The artificial neural systems that are computationally available today only implement these principles to an extent, especially when it comes to the processing of motion.

Existing neural network solutions to motion processing fall short of describing key motion dynamics. Purely feedforward architectures that typically perform well on image classification tasks require sophisticated preprocessing of motion sequences, which leaves the bulk of the motion processing burden to hard coded software solutions. This deviates considerably from how biological networks process motion, and one of the key differences between artificial and biological neurons that make it possible for the latter to process differences in motion instead of just static input information lies in their temporal dynamics — especially recurrence (Wang, 2001;

Wong & Wang, 2006). Because recurrence in a neural network enables sustaining activity signals over time, this both enables the network to process time dependent constructs like motion while serving as a testbed to study mechanisms like neural adaptation. Moving to implementation details, design choices used in the construction of the network directly affect the utility of the networks' responses. For example, using biologically realistic time constants wherever possible across the network will result in responses that can be directly compared with physiological and behavioural studies (Benda & Herz, 2003). One could argue that what is of greater importance, is the balance between constants, rather than their absolute values themselves. For example, for synaptic depression to work, the network must operate on timescales that are fast enough to enhance during transient stimulation yet slow enough to accumulate when the stimuli are prolonged (Abbott et al., 1997; Baccus & Meister, 2002; Zucker & Regehr, 2002). Energy constraints take this further, as they put the burden of balancing information transmission against energy costs, on biological systems. Adaptation as a mechanism works to uphold this balance, even as network parameters fluctuate within functional boundaries. The framework developed here in this thesis is to modify a feedforward motion processing network with recurrent connectivity and then incorporate neural adaptation into its flow. This architecture enables testable predictions—adaptation should lead to aftereffects in the network's responses, response latencies should vary compared to the baseline and a higher sensitivity to changes in stimuli should be accompanied by a decrease in activity in response to prolonged inputs. These predictions establish clear benchmarks to validate a computational model of adaptation.

**Studying neural dysfunction: multisensory integration**

A key challenge for collicular neurons is to determine whether signals from different senses were from a common external event. When a flash of lightning precedes thunder, or when watching someone speak, the brain must decide whether to treat these multimodal signals as coming from the same or different events. When done properly, multisensory integration provides significant computational benefits (Wallace et al., 2020). One such scenario is when the responses from individual senses are weak. Even though multiple modalities might signal an event at a particular location, if they are weak, the activity remains subthreshold, and the event will not elicit a percept. But neural recordings have shown that multisensory neurons can respond to combined

audiovisual stimulation with firing rates that exceed the sum of their individual responses. This phenomenon is called super additivity, and it is most pronounced when unisensory signals are weak (Stein & Stanford, 2008). Multisensory integration is defined by strict boundaries across space and time, with binding typically occurring only within roughly 30 degrees of spatial alignment and 200 to 300 milliseconds of temporal coincidence (Powers et al., 2009; Rohe & Noppeney, 2015; Wallace & Stevenson, 2014). Within these windows, cue combination is near optimal, and inputs to these multisensory neurons are weighted by their reliability. This approximates Bayesian inference, and consequently, integration can lead to more precise perceptual estimates than either of that sense could provide by itself (Alais & Burr, 2004; Ernst & Banks, 2002). To implement mechanisms of this resolution, there is a need for neural circuits capable of millisecond-precise coincidence detection.

The superior colliculus is perhaps the brain area that is most suited for mechanistic investigation, when it comes to multisensory integration. Deep and intermediate collicular neurons receive projections from both auditory and visual cortices, creating opportunities for cross-modal integration (King et al., 1998; Meredith & Stein, 1986; Stein & Stanford, 2008). When these inputs converge, they interact through synaptic mechanisms that determine when and how these signals combine. Faster acting channels like AMPA receptors provide almost immediate excitation lasting a few milliseconds, while slower NMDA channels maintain depolarization for 50 to 120 milliseconds (Rowland & Stein, 2007), by modifying the Mg gate op interval. This creates a system which accounts for a quick response latency while creating a temporal window during which disparate events can combine into a single percept. The boundaries of this window are then shaped by both the strength and timing of GABAergic inhibition, which prevents unrelated signals from being bound together. This interplay between excitatory and inhibitory currents lead to hallmark multisensory effects — superadditive enhancement for aligned stimuli and suppression of misaligned inputs. Any disturbance in this balance predictably leads to changes in integration. For example, blocking NMDA receptors reduces multisensory gain, and decreasing the strength of feedforward inhibition leads to a broadening of temporal binding windows (Binns & Salt, 1996; Felch et al., 2016). These effects are a direct demonstration of how changes in circuit parameters translate to behavioural differences. Because specific mechanisms like these translate cleanly to behaviour,

the superior colliculus is an ideal target for computational models to test how disruptions in network or synaptic parameters could affect multisensory integration.

The superior colliculus does not function as an isolated node, but instead as a multisensory hub in the midst of highly distributed cortico-tectal circuits (**Fig. 7**). Early experiments showed that removing the association cortex in cats would halt superadditive responses in collicular neurons, despite ascending neurons remaining intact (Jiang et al., 2001; Stein et al., 2014a). Even though the neurons continued to receive typical projections from audio and visual cortices, they failed to combine them effectively. Modern circuit mapping has shown that these cortico-tectal projections to the superior colliculus are consistent across species. This dependence of adequate multisensory integration on signals from the association cortex implies that this part of the cortex provides the drive essential for integration functionality. But the information coming into the superior colliculus from these higher order cortices is not redundant or arbitrary. Each top-down projection carries unique information, either about an event or an interaction with the environment. While input signals sent from the pre-frontal cortices are typically associated with cognitive influences, other regions like the anterior cingulate cortex and the frontal eye fields project sensorimotor information and orient response strength, respectively (Huda et al., 2020; Peel et al., 2017). These cortical influences tend to emerge slowly with development (Wallace & Stein, 1997; Yu et al., 2010). In particular, collicular neurons require cross modal experience postnatally to develop precision in integration of signals across modalities. From a network point of view, this development is a reflection of the interplay between collicular neurons and cortical “teaching” signals, with time. The layered architecture of the superior colliculus provides a starting point for the computational layout, and the identified cell types provide a direct way to validate circuit parameters against biology. The behavioural differences that are observed in neurodevelopment conditions like ASD provide pre-established tests to explore whether variances in superior colliculus -centric mechanisms can explain altered multisensory integration.

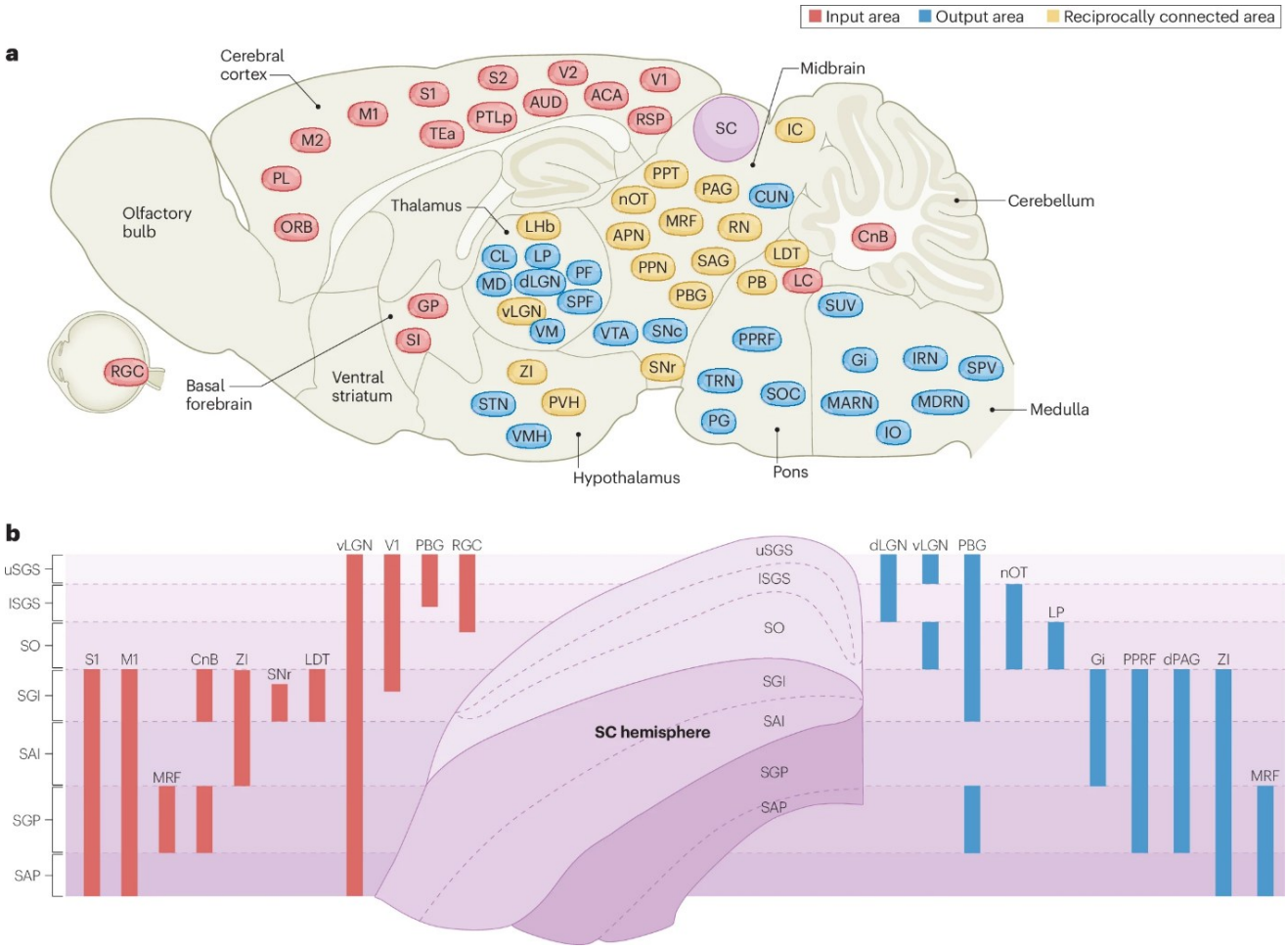


**Figure 7. Superior colliculus as a multisensory hub.** Brain-wide cortical sensory (visual, auditory, somatosensory) and associative inputs converge on SC; outputs and reciprocal links indicated; panel b shows laminar targeting. Reproduced from Cang et al. (2024).

In ASD, the activity of collicular neurons departs from typical integration in a manner that indicates which circuit mechanisms might be altered. The most frequently reproduced of these departures is a broadening of the temporal binding window, across both simultaneity judgement tasks as well as stimulus onset asynchrony in flash beep illusions (Foss-Feig et al., 2010) (**Fig. 8**). When asked to judge whether a flash and beep occurred simultaneously, neurotypical individuals typically accept offsets up to 200 ms, but autistic individuals often report simultaneity for delays exceeding 300 or even 400 ms (Powers et al., 2009; Stevenson, Siemann, et al., 2014). This difference is noted even across complex audiovisual speech, which indicates that it is a dysfunction in fundamental functionality like coincidence detection, rather than task specific. The consequences of this atypicality extend beyond perception. In noisy environments, where neurotypical individuals gain strong audiovisual integration benefits, these enhancements are reduced in autism (Beker et al., 2018; Foxe et al., 2015). A voice becomes easier to understand when you can see

the speaker's lips move, but this advantage is reduced in autism, particularly when temporal alignment is of importance. In contrast to the consistent differences seen in temporal binding, spatial integration in autism is also atypical, but the direction of difference varies considerably. Where certain individuals consider events with relatively larger spatial disparities as originating from the same source, others do not consider signals coming from even very small spatial disparities as causally linked (Pulliam et al., 2023). This heterogeneity in responses may be an indication that the atypical spatial binding window observed in ASD is a result of multiple underlying mechanisms. These multiple mechanisms may undergo different degrees of perturbation in ASD, leading to the varied differences across individuals. Importantly, the differences in these integration metrics in dysfunction raise targets for mechanistic exploration, which can be quantified. They could also suggest network level changes in how coincidences are detected, and cues are combined.

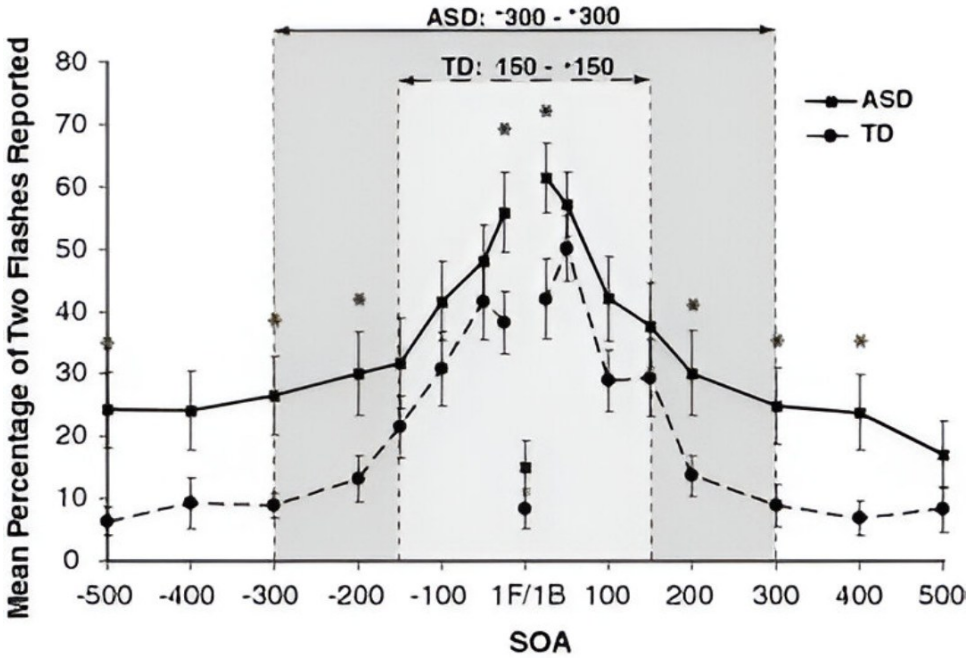


**Figure 8. Sound-induced flash illusion in children.** The temporal binding window (contiguous significant stimulus onset asynchrony (SOA)) is TD: –150 to +150 ms vs ASD: –300 to +300 ms, indicating an expanded window in ASD. Reproduced from Foss-Feig et al. (2010).

The behavioural differences seen in ASD point toward several candidate mechanisms that could lead to the dysfunction in integration seen in the condition. At the cellular level, successful multisensory binding is dependent on a narrow temporal binding window during which inputs can summate. This window is normally constrained to mere milliseconds, by inhibitory shunting sent from sensory cortices. If these inhibitory signals get delayed or lose their typical strength, the window may

expand (Pouille & Scanziani, 2001; Wehr & Zador, 2003). A second gating signal is provided by NMDA receptors through their voltage-dependent magnesium block. Because this voltage block only gets released under sufficient depolarization, NMDA receptors typically contribute substantial current when current flow from multiple sources sum together (Jalali-Yazdi et al., 2018; Nowak et al., 1984). This makes them ideal biological coincidence detectors. Consequently, disruptions in NMDA receptor kinetics could lead to dysfunctional integration dynamics. NMDA hyperfunction for instance, could directly affect the temporal binding window by extending the period during which events separated in time can interact. Alterations in E/I balance could degrade the signal-to-noise ratio that enables cross-modal signals to be enhanced (Gabernet et al., 2005; Rubenstein & Merzenich, 2003; Sohal & Rubenstein, 2019). At the systems level, atypical long range connectivity between brain regions may disrupt the synchronization in activity required to bind distributed representations (Khan et al., 2013; Uhlhaas et al., 2009). Each mechanism may produce a distinct pattern of altered integration. A chief issue in practice though, is that these mechanisms overlap in their functionality as well as dysfunction, making it difficult to isolate the specific circuit perturbations that contribute most to differences in response.

To determine links between circuit mechanism and response metrics, there is a need for methods that can isolate these pathways. Current experimental approaches face limitations in achieving this goal. Psychophysical studies can measure broadening or narrowing of integration windows, but face difficulties attributing these changes to specific mechanisms (Kawakami et al., 2020; Stevenson et al., 2014; Wallace & Stevenson, 2014). fMRI based approaches on the other hand provide information about where activity differs, but do not have the temporal resolution required to track the narrow windows during which integration occurs. Even fast tracking methods such as MEG, due to the inverse problem of source localization (uncertainty in implicating a specific causal mechanism, given response properties), are unable to identify precise circuit configurations that lead to observed outcomes (Baillet, 2017). Computational frameworks, especially those based on Bayesian inference, are effective at describing what is being computed, but typically abstract away the neural underpinnings behind that computation (Rohe & Noppeney, 2015). To remedy these issues in resolution, spiking neural models make circuit parameters explicit, and offer control over the desired level of abstraction (Brette & Gerstner, 2005; Brunel & Wang, 2001). By employing spiking networks for this study, each mechanism

can be varied along with its subcomponents, in detail. For example, lengthening NMDA's gate interval or delaying inhibition without varying its strength. As a result, each manipulation can lead to insights or testable predictions about how mechanisms alter integration. In the process, correlational observations in physiology are converted into hypotheses that can be validated against neural recordings and behavioural data.

**Thesis overview**

It is important to note that while this computational framework could provide testable insights about causal links in biological systems, it is not always straightforward to validate the hypotheses generated by these models against biology. This is especially true in the case of therapeutic intervention development. In biology, the link between various circuit mechanisms is still incompletely understood across brain areas. Homeostatic processes might link these mechanisms in such a dependent fashion that modifying one parameter might trigger compensatory changes in others, which could limit single target interventions. The superior colliculus, in particular, receives projections from several higher order brain regions, the computational roles of which are not yet fully understood. Cholinergic projections might control gain, while cortical feedback might set priors. But disentangling these functionalities would require a system that can implement pathway specific manipulations during natural behaviour. This is further complicated by the fact that developmental trajectories could further limit intervention windows by adding age-based constraints on plasticity. For example, the shift from slow to fast NMDA during development is accompanied by a narrowing effect on integration windows (Cathala et al., 2000), but it is unclear whether this narrowing can be reversed, once adulthood sets in. A broader theoretical question is whether biological systems explicitly implement optimization techniques, or whether such mechanisms emerge naturally as a result of other constraints. If the brain budgets its energy, parameters like the binding window should vary with task demands and the current metabolic budget. The answers to these questions could help resolve if task goals alone can predict neural organisation, or if explicit coding of parameters are necessary for biologically rooted simulations.

The two complementary studies described in this thesis illustrate how biologically constrained models can reveal mechanisms across the spectrum from adaptive efficiency to integration deficits. The first study presents AdaptNet, a recurrent neural network that learns motion processing through exposure to natural

image sequences while implementing neuronal adaptation inspired by cortical physiology. This network not only reproduces the classic motion aftereffect that has fascinated vision scientists for decades but also investigates potential functional benefits of adaptation. The network achieves comparable motion estimation accuracy while using dramatically less energy and responding faster to changes in the environment. These benefits emerge naturally from local circuit dynamics without any explicit optimization for efficiency. The second study shifts focus from adaptation to multisensory integration dynamics by constructing a detailed spiking model of the superior colliculus. After establishing that the model reproduces well-known integration phenomena like reliability-weighted cue combination and inverse effectiveness, systematic perturbations reveal how different neural alterations produce distinct patterns of sensory binding dysfunction. For example, reducing adaptation uniformly expands both spatial and temporal windows while degrading precision, whereas diminishing inhibition creates an unexpected dissociation where spatial windows narrow even as temporal windows broaden. These mechanistic insights suggest that the heterogeneous sensory profiles observed across autism spectrum populations might reflect different underlying circuit alterations rather than a single pathophysiology. Together, these studies establish that the same modelling philosophy can illuminate both why healthy circuits work and how they fail when key parameters shift.

**Energy efficiency and sensitivity benefits in a motion processing adaptive recurrent neural network**

Vishnu Mohan[1] & Reuben Rideaux[1,2]

[1]School of Psychology, The University of Sydney, Camperdown, Australia
[2]Queensland Brain Institute, The University of Queensland, St Lucia, Australia
corresponding author: *reuben.rideaux@sydney.edu.au*

Acknowledgements: This work was supported by Australian Research Council (ARC) Discovery Early Career Researcher Awards awarded to RR (DE210100790) a National Health and Medical Research Council (NHMRC; Australia) Investigator Grant (2026318).

**ABSTRACT**

Motion processing is a key function for the survival of many organisms and is initially implemented in the primary visual cortex (V1) and the middle temporal area (V5/MT) of the primate visual cortex. Advances in machine learning approaches have led to the development of motion processing neural networks that have elucidated several aspects of this process. However, it remains unclear how adaptation, a canonical function of sensory processing, influences motion processing. In this study, we developed two recurrent neural networks to study motion processing: MotionNet-R, a baseline model, and AdaptNet, a model that employs adaptive mechanisms inspired by biological systems. Both networks were trained on natural image sequences to estimate motion vectors. We found that both networks developed response properties that resembled those of neurons found in areas V1 and MT, e.g., speed tuning, and AdaptNet recapitulated the motion aftereffect phenomenon (i.e., *the waterfall illusion*). We show that the emergent computational properties that implement the phenomenon in AdaptNet confirm previous theoretical hypotheses. Further, we compared the performance of the two networks and found that AdaptNet processed motion more efficiently, operationalized as reduced activation. While AdaptNet incurred reduced accuracy in response to prolonged constant input, it was both more accurate and sensitive in response to changes in motion input. These results are consistent with theoretical explanations of adaptation as neural property that supports metabolic efficiency and increased sensitivity to change in the environment. Our findings provide novel insights into the neural mechanisms underlying motion adaptation and highlight the potential advantages of adaptive neural networks in modelling biological processes.

## INTRODUCTION

### Biological Basis of Motion Processing and Adaptation

The ability to process and interpret motion is one of the most fundamental requirements for survival in any environment. In the primate visual cortex, multiple areas work together in a hierarchical fashion to process increasingly complex forms of motion. Two key regions in this network are the primary visual cortex (V1) and the middle temporal area (V5/MT), which serve intrinsic roles in the early stages of motion processing. While V1 is primarily responsible for detecting local motion, MT integrates these local signals to compute global motion (Movshon & Newsome, 1996). This processing hierarchy in perhaps most prominently demonstrated by the responses to V1 and MT neurons in response to drifting sinewave and plaid gratings (Movshon et al., 1985).

A key feature of motion processing, and healthy brain function more broadly, is adaptation. Motion adaptation manifests in various perceptual phenomena, most notably the motion aftereffect (MAE) or "waterfall illusion", where prolonged exposure to motion in one direction leads to perception of motion in the opposite direction when subsequently viewing a stationary stimulus (Mather et al., 1998). While the MAE itself does not seem to enhance perception, it reflects underlying adaptive mechanisms thought to optimize neural resources and enhance sensitivity to changes in visual motion (Mather et al., 1998).

There have been significant advances in our understanding of motion processing (Born & Bradley, 2005; Burr & Thompson, 2011; Nishida, 2011) and its limitations (Edwards & Rideaux, 2013; Rideaux & Edwards, 2014). However, the neural mechanisms that underlie motion adaptation are not yet fully understood (Clifford et al., 2007; Glasser et al., 2011; Solomon & Kohn, 2014). Multiple factors contribute to this challenge. One such issue is that motion adaptation is distributed across several areas of the brain, which makes it difficult to isolate its effects on specific areas (Britten, 2008). Even within a single brain region, there is significant variability in both anatomy and response properties. For example in V1, the diversity of cell types, subcortical input adaptation, and complex changes in both gain and tuning preference of neurons present additional challenges (Carandini et al., 1999; Wissig & Kohn, 2012). This is further complicated by the wide range of adaptation timescales, from milliseconds to hours, which makes comprehensive experimental design difficult (Glasser et al., 2011). There is also an inherent variability in neural

responses, which obscures adaptive changes (Bair & Movshon, 2004). Studying adaptation in higher layers poses additional challenges due to the interplay between inherited and local adaptation effects, which can be difficult to disentangle (Patterson et al., 2013; Rideaux & Harrison, 2019; Zamboni et al., 2020). Additionally, factors such as the diversity of cell types in higher regions like area MT, which adapt differently to those in V1 (Ll et al., 2007), and the potential for top-down influences such as attention (Kohn & Movshon, 2004) further complicate the study of motion adaptation.

Despite the difficulty associated with studying motion adaptation, considerable progress has been made towards understanding this phenomenon. Johnston et al. (2006) revealed the effect of adaptation on speed perception, while the influence of adaptation on motion integration was explored by Patterson et al. (2014). Lee (2018) further built upon this by exploring the interplay between local and global motion under adaptation, uncovering bidirectional effects. Notably, adaptation can also improve motion detection capabilities in noisy conditions by improving sensitivity to motion signals that are relatively weaker (Hietanen et al., 2007). The scope of motion adaptation extends beyond simple 2D motion; for example, Sakano and Allison (2014) investigated motion-in-depth perception and found that adaptation to motion towards or away from an observer can induce an aftereffect in the opposite direction. Adaptation also impacts higher-level processes, such as biological motion perception in humans, as demonstrated by Theusner et al. (2011), who showed that adaptation to a walking figure can bias the perceived walking direction of a subsequently viewed figure. Additionally, Cuturi and MacNeilage (2014) highlighted that adaptation affects vestibular heading perception, illustrating its role in multisensory integration. This diverse body of research demonstrates how pervasive the effects of adaptation are across different forms of motion perception.

**Computational Approaches to Motion Perception**

Computational modelling has shown to be an effective tool for studying motion processing. Over the last few decades, there have been pioneering computational models of visual processing that have focused on both ventral and dorsal streams. In particular, Simoncelli and Heeger (1998) proposed an influential model of MT neurons that accounted for their direction and speed tuning. Rust et al., (2006) expanded on this work by implementing a more detailed and biologically plausible V1 layer. These

early models laid the groundwork to study motion processing in area MT using artificial networks.

In recent years, computational modeling combined with machine learning has increasingly been applied to investigate complex biological phenomena (Kriegeskorte & Douglas, 2018). Deep neural networks have been a useful tool for understanding the hierarchical structure of processing in the brain (Yamins & DiCarlo, 2016). Training these networks on natural images leads to representations that mimic those observed in the primate visual cortex (Cadieu et al., 2014; Guclu & Van Gerven, 2015; Khaligh-Razavi & Kriegeskorte, 2014). While many studies have used deep neural networks to investigate visual processing, they have predominantly focused on ventral stream functionality. Notable examples include the work of Yamins et al. (2014), who used deep learning to show that trained networks develop internal representations like those observed in higher visual areas of the ventral stream, and Kar et al. (2019), who used convolutional neural networks (CNNs) to predict responses in the ventral pathway during object recognition tasks.

There have been some more recent efforts to utilize machine learning techniques to understand dorsal stream processes. For instance, Rideaux and Welchman (2020) used a CNN trained on natural image sequences to model motion processing, successfully reproducing key properties of V1 and MT neurons and providing novel insights into the origins of motion illusions. Further, Qiao and Shen (2021) developed a model that learned to estimate motion from natural human videos and Gundavarapu et al. (2019) proposed a hierarchical model of motion processing that learned representations like those in the dorsal pathway. However, while the above artificial neural network (ANN) models successfully reproduced certain qualities of processing in the visual cortex, the effects of adaptive mechanisms on those qualities have been neglected.

Parallel to these developments, there has been considerable work investigating the benefits of adaptation in the field of neuromorphic computing. For example, adaptive mechanisms in spiking neural networks (SNN) produce efficiency gains (Ganguly et al., 2024; Indiveri & Liu, 2015) and optimizes sensory encoding (Mao et al., 2025) and the use of neuron models such as adaptive exponential neurons (AdEx) along with neuromorphic hardware has led to considerable gains in energy efficiency for certain tasks (Bellec et al., 2018, 2020). Such mechanisms have also been shown to enhance performanve in situations involving a change detection (Hu et al., 2021).

These studies highlight the importance of adaptation in spiking neural networks and suggest that incorporating adaptation can enhance computational efficiency in neuromorphic systems. However, the influence of adaptation in ANNs trained to perform visual tasks, in particular visual motion estimation, remains unexplored.

**Present Work**

While computational models of motion processing have provided considerable insights into this process, our understanding remains incomplete. Incorporating adaptation into neural networks may expand our understanding of motion processing across different areas of the visual cortex. Thus, here we developed novel ANNs that simulate motion processing and adaptation in the visual cortex, focusing on early to mid-level visual areas V1 and MT. These ANNs incorporate adaptation mechanisms in both V1- and MT-like layers, allowing us to study the role of adaptation in motion processing. By comparing the emergent properties of adaptive and non-adaptive networks trained on natural image sequences, we reveal novel insights into the neural mechanisms underlying motion adaptation in visual processing, complementing and extending previous theoretical and empirical work.

## METHODS

Two convolutional recurrent neural networks (conv-RNNs) were trained to estimate motion velocity from natural image sequences: MotionNet-R, a baseline model, and AdaptNet, which employs adaptive mechanisms. Our goal was to better understand the role of adaptation in motion processing by comparing the emergent properties within these networks. This comparison allows us to directly measure how adaptation mechanisms can influence motion processing, within a neural network.

***Training data.*** The network was trained with 60,000 natural image sequences, each containing ten frames, extracted from photographs in the Berkeley Segmentation Dataset (Martin et al., 2001). This approach has previously been used (Rideaux & Welchman, 2020, 2021; Simoncelli & Olshausen, 2001) and aims to reproduce the visual diet of biological visual systems. A sliding window method was used to generate motion sequences from natural images. The ground truth velocity values corresponding to each sequence were recorded by estimating pixels crossed by the sliding window during this process, for use in training. The sequences were kept relatively short to mitigate vanishing gradients. All natural images were converted to grayscale prior to sequence generation so that each frame contained a single luminance channel. Two consecutive frames were then stacked to form a dual-channel input tensor.

***Model architecture and theoretical foundations.*** We developed two ANNs to simulate motion processing and adaptation in the visual cortex, focusing on early to mid-level visual areas V1 and MT. The first network, which we named MotionNet-R, expands upon the original MotionNet architecture (Rideaux & Welchman, 2020, 2021) by incorporating a recurrent layer. The second network, AdaptNet, further builds on MotionNet-R by implementing adaptation mechanisms in both V1 and MT units. The only difference between MotionNet-R and AdaptNet was the implementation of the adaptation mechanism in the convolutional and recurrent layers. The structure of the two networks was the same: a two-dimensional (2D) convolutional layer (simulating V1), a recurrent layer (simulating MT), and a linear output layer. The networks' structure was intended to recapitulate the hierarchical organization of areas in the visual cortex (Born & Bradley, 2005; Movshon & Newsome, 1996). The fine tuning of parameters for training was done by trial and error. A dropout layer (dropout values were 0.3 for both the V1 and MT layers) was added after the convolutional and recurrent layers to improve regularization (Srivastava et al., 2014), and make the

training more robust. The dropout did not interact directly with the adaptation mechanism.

***Convolutional layer (V1 simulation).*** Following the input layer, the first hidden layer of the networks was a 2D convolutional layer with 16 kernels (size = 6×6 pixels; stride length = 1). This 2D convolutional layer has 2 input channels corresponding to consecutive frames of the input. These values were selected based on previous work (Rideaux & Welchman, 2020) to minimize network scale and complexity. Two successive images of the motion sequence were fed as input to this layer, with each image serving as a separate channel. The operation of a 2D convolutional layer over [i, j] with 2 input channels can be described as:

$$\boldsymbol{Y}[i,j,t] = \sum m \sum n \sum k \boldsymbol{K}[m,n,k] * \boldsymbol{X}[i+m, j+n, t+k] \quad (1)$$

where $\boldsymbol{Y}$ is the output, $\boldsymbol{X}$ is the input, $\boldsymbol{K}$ is the kernel, $i, j$ are spatial coordinates, $m, n, k$ are the kernel dimensions and * denotes convolution.

***Recurrent neural network layer (MT simulation).*** Area MT was modelled using a recurrent layer in both networks. This layer was responsible for analyzing temporal information across a series of V1 responses. The operation of area MT and other areas in the neocortex have previously been modelled with recurrent networks (Kar et al., 2019). Each unit in this layer uses a nonlinear activation function (rectified linear unit; ReLU) to introduce nonlinearity into the network. The ReLU function is defined as:

$$f(k) = \max(0, k) \quad (2)$$

where $k$ is the input activation at a ReLU unit.

***Adaptation mechanism.*** In AdaptNet, we implemented an adaptation mechanism in both V1 and MT units. We aimed to model this adaptive mechanism based on what is observed in biological neural networks like the visual area of the macaque (Kohn & Movshon, 2003; Krekelberg et al., 2006). Key to this implementation was an adaptation variable that accumulates over time (to reflect a decrease in response to a constant stimulus) and gradually decays (recovery). In the V1 layer, adaptation is implemented via the formula

$$\mathrm{y}_\mathrm{t}^{\mathrm{V1}} = \max\left(0, \mathrm{s}_\mathrm{t} - \mathrm{a}_{\mathrm{t}-1}^{\mathrm{V1}}\right)$$

where $\mathrm{y}_\mathrm{t}^{\mathrm{V1}}$ is the rectified V1 activity passed to the MT layer after subtracting the V1 adaptation $\mathrm{a}_{\mathrm{t}-1}^{\mathrm{V1}}$ from $\mathrm{s}_\mathrm{t}$, which is the pre-activation from the V1 (convolutional) layer to the adaptation layer. The adaptation is updated as

$$\mathrm{a}_\mathrm{t}^{\mathrm{V1}} = (1 - \beta_{\mathrm{V1}})\mathrm{a}_{\mathrm{t}-1}^{\mathrm{V1}} + \alpha_{\mathrm{V1}}\mathrm{y}_\mathrm{t}^{\mathrm{V1}}$$

with adaptation rate $\alpha_{V1} = 0.1$ and recovery rate $\beta_{V1}$ = 0.1. Similarly, the initial pre-activation in the MT layer is described by

$$p_t = W_x y_t^{V1} + b_{ih} + W_h h_{t-1} + b_{hh}$$

where $p_t$ is the pre-activation drive of the MT (recurrent) neurons, combining the adapted V1 signal via weights $W_x$, the previous hidden state $h_{t-1}$ via weights $W_h$, and two bias terms $b_{ih}$, $b_{hh}$. MT unit responses then calculated as

$$r_t = \max(0, p_t - a_{t-1}^{MT})$$

where $r_t$ is the rectified MT activity after subtracting MT adaptation $a_{t-1}^{MT}$, which is updated according to

$$a_t^{MT} = (1 - \beta_{MT}) a_{t-1}^{MT} + \alpha_{MT} r_t$$

with rates $\alpha_{MT} = 0.2$, $\beta_{MT} = 0.1$. Finally,

$$h_t = r_t$$

becomes the recurrent hidden state — the activation fed back at the next time-step and the internal memory of motion information. The adaptation variable $\boldsymbol{a}_t$ accumulates when the neuron is active (controlled by $\boldsymbol{a}_t$) and decays over time (controlled by recovery rate $\beta$). A higher adaptation rate ($\boldsymbol{a}_t$) in means these units show stronger or faster response reduction with sustained firing. We used an adaptation rate of 0.2 for the MT units and 0.1, for the V1 units. A recovery rate of 0.1 was used in both cases. In MotionNet-R, we omit the adaptation variable and associated adaptive logic. Hence, the recurrent layer and convolution layer outputs are passed as is, to the subsequent layer. We used a lower adaptation rate in the V1 layer compared to the MT layer to reflect the same difference in adaptation observed in V1 and MT of biological neural networks like those of the macaque (Patterson et al., 2014; Priebe et al., 2002; Solomon & Kohn, 2014).

***Linear layer (readout).*** The output layer of both networks was a linear layer that mapped the activity of the recurrent layer to two outputs: x and y. Here, x and y denote the estimated motion velocity (in pixels per frame) along the horizontal and vertical axes, respectively. Utilization of area MT's responses to estimate speed and direction has been observed in humans and adult male rhesus monkeys (Churchland & Lisberger, 2001). The operation of this layer can be described as:

$$\boldsymbol{q} = W\boldsymbol{p} + \boldsymbol{b} \quad (4)$$

where $\boldsymbol{q}$ is the output (motion estimate), $\boldsymbol{p}$ is the input from the recurrent layer, $\boldsymbol{W}$ is a weight matrix, and $b$ is a bias vector.

***Training procedure and evaluation.*** Both networks were trained using mean squared error (MSE) loss and the Adam optimizer (Kingma & Ba, 2017). The MSE is defined as:

$$MSE = \left(\frac{1}{N}\right)\sum_i (y_i - \hat{y}_i)^2 \quad (5)$$

where $N$ is the number of samples in a batch of data, $y_i$are the true values and $\hat{y}_i$are the predicted values.

We trained ten separate instances of the networks, each for 30 epochs. The variability between the models stemmed from random initializations and varied order of minibatch sampling. Having multiple networks to test allows us to quantify the variability of the results (Kriegeskorte & Douglas, 2018). The difference between the network's predictions and ground truth was quantified using Pearson's correlation coefficient.

***Spatial and temporal frequency tuning analysis.*** We extracted response profiles for each unit by exposing the network to drifting sinewave gratings and moving dot sequences, across a range of spatial and temporal frequencies (10 frame sequences, 32x32 pixels, moving dot diameter was 3 pixels unless specified otherwise). This approach mimics that used in neurophysiological experiments to characterize the tuning functions of neurons (De Valois et al., 1982). We generated sinewave grating stimuli using the following equation:

$$I(u, v, t) = Amp \times \sin(2\pi(f_u * u + f_v * v - f_t * t) + \varphi) \quad (6)$$

where $I(u, v, t)$ is the intensity at position $(u, v)$ and time $t$, $Amp$ is the amplitude (contrast), $f_u$ and $f_v$ are the spatial frequencies in the $u$ and $v$ directions, $f_t$ is the temporal frequency, and $\varphi$ is the phase.

We also tested the networks on plaid stimuli (generated by combining two sinewave gratings) to evaluate the units' responses to component and pattern motion. We varied spatial frequency logarithmically from 0.01 to 0.5 cycles/pixel and temporal frequency from 0.1 to 5 Hz. For each combination of spatial and temporal frequency, we presented gratings moving in eight different directions. For some of our analyses, directional and speed preferences were similarly calculated using moving dot sequences that varied in speed within a range between ±3 pixels/frame. The preferred direction, spatial and temporal frequencies of each V1 and MT unit was determined by identifying each unit's maximal response to the varying stimuli.

***Visualization of convolutional kernels.*** To gain insight into the features detected by the convolutional layer, we visualized the trained convolutional kernels (Zeiler & Fergus, 2013). We normalized the weights of each convolutional kernel $\boldsymbol{K}$ using the following equation:

$$\boldsymbol{K}_{norm} = \left( \frac{(\boldsymbol{K} - \min(\boldsymbol{K}))}{(\max(\boldsymbol{K}) - \min(\boldsymbol{K}))} \right) \tag{7}$$

We then applied Gaussian smoothing to highlight edge patterns, using the equation

$$K_{smooth} = G * K_{norm} \tag{8}$$

where $K_{smooth}$ is the smoothed kernel, $K_{norm}$ is the normalized kernel, * denoted 2D convolution and $\boldsymbol{G}$ is a 2D Gaussian kernel defined as

$$\boldsymbol{G}(u, v) = \left( \frac{1}{(2\pi\sigma^2)} \right) \exp\left( - \frac{(u^2 + v^2)}{(2\sigma^2)} \right) \tag{9}$$

where $u, v$ are the spatial coordinates in the 2D Gaussian kernel and $\sigma$ is the standard deviation that controles the amount of smoothing. We used σ = 1 for smoothing.

***Analysis of weight connections between directionally tuned units.*** To investigate how information is processed by the networks to support motion estimation, we analyzed the connections between V1 and MT units (V1-to-MT), and the recurrent connections between MT units (MT-to-MT) (Qian & Andersen, 1994; Snowden et al., 1992). We computed each V1 unit's average V1-to-MT weight by first aligning its preferred direction, and those of the MT units, to zero, before binning and averaging all weights within eight linearly spaced directions from 0-360 degrees.

***Waterfall effect analysis.*** To test for perceptual phenomena associated with adaptation in AdaptNet, we investigated whether the network exhibited the waterfall illusion, a well-known motion aftereffect (Mather et al., 1998). We modified testing sequences to probe for an aftereffect (natural image sequences that were 11 frames long; stationary initially for two frames to gauge any inherent network bias, then three frames of movement followed by six frames of stationary stimulus), presented this sequence to AdaptNet, and analyzed the output.

***Efficiency analysis.*** We tested the efficiency of both networks by comparing their response magnitude and accuracy. We exposed both networks to two types of moving dot sequences; one where the speed and/or direction of the moving dot varied every five frames and another kind where the moving dot maintained a constant trajectory with the same speed, throughout the duration of exposure. The MSE was calculated for a window of three frames after each input change point. Recurrent unit outputs

across all frames were then summed to obtain an analog of the energy used by the network to sustain a representation, under the assumption that implementation of the network as a hardware solution would lead to a linear translation of such energy constraints as well. Our aim was to test if AdaptNet displayed increased efficiency compared to MotionNet-R. Such an increase in efficiency with adaptation is supported by studies of biological visual systems (Barlow & Földiàgk, 1989; Wainwright, 1999). Practically, the test would help indicate if the reduced overall activation displayed by AdaptNet would lead to a lower net output when compared to MotionNet-R, without a substantial relative decrease in accuracy.

***Sensitivity Analysis.*** To examine the difference in sensitivity to a varying input stimulus between the networks, we exposed them to a variety of moving dot sequences with varied speeds. The sequences consisted of ten image frames, of which the first nine frames were one speed and the tenth frame was either the same or a different speed (32x32 images, speed varied from ±3 pixels/frame). This led to several initial-final speed combinations; for each of these combinations we presented 100 image sequences, each with varied initial dot locations. For each combination, we measured the networks' accuracy (as MSE) in estimating the correct motion direction of the final speed (separately) along x and y dimensions. This analysis produced a probability matrix that we could then compare with the ground truth. We then fit a sigmoid function to the diagonal values of these matrices to estimate the sensitivity of each network to stimuli with no change in final speed (congruent condition). The non-diagonal elements were averaged across the range of initial speeds and a sigmoid was fit to this data to estimate each networks' sensitivity to stimuli where final speeds varied from the initial speed (incongruent condition).

***Data availability.*** The code used to train and test the networks is publicly available at https://github.com/Vishnu-Mohan-USyd/Energy_efficiency_and_sensitivity_benefits_in_a_motion_processing_adaptive_recurrent_neural_network.git

## RESULTS

***Network performance evolution during training.*** Both MotionNet-R and AdaptNet learned to estimate motion reliably, following training with natural images. Both networks were structured with a convolutional layer simulating V1, a recurrent layer simulating MT, and a linear output layer for motion estimation (**Fig. 1a**). MotionNet-R displayed increasing accuracy over successive input frames (**Fig. 1b**), demonstrating the network's ability to integrate information over time to support reliable motion estimation. By contrast, while AdaptNet's accuracy initially increased with successive frames, it then subsequently decreased with further frames (**Fig. 1c**). This pattern reflects the impact of adaptation on the network's performance. In particular, the initial increase in accuracy is likely driven by temporal integration, but then the adaptation induced by the constant motion causes the network's response magnitude to decrease and the estimate to deviate from the ground truth, thus reducing the accuracy of motion estimation in response to later frames. We consider the reduction in accuracy to be meaningful because it was reliably present across all models, with relatively small variability, as reflected by the significance of the effect size. Given the 'toy' nature of the network, the relevance of the absolute magnitude is difficult to interpret in terms of its importance to commercial or biological networks. These networks are far larger and more complex; the magnitude may increase with increasing network scale/complexity. Further, small differences in performance may seem relatively insignificant for an isolated instance but applied at scale (across many networks and over time), the accumulated influence can have very significant implications.

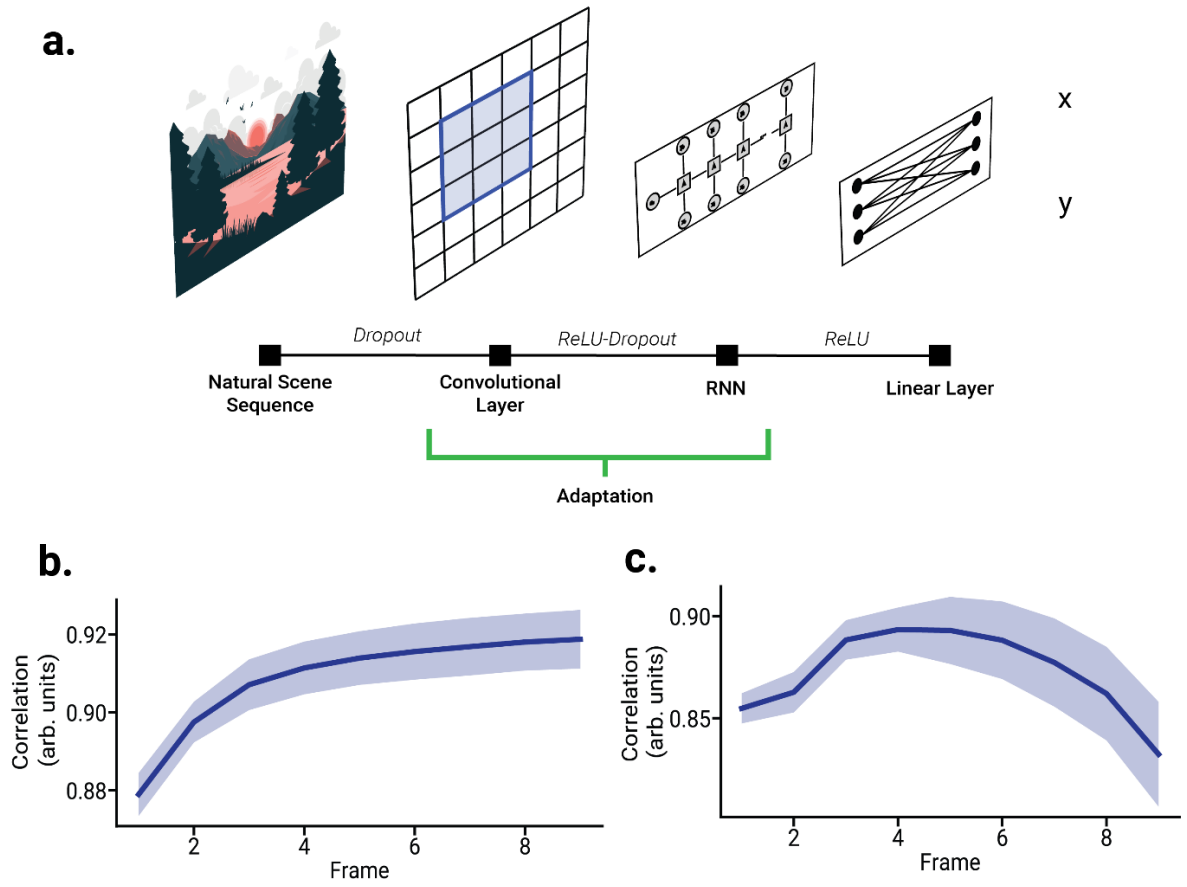


**Figure 1. Network Architecture and Performance.** **a**) Schematic diagram of the network architecture, showing the convolutional layer (simulating V1), the recurrent layer (simulating MT), and the linear output layer for motion estimation. **b, c**) Performance of (**b**) MotionNet-R and (**c**) AdaptNet, showing the correlation coefficient between predicted and ground truth motion values over time (successive image sequence frames). Shaded regions indicate ±SD across multiple networks.

***Spatiotemporal tuning properties in the networks***. Both networks developed response properties resembling those of biological neurons in areas V1 and MT. The distribution of speed tuning among convolutional (V1) and recurrent (MT) units was similar to neurophysiological observations in macaque (Maunsell & Van Essen, 1983; Priebe et al., 2006) (**Fig. 2a-b**). That is, V1 units were tuned to relatively lower speeds than MT units. This resembles the responses of neurons in area V1, which are typically more sensitive to lower velocities when compared to those of area MT.

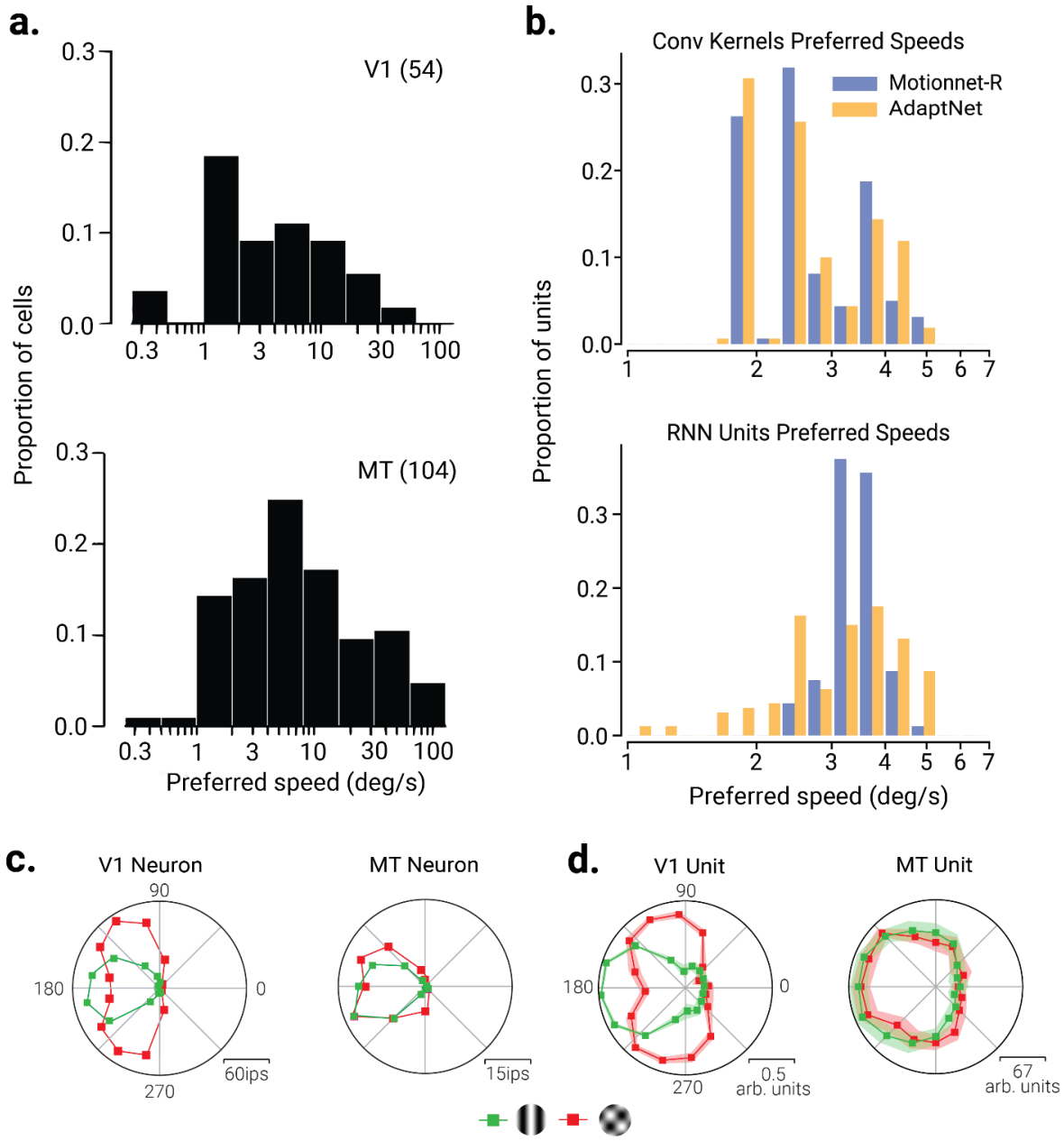


**Figure 2. Spatiotemporal tuning properties of network units. a**) Data from Priebe et al. (2006) showing the distribution of preferred speeds for (top) V1 and (bottom) MT neurons in macaque. **b**) The same as (**a**), but for V1 and MT units in MotionNet-R and AdaptNet networks. **c**) Replotted data from Adelson and Movshon (1982) showing single-neuron responses in (left) V1 and (right) MT to sinewave grating and plaid stimuli (135° separation) moving in different directions. **d**) Same as (**c**), but for responses obtained from MotionNet-R units. Shaded regions indicate ±SD across multiple networks.

A key distinction between V1 and MT neurons is that the former responds maximally to component motion, while the latter responds to pattern motion, which is thought to be due to pooling of signals between V1 and MT. This phenomenon is clearly observable in the responses of these neurons to drifting sinewave grating and plaid stimuli. V1 neurons respond maximally to the two components of the plaid stimuli,

whereas the MT neurons maximally respond to the combined pattern motion, which is consistent with perception of these stimuli (Movshon et al., 1985; Rust et al., 2006) (**Fig. 2c**). We tested the networks with these stimuli and found the same pattern of results; V1 units were selective for component motion while MT units responded maximally to the pattern motion (**Fig. 2d**). Together, the spatiotemporal tuning properties that emerged in the networks to perform motion estimation appear to resemble those observed in biological systems, e.g., non-human primates. The emergence of pattern motion selectivity in the higher layers occurs even in simpler models without recurrence or adaptation (Rideaux & Welchman, 2020) as it simply relies on the pooling of component motion signals from earlier layers.

***Emergent weight properties in the networks***. We analyzed the weights of MotionNet-R and AdaptNet to understand how the connectivity patterns in these networks supported motion processing. **Figure 3a** shows the learned convolutional kernels, which resembled edge detectors or Gabor filters. A shift in the phase of these Gabor-like kernels between the two channels, which receive input from successive image sequence frames, appears to have emerged to facilitate detection of motion energy. These kernels are analogous to the receptive fields of V1 simple and complex cells, which are sensitive to specific orientations and motion directions (DeAngelis et al., 1999; Hubel & Wiesel, 1962).

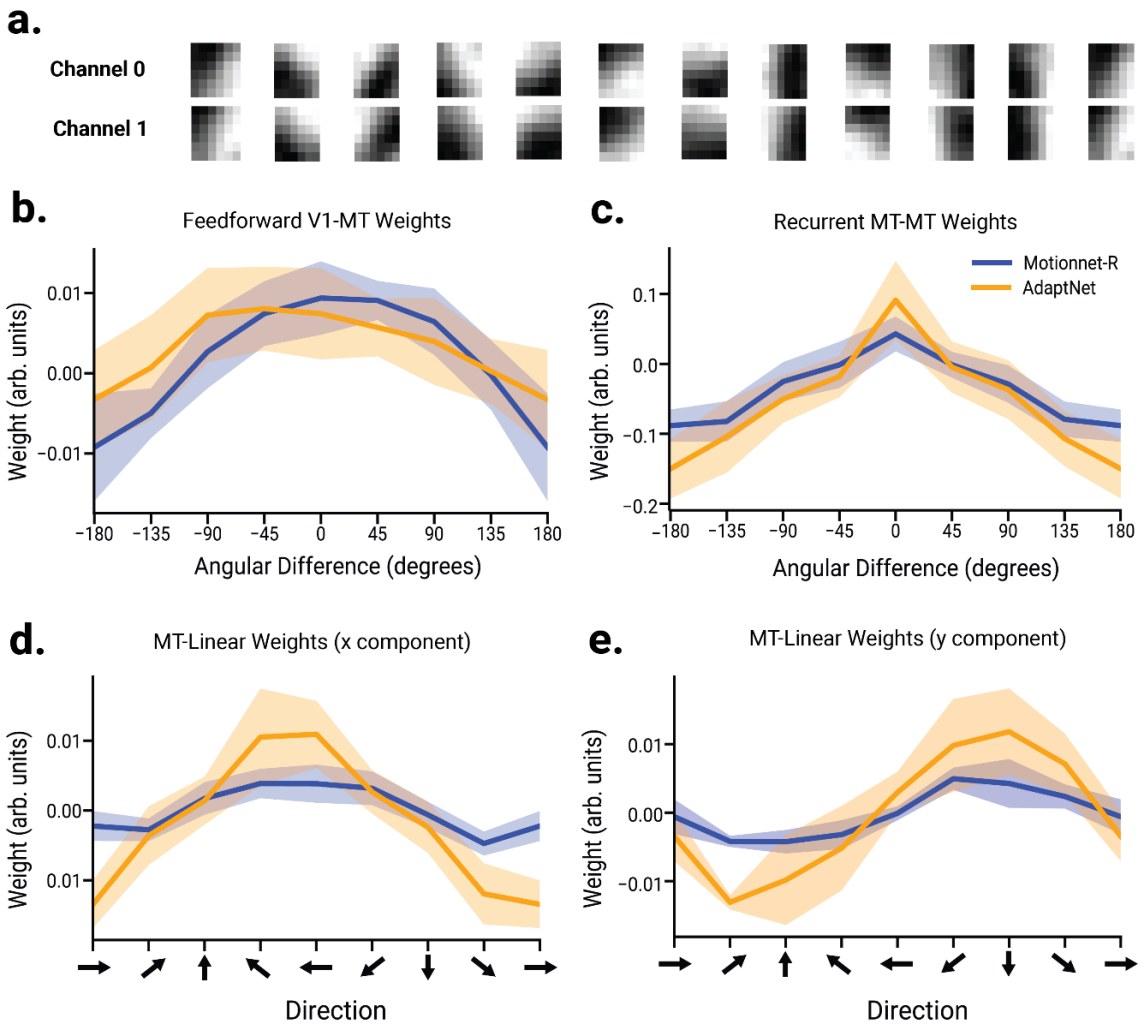


**Figure 3. Network connectivity.** **a**) Examples of convolutional (V1) kernels, resembling edge detectors or Gabor filters. Each column shows the two channels of a single kernel, corresponding to successive frames. **b**) Average feedforward connections from V1 to recurrent (MT) units as a function of directional tuning difference. **c**) Same as (**b**), but for recurrent connections between MT units (MT-to-MT). **d**, **e**) Average weights from MT units to the (**d**) x and (**e**) y component of the linear output layer as a function of the directional tuning of MT units. Shaded regions indicate ±SD across multiple networks. The legend in graph c also applies to graphs (b-e). Results are shown for both (blue) MotionNet-R and (orange) AdaptNet.

Assessment of the feedforward connections from V1 to MT units showed that there were more positive connections between units with a similar directional preference (**Fig. 3c**). This pattern of connectivity is consistent with previous neurophysiological observations between V1 and MT (Born & Bradley, 2005; Movshon & Newsome, 1996), and is thought to facilitate motion pooling (excitatory connections) and motion opponency (inhibitory connections). The recurrent connections between MT units (MT-to-MT) revealed that units with similar directional tuning are more positively connected (**Fig. 3b**). These connections likely serve similar motion pooling and noise reduction

purposes as those between V1 and MT, and are analogous to lateral excitatory and suppressive synapses in the visual cortex (Li et al., 2014; Tan et al., 2011).

Recurrent connections were relatively balanced between excitation and inhibition (**Fig. 3c**), which is consistent with neurophysiology (for a review on the topic, see Zhou & Yu, 2018). In particular, the emergent connectivity was excitatory among units with similar motion direction preference and inhibitory among units tuned to dissimilar directions. Within the context of biological motion processing, this appears to be consistent with motion opponency mechanisms (Heeger et al., 1999)

**Figures 3d** and **3e** show the connections from recurrent units to the output layer responsible for estimating the x and y components of motion. As expected, we found that units tuned to horizontal movement contributed more to the x component output, while those tuned to vertical movement contributed more to the y component. While the V1-to-MT weights were stronger in MotionNet-R, the recurrent MT-to-MT connections were weaker. This may be a product of the increased adaptation in the MT units. Further, the increased connection strengths between the MT and output layer may reflect a compensatory effect within AdaptNet in response to the habituated (reduced) activity in the MT layer.

The emergent connections of the networks seem to mirror key motion processing aspects observed in biological visual areas V1 and MT. The alignment of the learned weights with neurophysiological connections in these areas supports the biological validity of the models.

***Adaptation effects on motion perception and network efficiency***. Having found evidence supporting the biological validity of the emergent properties within the networks, we next tested how the networks respond to a stimulus that would typically elicit the motion aftereffect. The stimulus was comprised of three stages: an initial (baseline) stationary stage, an intermediate moving stage to induce adaptation, and then a final stationary stage to test for adaptation induced motion aftereffects (**Fig. 4**). As expected, MotionNet-R responded to the moving stimulus with increasing estimates, then gradually returned to baseline when the stimulus returned to stationary. By contrast, AdaptNet exhibited an overshoot in motion estimation following the cessation of stimulus movement, predicting motion in the opposite direction, which is a hallmark of the waterfall illusion observed in biological vision (Mather & Harris, 1998). To understand the computational basis for this motion aftereffect, we assessed the activity of the MT units across the different stages of stimulus processing (**Fig. 4**,

top; the x output was studied in this case, the y output is similar, as shown in **Supplementary Fig. 1**). At first, before movement was initiated, MT units were responding equally in all directions, maintaining balanced baseline activity (**Fig. 4**, top-left). Once motion was initiated, units tuned to the motion direction increased their activity, while those tuned to other directions were suppressed (**Fig. 4**, top-middle). When the motion stopped, the adapted units recovered at different rates, leading to a temporary imbalance manifesting as the motion aftereffect (**Fig. 4**, top-right). The overshoot occurred for a range of input velocities (**Supplementary Fig. 2**). The mechanism underlying the motion aftereffect in the network aligns with previous hypotheses of the corresponding phenomenon in humans. Namely, that adaptation perturbs the balanced state of mutual suppression between motion-selective neurons, which leads to the illusory perception of motion in the opposite direction when the stimulus ceases (Grunewald & Lankheet, 1996; Kohn & Movshon, 2003). As can be seen in **Figure 4**, prolonged activation of a subpopulation of units preferring the stimulus motion direction leads to their activity being relatively lower than units tuned to other directions when the stimulus ceases to move.

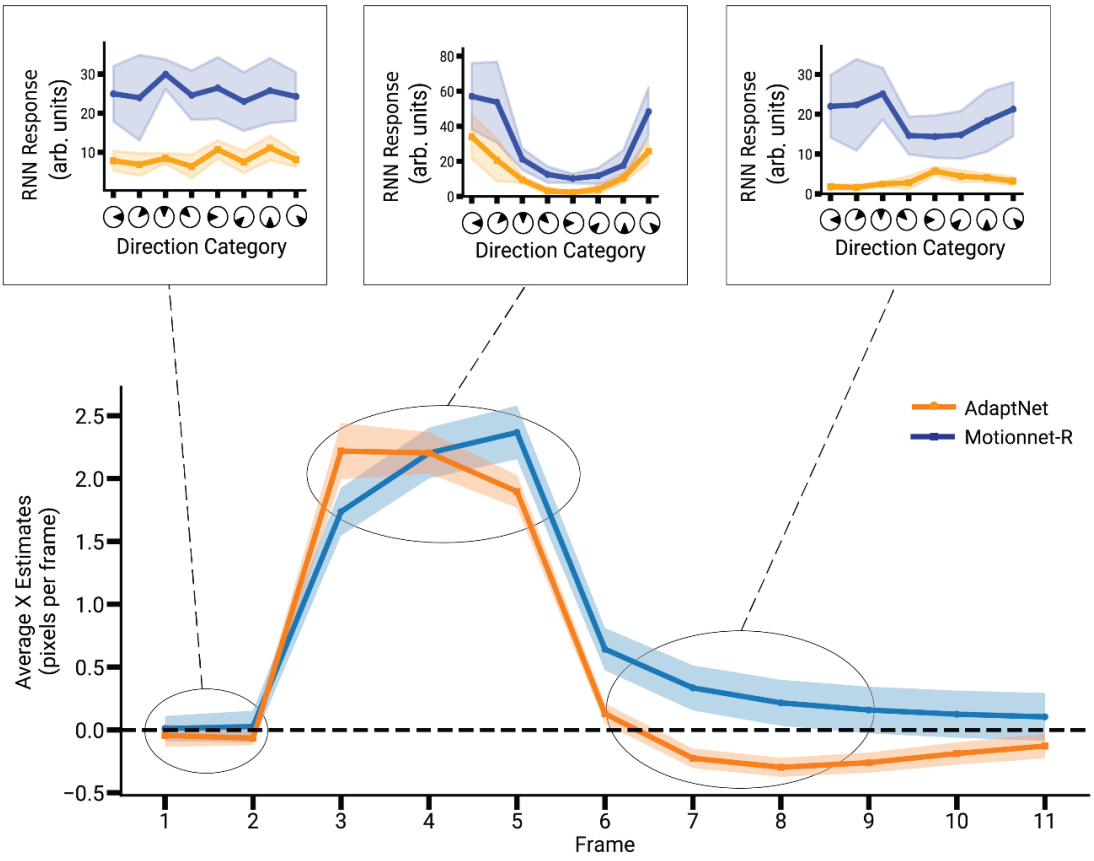


**Figure 4. Motion Aftereffect in AdaptNet**. Time course of the networks' responses to an image sequence consisting of a stationary stage (2 frames), followed by a moving stage (3 frames), and then a return to stationary (5 frames). The lower plot shows MotionNet-R and AdaptNet's motion estimation over time. The upper insets (showing RNN responses during frames 2, 4 and 7 representing the stationary, moving and final phases of the sequence respectively) show the average activity of MT units, binned according to their directional tuning, during different stages of the sequence. AdaptNet's response moving into the opposite (negative) illustrates the aftereffect displayed by this network. Shaded regions indicate ±SD across multiple networks.

This overshoot was consistent across a range of input velocities, indicating that the adaptation mechanisms in the network can account for the perception of illusory motion under various conditions (**Supplementary Fig. 2**). This result aligns with previous hypotheses that motion aftereffects result from the adaptation of motion-sensitive neurons, causing shifts in the perceived direction of motion when the stimulus changes or ceases (Grunewald & Lankheet, 1996; Kohn & Movshon, 2003). In particular, we found that adaptation perturbed the homeostatic state of mutual suppression between RNN units when exposed to a stationary input. As can be seen in Figure 4a, prolonged activation of a subpopulation of neurons preferring one direction reduced their activity after the stimulus was removed (which is most apparen immediately after motion cessation, where AdaptNet's response decreases to zero for

the previously active units, while in MotionNet-R there is no such activation reduction). During this refractory period, the previously active neural group fails to provide an equal and opposing response as it would, during stationary stimulus presentation, and hence there is a temporary shift in prediction that favors the opposite direction group. This temporary overshoot in motion estimation gives rise to the perception of the illusory waterfall effect.

Another notable difference between the responses of the MotionNet-R and AdaptNet is the latency with which they respond to the initiation of motion. As can be seen in **Figure 4**, AdaptNet reaches peak velocity estimation more quickly than MotionNet-R. AdaptNet's increased response speed may result from the reduced lateral suppression within the MT layer (passed from the previous time point). That is, the MT units tuned to the stimulus direction have less inertia to overcome at the onset of motion. To further investigate this phenomenon, we measured the average number of frames required by the MT units of each network to reach peak velocity estimation and found that AdaptNet consistently reached the peak 2-3 frames earlier than MotionNet-R, across a range of speeds (**Supplementary Fig. 3**).

Adaptation is thought to support healthy brain function by increasing sensitivity to changes in sensory input while reducing the otherwise high metabolic expenditure required for sustained cortical computation (Duong et al., 2023; Lennie, 2003). To test for this in our network, we compared the MSE between the actual and estimated motion, and the total MT layer activity, between AdaptNet and MotionNet-R in response to inputs with and without motion changes (**Figure 5a**). For image sequences of constant motion, AdaptNet's MSE was higher, reflecting reduced responsiveness to unchanging stimuli due to adaptation ($t_9$=-4.87, $p$=4.29e$^{-6}$). By contrast, for sequences with periodic motion changes, AdaptNet's MSE following each change was significantly lower than MotionNet-R, indicating better responsiveness in detecting change ($t_9$=10.09, $p$=8.45e$^{-24}$). This behavior is consistent with adaptive coding in sensory neurons, which prioritizes novel or changing stimuli to conserve metabolic resources and prevent saturation from constant stimuli (Fairhall et al., 2001). Further, AdaptNet showed significantly lower MT unit activity in both conditions (change: $t_9$=159.3 $p< 2.2\times10^{-16}$; constant: $t_9$=13.34, $p$=9.07e$^{-24}$; **Fig. 5a**, left), consistent with the hypothesis that adaptation enhances metabolic efficiency by reducing neuronal firing in response to prolonged or repeated stimulation (Ganguly et al., 2024;

Yi & Grill, 2019); **Fig. 5a**, left). This lower activity supports the hypothesis that adaptation enhances metabolic efficiency by reducing neuronal firing in response to prolonged or repeated stimulation (Ganguly et al., 2024; Yi & Grill, 2019). This reflects a real biological trade-off: adaptation conserves energy (lower firing over time) but can reduce fidelity for sustained stimuli. In nature, this is often acceptable because events that change are typically considered more ecologically relevant than those that remain the same (Tesileanu et al., 2022).

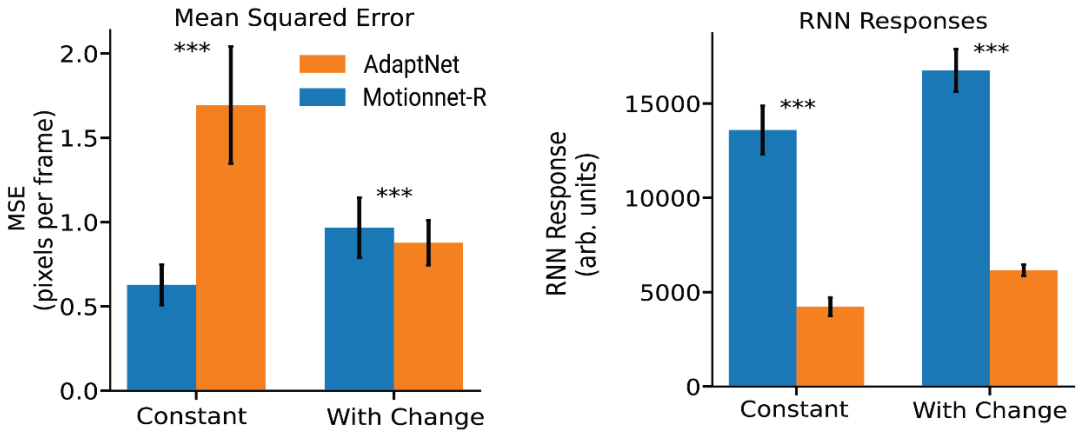


**Figure 5. Adaptation improves sensitivity to change and increases efficiency.** **a**) The mean squared error (MSE, left) and total MT layer activity (right) for MotionNet-R and AdaptNet for image sequences of constant motion (orange) and periodic motion changes (blue). Error bars indicate ±SD across multiple networks, and asterisks denote statistical significance ($p<.001$).

To further investigate the networks' sensitivity to constant and changing motion, we tested both with a dot-motion stimulus that moved in one velocity for nine frames, and then either remained the same or changed to a different velocity on the tenth frame. We recorded the direction of the networks' estimate for the final frame and compared this to the actual (ground truth) direction of the final velocity. Overall, we found that AdaptNet's estimates were closer to the actual velocity than those of MotionNet-R (**Fig. 6a**).

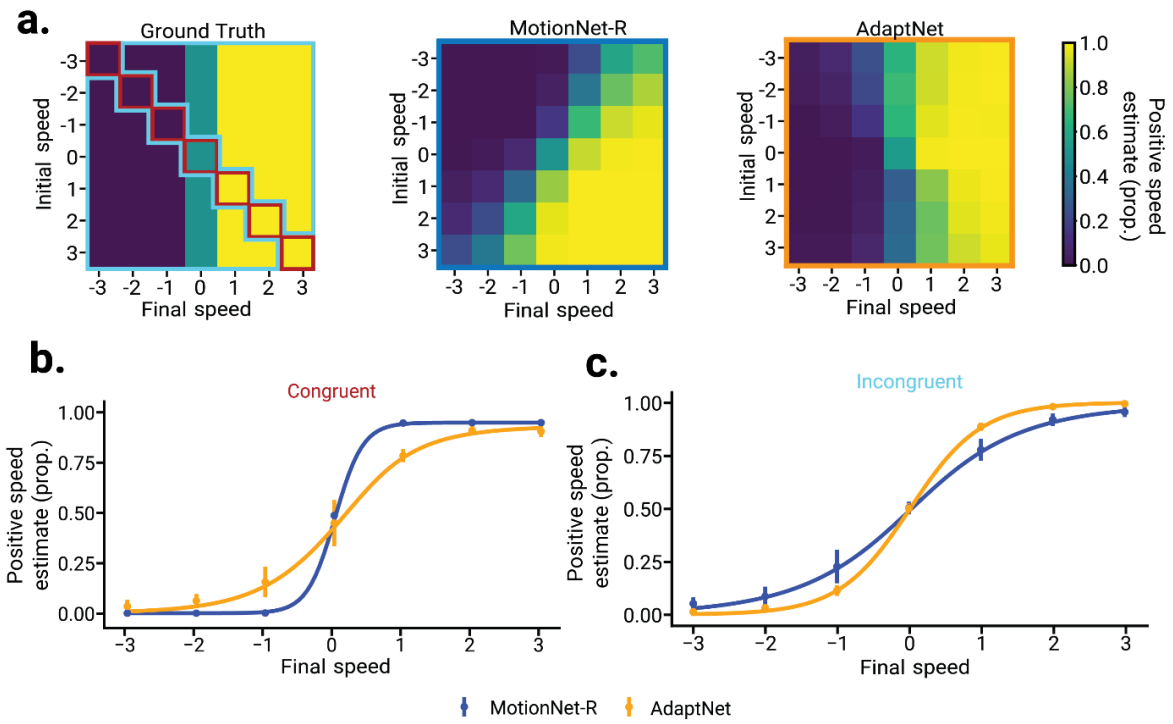


**Figure 6. Adaptation enhances sensitivity to change. a**) The proportion of positive velocity estimates along the (combined x and y) tested dimensions for each combination of initial (first nine frames) and final (tenth) frame speeds, for MotionNet-R (center) and AdaptNet (right); the ground truth (left) is displayed for reference. **b**) The same as (**a,** MotionNet-R & AdaptNet), but just for the (congruent) combinations of speeds along the diagonal (**a**, Ground truth, red bordered region). **c**) The same as (**a,** MotionNet-R & AdaptNet), but averaged across the remaining (incongruent) combinations of speeds (**a**, Ground truth, cyan bordered region). Sigmoid functions were fit to the data for both networks, and the steeper slopes indicate higher sensitivity. Error bars in (**b** & **c**) indicate ±SD across multiple networks.

We compared the sensitivity of each network to congruent and incongruent motion sequences by fitting their performance across final speeds with a sigmoid function (**Fig. 6b-c**). For the congruent condition, where the speed was constant across all frames, we found that MotionNet-R was more sensitive to speed (as indicated by the steeper slope; **Fig. 6b**). This is expected, because AdaptNet's accuracy reduces in response to constant stimuli. By contrast, for incongruent sequences, where the final speed changed, we found that AdaptNet was more sensitive (**Fig. 6c**). This increased sensitivity to change captures what is seen in biology across neural systems in different species, where adaptation is thought to amplify sensitivity to changes in the environment (Fairhall et al., 2001; Luczak & Kubo, 2022).

Neurons rapidly reset their adaptation when newly activated, suppressing previously adapted neurons, enhancing responsiveness to motion changes. Such improvement in response sensitivity supports the idea that incorporating adaptive mechanisms could introduce functional benefits in a neural network. Improved sensitivity to dynamic changes and increased processing efficiency have also previously been theorized to be the functional advantages of adaptation in biological systems. By capturing these key aspects of neural adaptation, AdaptNet offers a valuable model for exploring how adaptation shapes motion perception and neural computation.

## DISCUSSION

Here we trained two artificial neural networks, MotionNet-R and AdaptNet, to estimate motion from natural image sequences. Our primary aim was to investigate whether introducing adaptive mechanisms into motion processing networks would recapitulate phenomena associated with motion adaptation in biological neural networks and perception. Our results show that AdaptNet, but not MotionNet-R, exhibited the well-known perceptual phenomenon associated with motion adaptation, the MAE, and further provided a biologically explicit explanation for the effect. We then showed that AdaptNet was both more energy efficient and sensitive to changes in stimulus motion compared to the non-adaptive network (MotionNet-R).

The relevance of insights gleaned from ANNs into how biological neural networks operate is predicated on the correspondence between their functions. Thus, we began by validating the emergent properties of the ANNs with previously observed aspects of biological motion processing. We found similar hierarchical motion processing in the ANNs as observed in the visual cortex. In particular, the V1 units of both networks developed response properties that aligned with those of V1 neurons in macaque, such as the preference of V1 neurons for relatively lower speeds compared to MT neurons (DeAngelis et al., 1999; Hubel & Wiesel, 1962). The response of the units to plaid stimuli also varied considerably; while V1 units responded to individual components of the plaid grating, MT units responded to the pattern motion of the stimulus. This further validates the models' biological plausibility (Rideaux & Welchman, ; Zaharia et al., 2019) and reflects the role of MT in integrating local motion signals into a global percept (Maunsell & Van Essen, 1983; Perrone & Thiele, 2001).

We next tested our networks with stimuli that ceased moving after a period of constant motion, to compare their responses to those observed in psychophysical studies of motion adaptation (Mather & Harris, 1998). The adaptive network (AdaptNet) overshot the stationary (zero) motion estimate when the motion ceased, providing an estimate of motion in the opposite direction. This captures what is observed during psychophysical accounts of the phenomenon, suggesting that our network recapitulates a key aspect of adaptation. We then showed that the MAE in AdaptNet occurred because of a temporary reduction in the baseline activity of MT units, induced by prolonged exposure to a single motion direction, which perturbed the otherwise balanced mutual suppression between units tuned to different directions that

exists during exposure to static images. This mechanism has previously been hypothesized as the basis of the MAE (Allman et al., 1985; Barlow & Hill, 1963), and our findings provide empirical support for this account.

On analyzing the MT unit's responses during MAE, we also observed that AdaptNet showed a decreased latency in response to the onset of motion, compared to MotionNet-R. We investigated this further by measuring the number of frames required by each network to reach their peak output response following a change in the input motion and found that AdaptNet reached its peak 2-3 frames earlier than MotionNet-R. In particular, AdaptNet's response seemed to peak upon motion onset while MotionNet-R's response gradually increased over time. The former is consistent with rapid processing of changing input while the latter is more suited to integration of information over time. Our results may indicate that the degree to which biological neurons adapt may be related to their role as change detectors or temporal integrators.

Adaptation is thought to support healthy brain function by reducing the metabolic expenditure of processing sensory information (Kohn, 2007; Niven, 2016). Consistent with this, we found that AdaptNet used less energy to represent motion, both in V1 and MT, operationalized as reduced absolute unit activity within each layer. Efficiency is crucial in biological systems, where rapid and accurate sensory processing must be balanced with metabolic constraints (Lennie, 2003). The increased energy efficiency in AdaptNet came at the cost of reduced estimation accuracy for prolonged constant motion. However, we found that AdaptNet produced more accurate estimates in response to changes in motion. This improved accuracy was mirrored by a corresponding increase in sensitivity. These emergent properties support the notion that adaptation supports perception by increasing sensitivity to changes in sensory input (Fairhall et al., 2001; Rideaux et al., 2023; Wark et al., 2007).

This study addresses key gaps in the field of computational neuroscience. Previous models such as those by Simoncelli and Heeger (1998) and Rust et al. (2006), accounted for direction and speed tuning but did not incorporate adaptation. Accounting for this mechanism enabled us to provide a more realistic simulation that not only replicates the known tuning properties of motion processing neurons, but also captures the dynamic aspects of neural adaptation (Clifford & Wenderoth, 1999; Krekelberg et al., 2006).

The current study provides further insight into well-known perceptual phenomena (MAE), supports existing ecological explanations for adaptation, and

reveals a new potential benefit of this canonical neural feature (reduced latency). These findings extend the current understanding of motion processing and sensory adaptation, but they may also have important implications for artificial neural systems. That is, the increased sensitivity and reduced latency to motion changes in AdaptNet highlights the potential for adaptation mechanisms to improve the performance of artificial vision systems, particularly in dynamic environments where rapid detection of motion changes is desirable (Cox & Dean, 2014; Tan & van Dijken, 2023).

**Limitations**

We acknowledge some limitations of our study that should be considered. While AdaptNet successfully captured certain aspects of neural adaptation, the adaptation in our network was operationalized with a relatively simple mechanism. By design, this simplifies the complexity of adaptation in biological systems, such as the influence of neurotransmitters, ion channel dynamics, and modulatory inputs from other brain regions (Benda & Herz, 2003). Our study was conducted on a dataset of natural image sequences from the Berkeley Segmentation Dataset (Martin et al., 2001). While this provides a relatively naturalistic visual diet for our artificial systems, it does not capture all the variability present in real-world visual environments.

We did not compare the performance of AdaptNet with other existing motion processing networks because our networks were not designed to compete against computational benchmarks, rather, we sought to follow a biologically plausible training regime while constraining the network's size and complexity, in order to interrogate the properties that emerge. Further, we sought to study the isolated effects of adaptation. To this end we used MotionNet-R as a baseline network, as previous studies have validated the motion processing properties of similar architectures (Rideaux & Welchman, , 2021). This strategy allowed us to isolate the effect of adding adaptation to a relatively well-understood architecture.

**Future Work**

Future work could increase the biological plausibility of the network by using more realistic spiking models of neurons (Izhikevich, 2007). Extending the networks' input space to include more complex and varied stimuli like 3D motion could highlight other domains where adaptation influences sensory processing and perception (Idrees et al., 2024; Latimer et al., 2019; Rideaux et al., 2021).

With this study, we sought to demonstrate the role of adaptation mechanisms in motion processing systems. Incorporating adaptation into a motion processing network enabled us to replicate key biological phenomena that have been observed in the dorsal stream of the visual system. Further to this, we observed a higher energy efficiency and enhanced sensitivity to varying stimuli in a neural network with adaptation. These findings offer novel insights on the role of adaptation in motion processing and neural processing more broadly.

# From Spikes to Symptoms: Simulating SC-Driven Multisensory Deficits in Autism Spectrum Disorder

Vishnu Mohan[1] & Reuben Rideaux[1,2]

[1]School of Psychology, The University of Sydney, Camperdown, Australia

[2]Queensland Brain Institute, The University of Queensland, St Lucia, Australia

corresponding author: reuben.rideaux@sydney.edu.au

Acknowledgements: This work was supported by Australian Research Council (ARC) Discovery Early Career Researcher Awards awarded to RR (DE210100790) a National Health and Medical Research Council (NHMRC; Australia) Investigator Grant (2026318).

## ABSTRACT

Individuals with autism spectrum disorder (ASD) frequently exhibit altered multisensory integration, particularly enlarged temporal binding windows that impair speech perception and social communication. While various synaptic and cellular alterations have been implicated in ASD, the causal pathways linking these circuit-level perturbations to specific behavioural phenotypes remain elusive. To address this gap, we developed a biologically plausible spiking neural network of the superior colliculus, a key subcortical hub for audiovisual binding, incorporating realistic alpha-amino-3-hydroxy-5-methyl-4-isoxazolepropionic acid and N-methyl-D-aspartate (NMDA) receptor kinetics, γ-aminobutyric acid-mediated inhibition, and spike-timing-dependent plasticity. Through systematic parameter manipulation, we show that distinct neural alterations produce characteristic integration deficits: reduced neuronal adaptation uniformly expanded both spatial and temporal binding windows through sustained depolarization, whereas diminished feedforward inhibition contracted spatial windows while expanding temporal ones, indicating distinct roles for early inhibitory gating in space and time. Furthermore, NMDA conductance alterations bidirectionally modulated these windows, with hyperfunction generating permissive fusion and hypofunction curtailing integration. Each perturbation uniquely affected localization precision and multisensory benefit. Together, these results show how heterogeneous synaptic and cellular changes can converge on similar multisensory symptoms while leaving unique computational fingerprints. The framework yields testable predictions - linking, for example, restoration of adaptation or targeted augmentation of inhibitory control to normalization of binding - and suggests mechanism-specific avenues for intervention. By mapping synaptic alterations to measurable perceptual outcomes in a biologically grounded circuit, our work clarifies potential sources of phenotypic variability in autism and outlines principled targets for future experimental and translational work.

## INTRODUCTION

Our experience of the world is constructed from sensory inputs that are inherently partial and frequently ambiguous. To form coherent perceptions, the brain integrates multiple signals, each governed by distinct constraints. For example, determining the shape of a nearby object may involve combining various visual cues — such as perspective, shading, and texture — as well as inputs from other senses, like size information from both vision and touch (Ernst & Banks, 2002; Georgieva et al., 2008; Norman et al., 2003). This integration helps to resolve ambiguities and can lead to faster and more precise judgments (Hagmann & Russo, 2016).

The ubiquitous nature of multisensory integration in neural processing renders it particularly susceptible to the disruptive effects of neurodevelopmental disorders. One of the most prevalent and complex of these disorders, which is associated with multiple multisensory integration deficits, is autism spectrum disorder (ASD; Feldman et al., 2018). Population studies indicate that ~90% of autistic individuals report hyper- or hypo-reactivity across sensory modalities (Balasco et al., 2020). In particular, psychophysical work has shown that individuals with ASD have enlarged spatiotemporal binding windows (i.e., broadened spatial fusion zones and reduced precision in spatial localization) for audiovisual stimuli (de Boer-Schellekens, Eussen, et al., 2013; Foss-Feig et al., 2010). These sensory irregularities could potentially accumulate across modalities, leading to effects which could compound and affect higher level processing which could in turn impact daily functioning, making social environments overwhelming and leading to behaviours such as withdrawal or distress (Kawakami & Otsuka, 2021; Thye et al., 2018).

The superior colliculus (SC) is a brain area situated in the midbrain tectum, and has emerged as a key region for understanding multisensory integration deficits in ASD (Jure, 2019). The SC functions as a principal node for audiovisual integration, receiving convergent inputs from multiple sensory modalities (Benavidez et al., 2021). Within the SC, multisensory neurons receive congruent retinal and brainstem auditory afferents, aligning cross-modal inputs originating from common external events (Meredith & Stein, 1986). This part of the brain permits robust cross-modal enhancements of responses detectable by both human neuroimaging studies and animal electrophysiology (Calvert et al., 2001; Stein & Rowland, 2020). Notably, the neural responses of this part of the brain are maximal when the audiovisual events co-

occur during a narrow time window, providing a cellular correlate for the coincidence detection underlying multisensory binding (Meredith et al., 1987). The computational processes key to such temporal summation depends on a delicate balance between fast α-amino-3-hydroxy-5-methyl-4-isoxazolepropionic acid (AMPA) receptor-mediated excitation, slower N-methyl-D-aspartate (NMDA) receptor-mediated excitation, and γ-aminobutyric acid (GABA)ergic inhibition (Binns & Salt, 1994). Increasing developmental and clinical evidence supports the view that these integrative gains for such binding are attenuated by ASD, providing a robust case for a relationship between early dysfunction of the SC circuitry and the typical phenotypes of the senses evident by autism (Siemann et al., 2020).

Several lines of evidence implicate specific neural mechanisms of the SC in the sensory deficiencies of ASD, but these neural pathway perturbations need to be translated into measures of perception as a significant barrier. Deficits of multisensory integration characteristic of ASD correspond with disruptions of the SC, whereby audiovisual responses are invariably decreased both for autistic groups and mouse models of the disorder (Jure, 2019; Siemann et al., 2017). Postmortem, genomic, and pharmacological data demonstrate that altered NMDA expression, particularly GluN2B reductions, are associated with atypical audiovisual temporal and spatial binding windows (Bahry et al., 2021; Lee et al., 2024; Wallace & Stevenson, 2014). Electrophysiological research also uncovered decreased sensory adaptation and elevated excitation-inhibition (E/I) ratio of SC circuits, with each of these perturbations accompanying corresponding internal shifts in sensory processing capabilities (Rubenstein & Merzenich, 2003; Turi et al., 2016). Despite substantial associative evidence, direct causal pathways between specific circuit perturbations and sensory response alterations have not yet been established.

Traditional experimental methods face inherent limitations in establishing these causal mechanistic links (Wolff & Ölveczky, 2018). Single unit electrophysiology, psychophysics, and focal lesion studies have identified associations between neural activity and multisensory behaviour (Meredith & Stein, 1983; Stein & Stanford, 2008). But these approaches are not typically capable of establishing causality, as they sample only fragments of distributed circuits. In addition to this, it is experimentally challenging to vary synaptic parameters in living tissues (Reid et al., 2019; Wolff & Ölveczky, 2018). As a result, it would not be possible to use such methods to link alterations in spatiotemporal binding window metrics in ASD to specific collicular

mechanisms (Crosse et al., 2022). Computational models seek to overcome this limitation through controlled parameter sweeps that enable identification of causal links between circuit perturbations and behaviour (Jun et al., 2021), which produces hypotheses of SC function that can be tested experimentally.

Current computational models of multisensory integration have given us valuable theoretical advances while also uncovering critical methodological gaps which restrict them from being used for explaining ASD-related dysfunction on a level of neural circuits (Loosen et al., 2025; Stein et al., 2014). These approaches act at various levels of analysis, each of which yields unique advances but also significant gaps in understanding. At a statistical level, Bayesian causal inference models demonstrate how the brain optimally balances sensory evidence in order to decide whether signals arise from a common or from independent sources (Lerousseau et al., 2022); a computation that appears to be altered in ASD (Sapey-Triomphe et al., 2023). Still following a statistical approach but at a biophysically informed generative-modeling level, dynamic causal modelling uses fMRI data to estimate directed connectivity between brain regions during multisensory tasks, revealing how effective connectivity changes with stimulus conditions (Bouton et al., 2020). Meanwhile at the neural implementation level, neural networks such as MultiNet demonstrate how this causal inference arises from populations of neurons which have congruent and opposite tuning features, akin to those which exist for macaque MSTd cortex (Rideaux et al., 2021). While these models provide useful insights into multisensory integration, they typically omit explicit representations of receptor kinetics and other synapse specific dynamics (Barri et al., 2022; Stein et al., 2014), which limits their capacity to trace neurotransmitter level perturbations directly to behavioural observations (Barri et al., 2022; Gjorgjieva et al., 2016). Defining these mechanistic links is key to explaining how synaptic abnormalities in the SC cause the multisensory symptoms seen in ASD.

Biologically plausible spiking neural networks (SNNs) represent a promising approach to address these shortcomings by incorporating the detailed synaptic mechanisms that are missing from current models (Agnes & Vogels, 2024; Saponati & Vinck, 2023). SNNs can embed explicit AMPA and NMDA conductance dynamics, GABAergic inhibition, and spike-timing-dependent plasticity (STDP) at millisecond temporal resolution (Brunel & Wang, 2003; Maass et al., 2002; Wang, 1999). Detailed modelling of these biological features allow synapse-specific hypotheses about ASD-

related dysfunction to be tested computationally. Rate-coded SC models, such as those developed by Cuppini et al. (2011), have successfully reproduced key features of multisensory integration including superadditive audiovisual gain, demonstrating the potential explanatory power of network-based approaches with detailed spiking-level implementations. Large-scale integrate-and-fire reconstructions of SC circuitry have also confirmed that SNN architectures can accurately model the fundamentals of collicular circuits computationally (Alizadeh & Van Opstal, 2022). However, SNNs modelling multisensory integration processes in the SC have not yet been used to interrogate ASD-related circuit anomalies. This represents a clear opportunity to extend biologically grounded computational frameworks to test how NMDA receptor dysregulation, altered E/I balance, or other synaptic perturbations could reshape multisensory tuning properties in the SC and explain perceptual impairments associated with ASD.

Here we introduce a biologically constrained SNN model of the SC that allows NMDA conductance, E/I balance, and synaptic adaptation parameters to be independently manipulated and systematically varied. Through focused parameter sweeps, we show that specific changes in synaptic properties lead to evidence of multisensory integration difficulties similar to those seen in persons with ASD. By isolating these causal pathways under tightly controlled conditions, the model makes testable predictions regarding how unique circuit alterations may accumulate to generate the sensory processing differences present in ASD. By manipulating these causal mechanisms under tightly controlled conditions, the model makes predictions linking specific network perturbations to the disruptions in behaviour seen in autism.

## METHODS

***Network architecture.*** The SC integrates sensory information through a precise laminar organization, where unisensory inputs converge onto multisensory neurons through both direct excitatory and indirect inhibitory pathways (Gehr et al., 2023; May, 2006; Stein et al., 2014). To capture these fundamental organizational principles, we constructed an SNN comprising four interconnected layers that mirror the SC's functional architecture. The auditory (A) and visual (V) input layers each contained 180 excitatory neurons representing azimuthal space from 0° to 179°, reflecting the topographic maps observed in the superficial and intermediate SC layers (Ito & Feldheim, 2018). These unisensory representations projected to both a multisensory integration excitatory layer (180 neurons) and a multisensory integration inhibitory layer (54 neurons), with the 30% inhibitory proportion matching the typical density of interneuron cells found in mammalian neural circuits (Essig et al., 2021; Feldmeyer, 2012).

To model the individual neurons' spiking behaviour, we used the Izhikevich neuron, which couples a quadratic membrane equation with a recovery variable and an after-spike reset to reproduce the spiking patterns observed in SC recordings, while maintaining ease of computation for large-scale simulations (Izhikevich, 2003). The state equations of the neuron model are

$$\frac{dv}{dt} = 0.04v^2 + 5v + 140 - u + I(t),$$

$$\frac{du}{dt} = a(bv - u),$$

with the spike/reset condition

$$v \geq 30\text{mV} \Rightarrow \{\, v \leftarrow c,\ u \leftarrow u + d \,\}$$

where $v$ is membrane potential, $u$ is a recovery variable and $I(t)$ denotes the net synaptic input current at time $t$. In this formulation, $a$ sets the time scale of recovery (smaller $a \rightarrow$ slower adaptation), $b$ controls how strongly $u$ couples to $v$ (restorative feedback near rest), $c$ is the post-spike reset potential, and $d$ is the after-spike increment to the recovery variable. An added advantage of the Izhikevich model was that we could switch between several neuron behavioural modes by controlling a few key parameters. For example, regular-spiking dynamics ($a$ =0.02, $b$=0.2, $c$ =-65, $d$ =8) captured the sustained firing patterns of excitatory projection neurons, while fast-spiking parameters ($a$ =0.1, $b$=0.2, $c$ =-65, $d$ =2) reproduced the rapid, non-adapting

responses characteristic of inhibitory interneurons that mediate feedforward inhibition in the SC. This distinction proved to be important for establishing the timing relationships between excitation and inhibition that underlie multisensory integration windows (Gingras et al., 2009).

The network operated at millisecond resolution (dt = 0.1 ms) with 100 sub-steps per frame (each frame was 10 ms long), as this level of temporal detail enables fine-scale coincidence detection that distinguishes true multisensory events from false correlations (Wu et al., 2025; Zenke & Gerstner, 2014). This high temporal resolution also allowed synaptic current computations to evolve realistically and enabled STDP mechanisms to shape connectivity based on the correct temporal relationships between pre- and postsynaptic activity (Shouval et al., 2010).

***Training protocol and stimulus generation.*** The networks we trained acquired topographically aligned multisensory representations, through exposure to naturalistic stimulus statistics during an 80-epoch unsupervised training phase. Each epoch comprised 1,000 synthetic audiovisual sequences and each lasted 20 frames (200 ms). Each sequence consisted of events spanning 50 ms, and event locations were represented by Gaussian waveforms which occurred at random azimuthal locations with probabilities that were pre-set: 60% bimodal (spatially congruent audiovisual), 20% audio-only, and 20% visual-only, reflecting the predominance of multisensory events in natural environments while ensuring robust unisensory responses (De Gelder & Bertelson, 2003; Stevenson, Ghose, et al., 2014). A maximum of two events could occur simultaneously.

To make sure the network could tolerate minor deviations in spatial alignment, during each bimodal event the auditory and visual components were independently jittered with 60% probability by a small lateral offset drawn uniformly from ±3°, such that either modality (or both) could be displaced while the other remained aligned. Before entering the unisensory A and V layers, each event profile was converted into a population of Poisson-distributed spikes (0–300 Hz, 10 ms bins), providing physiologically realistic spiking input for synaptic plasticity (Thieu & Melnik, 2025). Input intensities varied logarithmically between 0.4 and 1.0 to encourage contrast-invariant responses, and Gaussian spatial profiles were corrupted with additive zero-mean Gaussian noise ($\sigma$ = 0.02, applied independently to every neuron

and frame in both modalities) to simulate sensory uncertainty and avoid overfitting to noise-free inputs (Faisal et al., 2008; Hasinoff, 2014).

The network's operating regime required careful calibration to balance sensitivity against saturation. By trial and error, we identified an input scaling factor that elicited approximately ten multisensory spikes in response to a single unimodal pulse over a second, a level that permitted robust responses without ceiling effects. Feedforward inhibitory gain was set to match a physiologically accurate excitation/inhibition balance that supported both reliable detection and dynamic range for multisensory enhancement (Bhatia et al., 2019).

***Synaptic dynamics and receptor dynamics.*** Multisensory integration in the SC depends on the interactions between fast and slow excitatory currents that create temporal windows for coincidence detection (Binns & Salt, 1996; Meredith et al., 1987). To simulate such time-varying dynamics, we modelled dual-component excitatory synapses into our network, with physiologically constrained AMPA and NMDA conductances. AMPA receptors are responsible for fast synaptic transmission with a 2.5 ms decay constant, which gives them the precision needed to detect simultaneous events. In contrast, NMDA receptors exhibit slower kinetics with decay constants set to 80 ms, which leads to extended temporal activity, over which events farther apart in time could summate.

The NMDA conductance incorporated a voltage-dependent $Mg^{2+}$ block, a key nonlinearity that makes these receptors function as coincidence detectors at the molecular level:

$$I_{NMDA} = g_{NMDA} m_{NMDA} \left( \frac{E_{NMDA} - V}{1 + e^{-0.062 * (V + 35)}} \right)$$

where $g_{NMDA}$ is the maximal synaptic conductance, $m_{NMDA}$ is the fraction of receptors with ligand-gated channels open, $V$ is the postsynaptic membrane potential, $1 + e^{-0.062 * (V + 35)}$ is the voltage-dependent $Mg^{2+}$-block relief factor, and $E_{NMDA}$ ($\approx$ 0 mV) is the reversal potential driving the current. This formulation meant that NMDA receptors contributed minimal current at resting potentials but as neurons depolarized, these receptors became more active, which then created a positive feedback mechanism that amplified responses to coincident inputs (Trpevski et al., 2023; Zoicas & Kornhuber, 2019). The half-activation voltage of -35 mV and steepness factor of 0.062 $mV^{-1}$ matched measurements recorded from SC neurons.

The AMPA synapses were also modelled to display synaptic depression, following delayed relative firing of the pre- neurons. Short-term synaptic depression on AMPA-mediated connections followed the Tsodyks-Markram formula:

$$\frac{dR}{dt} = \frac{1 - R}{\tau_{rec}} - \mathrm{U}\, R\, \delta_{(t - t_{spike})}$$

where $R$ represents the fraction of available synaptic resources, $\tau_{rec}$ = 400 ms is the recovery time constant, $U$ = 0.7 is the utilization parameter determining the fraction of resources consumed per spike, and $\delta_{(t-t_{spike})}$ represents spike times. This activity-dependent attenuation prevents response saturation during sustained stimulation as is observed in SC neurons (Lee et al., 2020). This depression manifested as the sensory adaptation displayed by neurons in the multisensory layer.

To prevent runaway excitation and establish competitive dynamics between spatial locations, we implemented three distinct inhibitory mechanisms to modulate the main excitatory pathways in our network. Feedforward inhibition from unisensory layers to multisensory neurons arrived with controlled delays, narrowing the temporal window of integration (Kardamakis et al., 2016). Recurrent inhibition from the multisensory inhibitory population provided divisive gain control, which normalized responses across stimulus intensities (Mahajan & Mysore, 2022; Ohshiro et al., 2011). Within the multisensory excitatory layer, lateral inhibition was designed with a Mexican-hat pattern with local excitation (radius of four neurons) and surround suppression, which sharpened spatial tuning through competitive interactions (Cuppini et al., 2011). We designed this multi-scale inhibitory architecture to reproduce the centre-surround receptive fields characteristic of SC multisensory neurons.

***Connectivity and topographic organisation.*** The SC plays a key role in the alignment of auditory and visual spatial maps even though they come from different topographic origins, which represents a fundamental goal of multisensory integration (King et al., 1988). We attempted to model this ability through structured connectivity patterns that promoted map alignment while allowing for flexibility during learning (Cuppini et al., 2011). The initial feedforward connections from unisensory to multisensory layers followed Gaussian spatial profiles centred on corresponding topographic positions (Ottes et al., 1986), providing a coarse scaffold for integration:

$$W_{ij} = A\, e^{\left[-\frac{(i-j)^2}{2\sigma^2}\right]}$$

where $W_{ij}$ represents the connection strength from neuron $j$ in the unisensory layer to neuron $i$ in the multisensory layer, $A$ is the peak amplitude, and $\sigma$ = 5 neurons determine the neural radius of connectivity. These feedforward connections were present for both AMPA and NMDA synapses and remained plastic, allowing learning experience to shape the alignment between modalities.

To maintain Dale's principle while enabling gradient-based learning, we employed a soft-plus reparameterization for excitatory weights that ensured the network's weights would stay non-negative while maintaining the differentiability needed for learning (Wiemann et al., 2024).

$$W = ln\left(1 + e^{\theta}\right) - ln(2)$$

This formulation allowed for stable STDP-driven organization of topographic maps.

Neurophysiological studies demonstrate that auditory and visual information arrive at SC neurons with characteristic delays reflecting subcortical processing times (Keetels & Vroomen, 2012). We incorporated these timing differences through pathway-specific conduction delays: auditory signals were delayed by 10 ms and visual signals by 26 ms relative to multisensory neurons. These delays, derived from *in vivo* measurements of SC response latencies, created realistic temporal relationships between converging inputs and enabled the network to learn appropriate integration windows through STDP mechanisms (King, 2004).

***Learning rules and homeostatic mechanisms.*** The development of aligned multisensory maps in the SC involves interactions between Hebbian plasticity, which strengthens correlated inputs, and homeostatic mechanisms that maintain stable firing rates and prevent pathological synchrony (Wu et al., 2020). We implemented this learning structure through multiple plasticity rules operating at distinct timescales (Daoudal & Debanne, 2003; Wu et al., 2020).

STDP learning shaped feedforward connections based on the temporal relationship between pre- and postsynaptic spikes (Vogels et al., 2013):

$$\Delta W = A_{stp}\, e^{-\frac{\Delta t}{\tau_{stp}}}, \quad \Delta t > 0$$

$$\Delta W = -A_{std}\, e^{\frac{\Delta t}{\tau_{std}}}, \quad \Delta t < 0$$

where $\Delta W$ is the weight change, $\Delta t$ is the spike timing difference, $A_{stp} = A_{std}$ = 1.0 are the maximum potentiation and depression amplitudes, and $\tau_{stp} = \tau_{std}$ = 20 ms are the time constants determining the temporal window for plasticity. When presynaptic

spikes preceded postsynaptic firing, synapses potentiated, which then stremgthened inputs that reliably drove postsynaptic responses (Zannone et al., 2018). Conversely, a reversal in these dynamics led to depression, which would further eliminate connections that failed to contribute to output generation. Learning rates of 0.02 for unisensory pathways were chosen to balance rapid map formation against stability. Multisensory connections adapted more slowly to preserve established topography.

Recognising that NMDA receptors carry a larger fraction of charge than AMPA receptors at mature SC synapses, we maintained an AMPA:NMDA weight ratio of 1: 3 throughout training (Zhao et al., 2014). After every STDP update, the summed synaptic strength of each unisensory to multisensory row was renormalised so that 25% of the weight resided in the fast AMPA component and 75% in the slow NMDA component, ensuring physiologically realistic but NMDA-dominated transmission while still allowing activity-dependent refinement of both receptors.

Unconstrained Hebbian plasticity has previously been shown to lead to instability through positive feedback loops (Wu et al., 2020). To counter such instability, we incorporated three homeostatic mechanisms operating at complementary timescales (Zenke et al., 2017). Fast Oja-type normalization, applied every external frame, maintained constant L2 norms for each neuron's afferent weight vector, implementing a form of hetero-synaptic competition (Witten et al., 2008). Medium-timescale inhibitory plasticity followed the Vogels-Abbott rule:

$$\Delta W_{inh} = \eta_i \left(\rho_{post} - \rho_{target}\right) s_{pre}$$

where $\Delta W_{inh}$ is the inhibitory weight change, $\eta_i$ = 0.01 is the learning rate, $\rho_{post}$ is the postsynaptic firing rate, $\rho_{target}$ = 5 Hz is the target firing rate, and $s_{pre}$ indicates presynaptic spikes. This homeostatic inhibition prevented runaway excitation while preserving stimulus selectivity. Finally, slow multiplicative scaling operated every 100 ms, gently nudging all synaptic weights toward a mean of 0.006 through soft rescaling (Wu et al., 2020). This three-faced homeostatic system reproduced the remarkable stability of SC responses despite ongoing plasticity.

***Autism spectrum disorder model implementation.*** Converging evidence implicates specific synaptic alterations in the sensory processing differences observed in ASD (Chen et al., 2020; Robertson & Baron-Cohen, 2017; Siemann et al., 2017). We instantiated these findings through targeted parameter modifications that preserved overall network architecture while selectively altering synaptic transmission properties.

NMDA conductance was reduced by 60% (from 0.05 to 0.02 normalized units), directly modelling the decreased NMDA receptor expression (Gandal et al., 2012), particularly of GluN2B subunits, reported in postmortem studies of autistic individuals. We then modelled for NMDA hyper-expression, by setting the NMDA conductance at 0.15, which is a threefold increase from the training baseline (Marotta et al., 2020). These alterations affected the slow integrative component of excitatory transmission without affecting fast AMPA-mediated responses.

In addition to synaptic mechanisms, alterations in network and neuronal dynamics have also been implicated in ASD pathology. One such observation frequently linked to differences in responses is altered E/I balance. We attempted to replicate the elevated E/I balance observed in ASD by proportionally reducing inhibitory tone, by reducing feedforward inhibition by 50% (Manyukhina et al., 2022). These changes weakened the competitive dynamics that normally sharpen spatial tuning and temporal precision.

Behavioural differences in ASD have also been linked to decreases in sensory adaptation (Lawson et al., 2015). To investigate the extent of change in responses induced by such a decrease, we reduced the neuronal sensory adaptation exhibited by the multisensory units. We did this by altering the Izhikevich variables of the neurons corresponding to recovery and reset. This combination of altered NMDA conductance, decreased inhibition, and lower sensory adaptation created a coherent model of ASD-related synaptic dysfunction grounded in empirical observations.

**Behavioural Assays**

***Temporal binding window.*** The temporal window over which the brain integrates multisensory information provides a fundamental measure of integration capacity (Marsicano et al., 2022). We quantified this window using a psychophysical fusion probability approach, systematically varying audiovisual onset asynchronies from -500 to +500 ms in 10 ms increments, where negative values indicated visual-leading and positive values indicated auditory-leading stimuli. For each offset, we presented five-frame (50 ms) stimulus pulses at 90° azimuth and recorded the integrated multisensory population response over a 100 ms window following the later stimulus onset. This integration period captured both immediate responses and NMDA-mediated sustained activity that bridges temporal gaps between inputs.

To derive fusion probabilities from neural responses, we transformed the integrated spike counts using a percentile-based normalization that preserved peak

structure while mapping responses to a 0-1 probability scale. Specifically, we computed baseline and peak responses using the 10th and 90th percentiles respectively, then applied a soft-clipping transformation to maintain relative differences at high response levels. The resulting fusion probability curve was fit with a Gaussian function, and the temporal binding window was defined as the range of asynchronies maintaining fusion probability above 50%. This metric directly relates to psychophysical measurements of perceived simultaneity in human subjects, where individuals with ASD consistently show broader temporal windows indicating less precise coincidence detection (Vogel et al., 2022).

***Spatial binding window (SBW).*** While temporal alignment provides one binding cue, spatial congruence offers another critical constraint on multisensory integration. We assessed the network's spatial binding characteristics by presenting simultaneous audiovisual stimuli with systematically varied spatial disparities ranging from 0° to 80°. For each disparity level, we ran multiple trials with randomized absolute locations while maintaining the specified angular separation. The network's multisensory response pattern was analysed to determine whether it exhibited a single unified peak (indicating perceptual fusion) or multiple distinct peaks (indicating segregated processing).

We employed automated peak detection with Gaussian smoothing ($\sigma = 2$ neurons) to identify response maxima. A response was classified as "fused" if it contained a single peak above 20% of maximum amplitude, or if multiple peaks existed but the valley between them exceeded 60% of the lower peak height — indicating insufficient separation for independent representation. The proportion of fused responses across trials yielded a fusion probability curve as a function of spatial disparity. This curve was fit with a pedestal function to extract the spatial binding window width, defined as the disparity range maintaining 50% fusion probability. This measure captures the spatial principle of multisensory integration and its disruption in ASD, where enlarged spatial windows reflect reduced selectivity to spatial congruence.

***Multisensory localization sensitivity.*** Multisensory integration should enhance perceptual sensitivity beyond what unisensory performance typically is, with the magnitude of enhancement depending on the relative reliability of each modality. We accounted for localization sensitivity by measuring the precision of spatial discrimination under audio-only, visual-only, and bimodal conditions. For each

modality configuration, we generated sequences of 10-frame stimulus events at multiple azimuthal locations (5 trials per location) with fixed intensity (0.8) and added sensory noise (σ = 0.1).

Following each stimulus presentation, we decoded the perceived location using center-of-mass analysis of the multisensory population response. The signed localization error — the difference between decoded and true location — was computed for each trial. From the distribution of these errors, we calculated sensitivity as the inverse of the standard deviation:

$$\text{sensitivity} = \frac{1}{\sigma_{error}}$$

where $\sigma_{error}$ represents the standard deviation of localization errors in degrees. Higher sensitivity values indicate more precise localization. We computed three sensitivity measures: $s_A$ (auditory), $s_V$ (visual), and $s_B$ (bimodal). The multisensory enhancement of sensitivity was then quantified by comparing multisensory performance against the better unisensory modality. This measure revealed whether the network achieved optimal integration and whether this enhancement was preserved or diminished in the ASD model.

***Cue reliability weighting.*** Optimal multisensory integration requires weighting sensory inputs according to their reliability — a computation fundamental to Bayesian theories of perception. We tested whether the network learned statistically optimal cue combination by independently manipulating the spatial uncertainty of auditory and visual inputs. Stimulus reliability was controlled by varying the spatial spread (σ) of Gaussian input profiles from 2° to 20° in 2° increments, with larger spreads representing less reliable spatial information.

For each combination of auditory and visual reliabilities, we presented spatially disparate stimuli with auditory input centered at 80° and visual input at 100° azimuth. To maintain equal total input despite varying spatial spreads, we applied gain normalization proportional to

$$\frac{\sigma_{ref}}{\sigma}$$

where $\sigma_{ref}$ = 2° was the reference width. After 10 frames of stimulation, we decoded the perceived location from the integrated multisensory response and computed the visual weight as:

$$w_V = \frac{\text{decoded\_location} - 80^\circ}{100^\circ - 80^\circ}$$

This weight represents the relative influence of visual information on the final percept, ranging from 0 (purely auditory) to 1 (purely visual). According to maximum likelihood estimation theory, the optimal visual weight should equal:

$$w_V^* = \frac{\sigma_A^2}{\sigma_A^2 + \sigma_V^2}$$

We compared empirically observed weights against these theoretical predictions across the full reliability matrix. The network's adherence to optimal cue combination was quantified through the mean absolute deviation between observed and predicted weights, as well as correlation analysis. This test revealed whether unsupervised learning through STDP could discover statistically optimal integration rules without explicit training on reliability-weighted tasks.

***Inverse effectiveness.*** The principle of inverse effectiveness, whereby multisensory enhancement is greatest when unisensory responses are weakest, represents a fundamental computation that optimizes information gain under uncertainty. We quantified this phenomenon by measuring spatial localization performance under audio-only, visual-only, and bimodal conditions across six logarithmically spaced stimulus intensities (0.05 to 1.6 arbitrary units). For each intensity and modality combination, we presented 10-frame stimulus pulses at 90° azimuth and recorded the integrated multisensory spike count over 20 frames.

The multisensory enhancement index (MEI) was computed as:

$$\text{MEI} = \frac{R_{AV} - \max(R_A, R_V)}{\max(R_A, R_V)}$$

where $R_{AV}$ represents the multisensory response and $\max(R_A, R_V)$ represents the stronger unisensory response at each intensity. By plotting MEI against stimulus intensity on a logarithmic scale, we assessed whether the network exhibited the characteristic negative relationship indicative of inverse effectiveness. This nonlinear relationship would indicate that multisensory integration provides maximal benefit when sensory signals are weakest and most ambiguous, precisely when enhanced detection would be most behaviourally advantageous.

***Distance-dependent noise correlations.*** We quantified the spatial scale of shared trial-to-trial variability by computing pairwise spike-count noise correlations between multisensory neurons and binning them by separation along the azimuthal map. For

each trained model, we ran repeated, identical bimodal (simultaneous A+V) trials at a fixed location and accumulated per-trial multisensory spike counts over the stimulus sequence. Counts were z-scored across trials for each neuron and noise correlation was defined as the Pearson correlation coefficient of the resulting per-trial spike counts for each neuron pair, a standard measure for $r_{sc}$ (i.e., spike-count correlation). Neuron positions were mapped to azimuth on a 0–180° ring; pairwise separation was the minimal circular distance $d = min(|\Delta|, 180 - |\Delta|)$ restricted to unique distances $d \in [0, 90°]$.

To prevent inflation of the near-zero bin by self-pairs and clone-like receptive fields, we excluded all pairs with $d$ lesser than one neuron pitch (degrees per neuron). Remaining pairs were grouped into 1-pitch bins using half-open edges $(a, b]$, beginning at 1×pitch, and we computed the mean correlation within each bin. This produced a per-model curve that was then aggregated across $n = 10$ independently trained networks to obtain the pooled mean ± SEM at each distance; for visualization only, the pooled trace was lightly smoothed with a Gaussian kernel ($\sigma$ = 1.2 bins) using reflect boundaries to avoid edge artifacts.

***Response latency analysis.*** Multisensory integration in the SC not only enhances response magnitude but also accelerates reaction times, a phenomenon critical for rapid orienting behaviours. We measured first-spike latencies by presenting 10-frame stimulus pulses under audio-only, visual-only, and bimodal conditions, then detecting the first multisensory spike that exceeded baseline activity. The network was run for 40 frames total to ensure capture of delayed responses, with latency recorded as the time from stimulus onset to first spike in milliseconds.

For each network, we computed the mean unisensory latency (averaging audio and visual conditions) and compared it to the multisensory latency. The latency reduction

$$\Delta\text{latency} = \frac{L_A + L_V}{2} - L_B$$

quantified the temporal advantage conferred by multisensory integration. This measure allowed us to compare our latency measurements to behavioural studies showing reduced multisensory facilitation of reaction times in individuals with ASD, potentially reflecting weakened temporal summation mechanisms.

## RESULTS

***Model validation and characterisation*.** We developed a two-layer SNN to investigate how synaptic alterations affect multisensory processing in the SC. The architecture incorporated separate auditory and visual input layers that projected to a multisensory integration layer through both excitatory and inhibitory pathways (**Fig. 1a**). Following 80 epochs of unsupervised training with pre-set stimulus statistics (60% bimodal, 20% audio-only, 20% visual-only events), we measured the ratio of inhibitory to excitatory currents in response to centered bimodal stimuli. The network maintained an E/I ratio of 0.98 ± 0.04 across ten independent instantiations (**Fig. 1b**), consistent with the approximately 1:1 balance documented in cortical and subcortical circuits. This balance emerged despite implementing a 30% proportion of inhibitory neurons and three distinct inhibitory mechanisms (feedforward, recurrent, and lateral), suggesting that STDP mechanisms successfully regulated synaptic weights to prevent unstable dynamics.

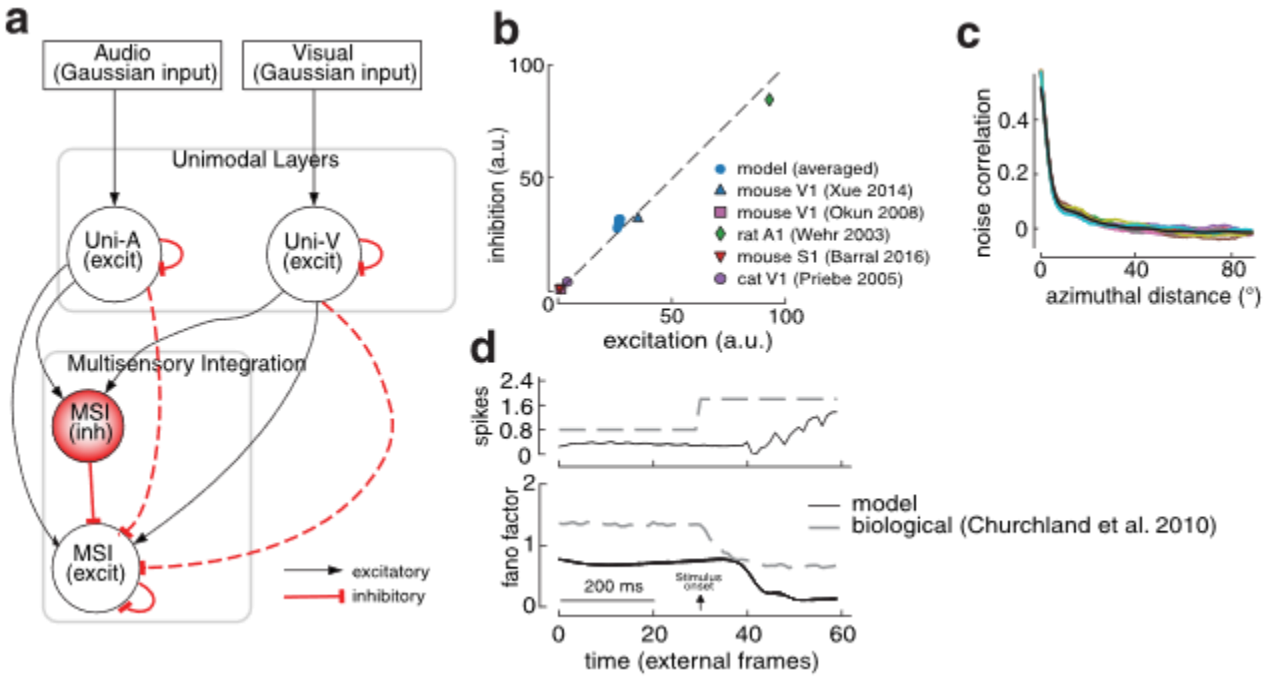


**Figure 1. Network architecture and validation of key physiological properties.** **a**) Two-layer spiking neural network with auditory and visual input layers projecting to multisensory (MSI) layers through excitatory (black) and inhibitory (red) connections. **b**) Excitation-inhibition balance comparing model results (blue circle, averaged across instantiations) to biological measurements from various cortical regions and species; dashed line indicates 1:1 ratio. **c**) Spike-count noise correlation as a function of azimuthal distance between neuron pairs in the multisensory layer. **d**) Fano factor dynamics showing spike count variability (top) and fano factor (bottom) following stimulus onset; black line shows model, gray dashed line shows biological reference data from Churchland et al. (2010).

To validate the mesoscale coupling in the multisensory layer, we quantified spike-count "noise" correlations ($r_{sc}$) across repeated presentations of identical stimuli

and binned neuron pairs by their separation on the azimuth map (0–80°). Correlations were strongest for nearby pairs and declined monotonically with azimuthal distance, approaching near-zero at large separations (**Fig. 1c**). This spatial fall-off is the expected footprint of local shared input in sensory populations and mirrors well-established distance-dependence of correlated variability in primate cortex and, specifically for SC, the observation that $r_{sc}$ depends on pairwise proximity and functional class. Together with the near-balanced E/I ratio, this shows the trained network learns realistic local coupling without imposing spurious long-range common noise.

We examined trial-to-trial variability by computing the Fano factor (variance/mean) of spike counts in 10 ms bins. During spontaneous activity, the network exhibited a Fano factor of 0.73 ± 0.05, which decreased to 0.21 ± 0.03 within 100 ms following stimulus presentation (**Fig. 1d**). This reduction occurred concurrently with an increase in mean firing rate from 0.4 to 1.6 spikes per bin. The temporal dynamics and trend of this variability reduction paralleled recordings from macaque middle temporal (MT) cortex, where Fano factors decrease from ~1.5 to ~0.7 following motion stimulus onset. The observed variability suppression likely resulted from stimulus driven engagement of inhibitory circuits that reduced ongoing fluctuations while preserving evoked responses, a mechanism that could potentially be disrupted by alterations in EI balance.

***Emergent multisensory integration properties.*** Having established that the network maintained balanced E/I and correlated noise activity, we next examined whether it reproduced characteristic signatures of multisensory integration observed in SC neurons and psychophysical studies. We evaluated five fundamental properties: enhanced localization sensitivity, spatial and temporal binding windows, optimal cue weighting, accelerated response latencies, and inverse effectiveness

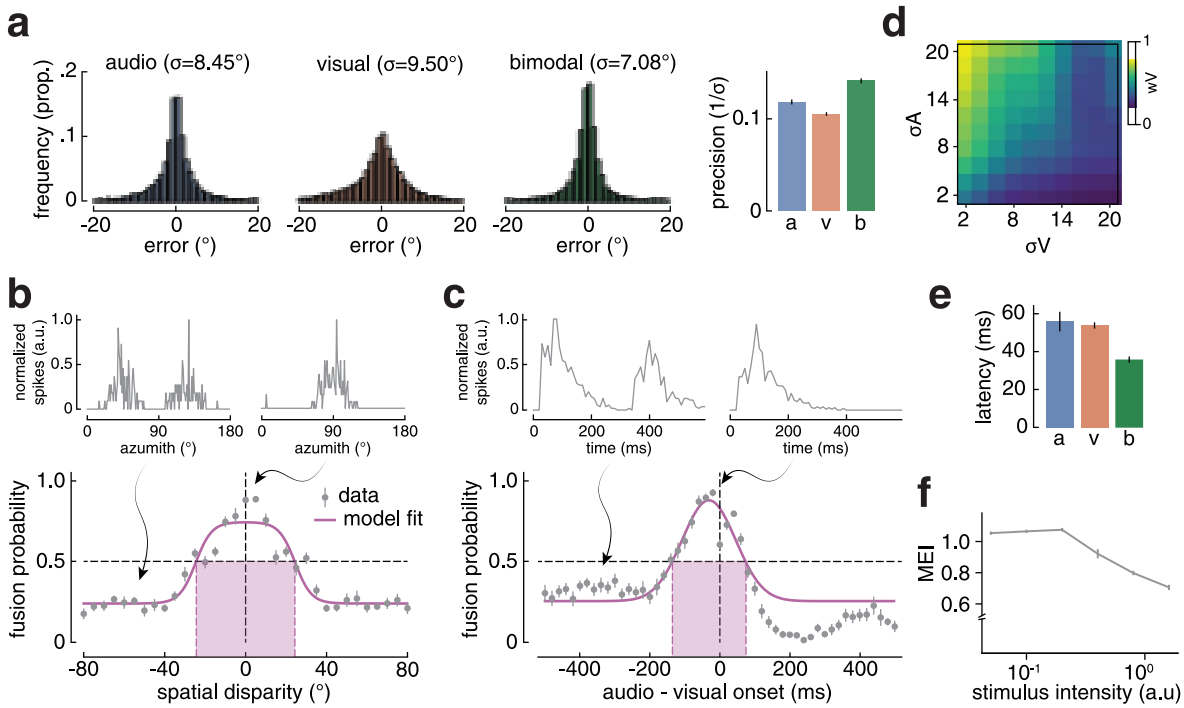


**Figure 2. Multisensory integration properties in the trained network.** **a**) Frequency distributions of signed localization errors for auditory (σ=8.47°), visual (σ=9.59°), and bimodal (σ=7.08°) stimulus conditions (left histograms) with corresponding mean precision values (1/σ) averaged across ten network instantiations (right bar plot). **b**) Spatial binding window analysis. Upper panel: example multisensory population spike activity across azimuthal positions (0-180°) showing fused and segregated responses at different audiovisual spatial disparities. Lower panel: Fusion probability as a function of spatial disparity between audiovisual stimuli, with shaded region indicating the binding window where fusion exceeds 50%. **c**) Temporal binding window analysis. Upper panel: multisensory population spike activity over time showing responses to temporally aligned and asynchronous audiovisual stimuli. Lower panel: Fusion probability as a function of audiovisual onset asynchrony (negative values: visual-leading, positive: auditory-leading), with shaded region marking the temporal binding window. **d**) Heat map displaying visual weight (wV) in multisensory localization as a function of auditory (σA) and visual (σV) stimulus reliability, where larger σ values represent less reliable spatial information. **e**) Mean first-spike latencies for auditory, visual, and bimodal stimulus conditions. **f**) Multisensory enhancement index (MEI) plotted against stimulus intensity on a logarithmic scale. Error bars indicate ±SEM across ten independent network instantiations. Gray dots in panels b and c represent mean trial measurements across ten independent network instantiations; solid lines show fitted curves.

The network demonstrated enhanced spatial localization when both sensory modalities were present compared to either alone (**Fig. 2a**). Analysis of signed localization errors revealed that auditory-only trials produced a broad error distribution (σ = 8.47°), while visual-only trials showed comparable but slightly lower precision (σ = 9.59°). Bimodal stimulation yielded the highest localization sensitivity (σ = 7.08°), corresponding to a 19% improvement over the better unisensory condition. This enhancement pattern mirrors the multisensory integration effects observed in SC neurons of behaving animals, where responses to bimodal stimulation typically outperform unimodal spatial discrimination under optimal stimulus conditions (Stanford et al., 2005). Such multisensory enhancement is also observed across

human behavioural responses to spatial discrimination tasks (Alais & Burr, 2004; Battaglia et al., 2003; Binda et al., 2007). The error distributions for all three conditions approximated Gaussian profiles centred around zero, indicating unbiased spatial representations.

The spatial window over which the network integrated multisensory information revealed distance dependent constraints on binding (**Fig. 2b**). We presented simultaneous audiovisual stimuli with varying angular disparities and measured the probability of observing a unified or segregated population response (i.e., either one or two distinct peaks in activity in the multisensory layer as shown in the upper panel of **Fig. 2b**). The network maintained fusion probability above 50% for disparities up to ±26°, beyond which fusion declined to baseline levels by ±40°. This spatial binding window corresponds to the receptive field overlap required for multisensory enhancement in SC neurons. On the other hand, the temporal binding window, assessed by varying audiovisual onset asynchronies, exhibited marked asymmetry in integration capacity (**Fig. 2c**). Fusion probability remained above 50% for asynchronies ranging from -150 ms (visual leading) to +70 ms (auditory leading), with peak integration at slight visual-lead offsets. This asymmetry aligns with the differential conduction delays in the network architecture: visual signals required 26 ms to reach multisensory neurons while auditory signals required only 10 ms, creating a natural bias toward visual-preceding-auditory sequences that may compensate for faster auditory processing in natural environments.

To assess whether the network learned appropriate cue combination strategies, we manipulated the spatial reliability of auditory and visual inputs by varying their spatial spread from $\sigma = 2°$ to 20°. When both modalities had equal reliability, the network assigned similar weights to each input ($wV = 0.51 \pm 0.03$). As we decreased visual reliability relative to auditory, visual weight decreased systematically to $0.04 \pm 0.04$ when $\sigma V = 20°$ and $\sigma A = 2°$ (**Fig. 2d**). This pattern suggests that the network learned to dynamically weight sensory inputs based on their reliability, with more reliable modalities receiving stronger weights. The empirical weights showed a strong correlation with maximum likelihood estimation predictions ($R^2 = 0.71$), with a mean absolute error of 0.13, indicating that exposure to correlated multisensory events during training was sufficient for the network to learn reliability-based integration. While not numerically optimal, this weighting strategy approximates the principles of statistically optimal integration, allowing the network to rely more heavily on the

sensory channel providing higher quality information (Alais & Burr, 2004; Battaglia et al., 2003).

Response timing analysis demonstrated that multisensory stimulation accelerated neural responses relative to unisensory conditions (**Fig. 2e**). Mean first-spike latencies were 56 ± 5.2 ms for auditory, 54 ± 1.6 ms for visual, and 36 ± 1.6 ms for bimodal stimulation across network instantiations. The 19 ms reduction in multisensory latency represents a 35% acceleration compared to the mean unisensory latency, an effect size comparable to reaction time benefits observed in multisensory detection tasks. This latency reduction emerged from the convergence of subthreshold inputs that, when combined, reached spike threshold earlier than either modality alone. We also tested for the principle of inverse effectiveness, whereby multisensory enhancement is greatest for weak stimuli, manifested in the network's responses across stimulus intensities (**Fig. 2f**). The multisensory enhancement index (MEI) decreased from 1.1 at the lowest intensity (0.05 a.u.) to 0.78 at the highest (1.6 a.u.), broadly following a power-law relationship on logarithmic axes. This inverse relationship ensures that multisensory integration provides maximal benefit when unisensory signals are least reliable, a computational strategy that optimizes behaviour under conditions of sensory uncertainty.

***Reduced neuronal adaptation.*** Diminished sensory adaptation has emerged as a potential mechanism underlying atypical sensory processing in autism, with individuals showing reduced habituation to repeated stimuli across multiple sensory modalities. To probe how diminished spike-frequency adaptation shapes multisensory behaviour, we re-parameterised multisensory neurons from regular-spiking (a = 0.02, d = 8) to near tonic (a = 0.0001, d = 0.01, b = 0.2, c = -60 mV), greatly reducing the after-hyperpolarising current that curtails sustained firing. This manipulation allowed us to examine whether altered intrinsic excitability could contribute to the characteristic sensory integration differences observed in autism spectrum disorder (Millin et al., 2018).

The spatial binding window expanded significantly following adaptation reduction (**Fig. 3a**). While the control networks maintained fusion probability above 50% for audiovisual disparities within ±26°, perturbed networks extended this range to ±34°, a 25% increase in spatial tolerance. Additionally, the fusion probability curve developed a flat-top plateau, maintaining near-perfect fusion ($P \approx 1.0$) across the

central ±20° range rather than the narrower window observed in controls. This resembles reports that individuals with ASD often show more implicit integration at large spatial disparities but narrower explicit spatial binding windows. (Noel et al., 2022). The distortion of graded spatial selectivity we see in our perturbed networks could suggest that reduced adaptation may prevent the competitive dynamics necessary for precise spatial discrimination, allowing disparate inputs to drive sustained multisensory responses (Stein et al., 2014).

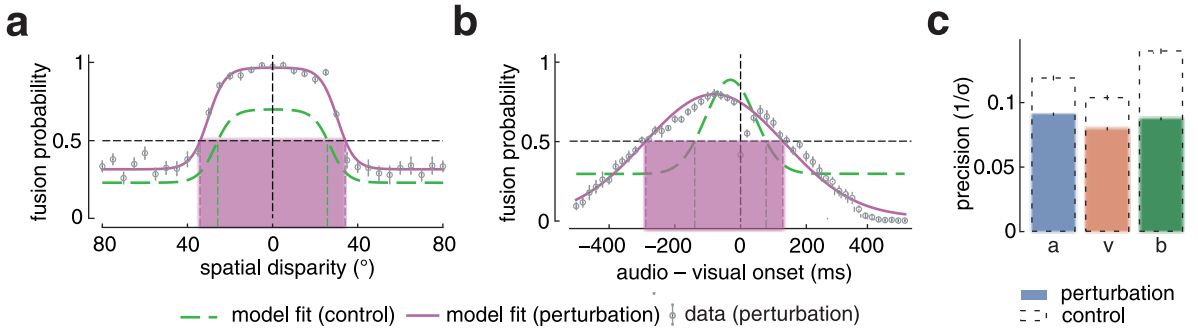


**Figure 3. Effects of reduced neuronal adaptation on multisensory integration.** **a**) Fusion probability as a function of spatial disparity for control (green dashed line) and reduced adaptation (magenta solid line) networks. **b**) Fusion probability as a function of audio-visual onset asynchrony for control and perturbed networks. **c**) Localization precision (1/σ) for auditory, visual, and bimodal conditions; coloured bars show perturbed networks with black dashed lines indicating control values. Vertical green dashed lines and shaded regions in (**a**, **b**) indicate where fusion probability exceeds 50% for control and perturbed networks, respectively; negative asynchronies in (**b**) indicate visual-leading stimuli. Error bars indicate ±SEM across ten network instantiations.

Temporal integration constraints showed comparable alterations. Post manipulation, fusion tolerance to onset asynchrony increased dramatically, expanding from -139 to +76 ms (215 ms total) in controls to -288 to +128 ms (416 ms total) post manipulation, with the bulk of the expansion occurring on the visual lead side (**Fig. 3b**). Both the magnitude and asymmetry of this temporal expansion aligns with behavioural studies in ASD, where individuals consistently show temporal binding windows ~400 ms on flash-beep simultaneity judgments and demonstrate particular difficulty rejecting visual first sequences (de Boer-Schellekens, Keetels, et al., 2013; Foss-Feig et al., 2010; Stevenson, Siemann, et al., 2014). Within the network architecture, reduced adaptation (and thus uncontrolled spiking) prolongs NMDA-mediated depolarization, potentially extending the window during which late arriving auditory signals can trigger multisensory enhancement. This mechanism is consistent with evidence of altered NMDA receptor expression and function in ASD, particularly in subcortical structures involved in sensory integration (Won et al., 2012).

The expanded binding windows exhibited by the modified network were accompanied by degraded localization performance (**Fig. 3c**). Sensitivity (1/σ) decreased by approximately 23% for unimodal and 37% for bimodal stimulation, relative to controls. The typical multisensory benefit (whereby sensitivity to bimodal stimulation exceeds that to both unimodal stimuli) was substantially diminished in adaptation-reduced networks. Control networks showed 19% enhancement for multisensory compared to (best) unisensory performance, while perturbed networks showed a 4.6% diminution. These findings suggest that the mechanism contributing to broadening of the integration windows may also increase response variability, degrading the signal-to-noise ratio that typically enhances multisensory localization. Our results parallel the contrasting combination of enhanced binding yet reduced behavioural benefit from multisensory integration commonly observed in ASD (Noel et al., 2022; Ostrolenk et al., 2019).

Reducing spike-frequency adaptation fundamentally altered network dynamics by allowing multisensory neurons to maintain prolonged depolarisation, thus extending the window over which incoming sensory signals could summate effectively. Under normal conditions, adaptation currents quickly repolarise neurons after firing, sharply restricting the temporal window for multisensory integration. Without this rapid repolarisation, NMDA receptors remained partially unblocked for an extended duration (17% compare to 10%), increasing the cumulative NMDA-mediated excitation, which resultantly increased the share of NMDA charge, relative to AMPA (by ~40% on average). This sustained excitation effectively overwhelmed inhibition that, although recruited at the same latency as control conditions (~2 ms after excitation), was insufficient to rapidly repolarise multisensory neurons. At the same time, the prolonged NMDA currents and excitation also affected neighbouring neurons, manifesting as persistent local recurrent excitation that overpowered the inhibitory surround (the increased NMDA current into the neurons decreased the depth of the firing activity valley between two adjacent spiking neural populations and resulted in increased fusion across spatial disparities, despite surround inhibition increasing from 1.5 to 2.6 following reduced adaptation). Consequently, the prolonged excitation resulted in the expanded temporal and spatial binding windows, coupled with a reduction in localisation precision. This pattern of indiscriminate fusion and reduced precision closely mirrors sensory processing anomalies frequently reported in ASD populations (Noel et al., 2022). Such findings support the notion that diminished neuronal

adaptation may underlie core aspects of multisensory integration deficits observed in autism.

***Reduced feedforward inhibition.*** Disrupted excitation-inhibition balance represents one of the most widely documented circuit alterations in autism spectrum disorder, with evidence spanning from genetic mutations affecting GABAergic signalling to altered inhibitory neuron density in postmortem tissue. We next sought to examine how altered E/I balance affects multisensory integration and to that extent, we scaled feedforward GABAergic inhibition from unisensory to multisensory layers to 30% of their baseline values. This manipulation increased the epoch-integrated E/I charge ratio from approximately 1.1 in control networks to 3.0 in perturbed networks, mimicking the reduction in cortical inhibition hypothesized in ASD (Antoine et al., 2019; Rubenstein & Merzenich, 2003; Sohal & Rubenstein, 2019). This intervention produced integration deficits distinct from those observed with reduced adaptation, which may reflect the way different circuit perturbations generate heterogenous sensory phenotypes within the autism spectrum (Hahamy et al., 2015; Lombardo et al., 2019; Sohal & Rubenstein, 2019; Zerbi et al., 2021).

The spatial binding window contracted following inhibition reduction, with the 50% fusion threshold narrowing from ±26° to ±20°, a 23% decrease in spatial tolerance (**Fig. 4a**). By analogy with the adaptation manipulation, where reduced adaptation broadened the SBW via greater NMDA conductance and more persistent excitation (**Fig. 3a**), a simple E/I account would predict that feedforward disinhibition should likewise widen, not narrow, the SBW. This seemingly paradoxical result may reflect a relative increase in centre surround inhibition under conditions of feedforward disinhibition (the charge contributed from the surround inhibition increased by 19% while feedforward inhibition decreased by 45% along with the NMDA/AMPA ratio which also fell from 0.3 in control to 0.171 after disinhibition), potentially tightening the receptive fields of the multisensory layer neurons and sharpening spatial tuning. This was further supported by the finding that abolishing surround inhibition greatly reduced the deficits produced by reducing feedforward inhibition (**Supplementary Fig. 4**). The steeper decline in fusion probability with increasing disparity resembles findings in certain ASD cohorts, where individuals show reduced likelihood of perceiving common-cause relationships for moderately disparate audiovisual stimuli, despite accepting larger disparities in other paradigms (Noel et al., 2022).

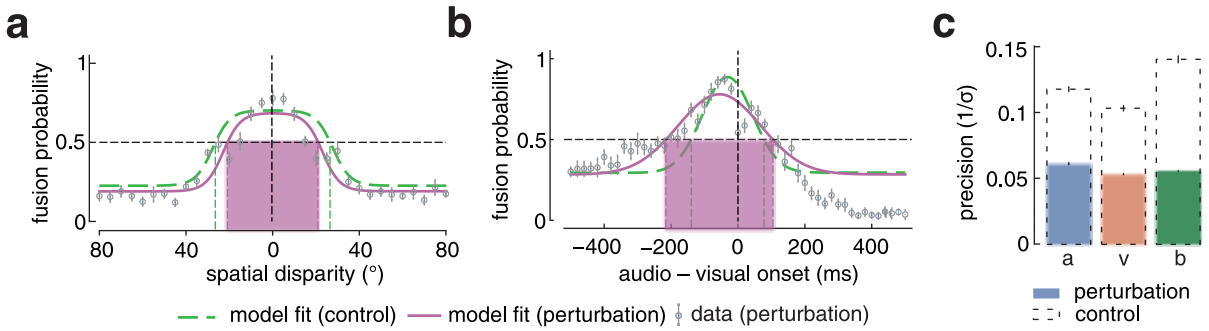


**Figure 4. Effects of reduced feedforward inhibition on multisensory integration. a**) Fusion probability as a function of spatial disparity for control (green dashed line) and reduced feedforward inhibition (magenta solid line) networks. **b**) Fusion probability as a function of audio-visual onset asynchrony for control and perturbed networks. **c**) Localization precision (1/σ) for auditory, visual, and bimodal conditions; coloured bars show perturbed networks with black dashed lines indicating control values. Vertical green dashed lines and shaded regions in (**a**, **b**) indicate where fusion probability exceeds 50% for control and perturbed networks, respectively; negative asynchronies in (**b**) indicate visual-leading stimuli. Error bars indicate ±SEM across ten network instantiations.

While spatial integration became more restrictive, temporal binding showed the opposite pattern, expanding from -139 to +77 ms (216 ms total) in controls to -215 to +104 ms (319 ms total) following disinhibition (**Fig. 4b**). This 32% expansion of the temporal window showed characteristic asymmetry, with visual-leading asynchronies extending by 76 ms compared to 27 ms for auditory-leading offsets. This temporal expansion coincided with prolonged NMDA-mediated depolarization, as indicated by increased average $Mg^{2+}$ gate relief (12.5% compared with 10.4% in controls). Under these conditions, sensory inputs separated by up to ~300 ms could potentially summate effectively, particularly when visual stimuli preceded auditory ones. This finding was expected, given that feedforward inhibition typically narrows the temporal integration window (Gabernet et al., 2005; Pouille & Scanziani, 2001). Extended audiovisual temporal binding windows are a robust sensory marker of ASD, appearing across flash-beep, speech, and complex stimulus paradigms (Stevenson, Siemann, et al., 2014; H. Zhou et al., 2018).

Concurrent with spatiotemporal binding alterations, reduced feedforward inhibition led to less precise localization across all conditions, with sensitivity declining by 48% for auditory, 48% for visual, and 60% for bimodal stimuli (**Fig. 4c**). Control networks showed 19% enhancement for multisensory compared to (best) unisensory performance, while perturbed networks showed a 10% diminution. The disproportionate impact on multisensory performance indicates that elevated excitation not only increased baseline response variability but specifically disrupted the variance reduction mechanisms that might otherwise enhance multisensory

precision (Dinstein et al., 2012). Such loss of spatial acuity parallels experimental findings where GABA receptor blockade or optogenetic silencing of interneurons in the superior colliculus produces comparable degradation of spatial discrimination and multisensory gain (Binns & Salt, 1997; Wang et al., 2020).

The dissociation observed in our networks (expanded temporal binding coupled with contracted spatial binding and reduced precision) indicates that E/I imbalance differentially affects distinct aspects of integration (Pouille & Scanziani, 2001; Wilson et al., 2012). Our findings indicate that while reduced adaptation produces uniformly expanded binding across spatial and temporal domains, an elevated E/I ratio generates opposing effects. Such mechanistic diversity could potentially account for the variable sensory profiles observed clinically (Noel et al., 2022; Weiland et al., 2023; Zhou et al., 2018), though direct experimental validation would be necessary to establish whether similar dissociations occur in biological systems.

***NMDA alterations.*** Exome sequencing has identified mutations in NMDA receptor subunit genes (GRIN1, GRIN2A, GRIN2B) in individuals with autism spectrum disorder, with both receptor hypofunction and hyperfunction implicated in different contexts (Cha et al., 2025; De Rubeis et al., 2014; O'Roak et al., 2011). To investigate how NMDA receptor function shapes multisensory integration, we systematically altered NMDA conductance in both directions, reducing NMDA expression from 0.05 to 0.02 (60% reduction) and increasing it to 0.15 (threefold increase). These manipulations allowed us to examine whether NMDA receptors primarily contribute to the temporal precision of coincidence detection or more broadly regulate the spatiotemporal constraints of multisensory binding.

Reduced NMDA conductance produced consistent narrowing of integration windows across both spatial and temporal domains (**Fig. 5a**, **b**). The spatial binding window contracted from ±25° to approximately ±17°, with fusion probability declining more steeply as audiovisual disparities increased. This narrowed spatial tolerance may reflect limited capacity for sustained depolarization when NMDA-mediated currents are weakened (Ewald et al., 2008; Mayer et al., 1984), potentially restricting the spatial extent over which convergent inputs can fuse. Temporal integration showed minimal constriction, with the binding window shrinking from -139 to +76 ms (215 ms total) in controls to -139 to +60 ms (199 ms total) following NMDA reduction. The asymmetric nature of this minimal narrowing, with evident impact only on audio leading

asynchronies, could result from insufficient slow integrative currents to bridge the temporal gap between early auditory and delayed visual inputs (Drotos et al., 2024). Localization sensitivity declined across all conditions, with multisensory precision showing relatively more degradation (30% degradation across unisensory sensitivities and 33% for multisensory; **Fig. 5c**). The reduced multisensory enhancement (18% multisensory enhancement for control compared to 10% enhancement following manipulation) supports previous claims that adequate NMDA function is key for deriving signal processing benefits from combining sensory information (Lebedeva et al., 2019; Li & Gulledge, 2021).

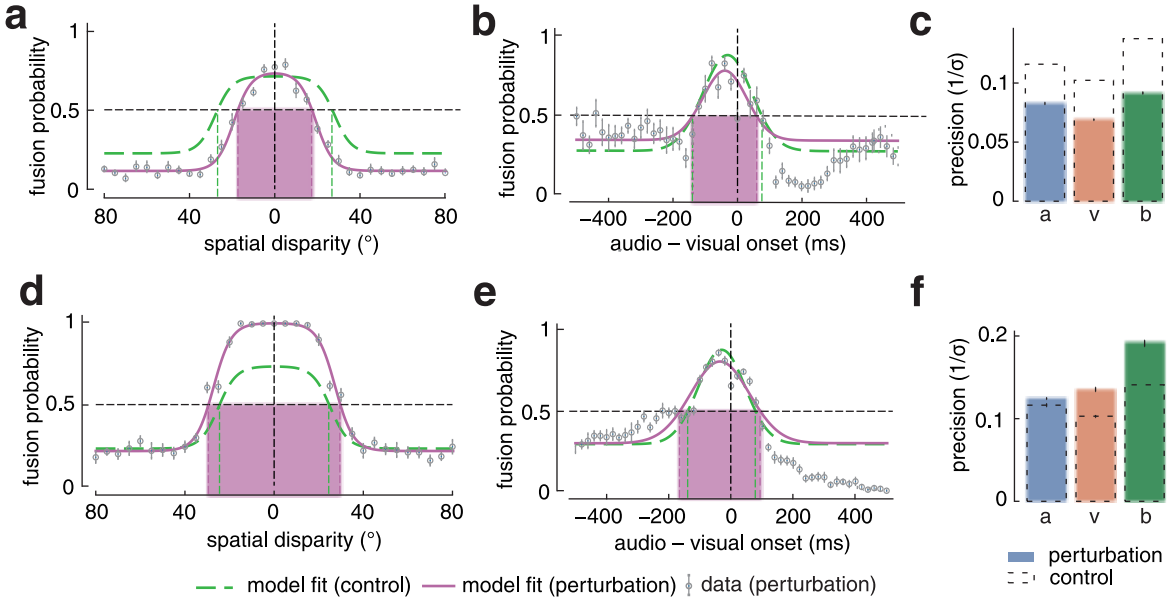


**Figure 5. Bidirectional effects of NMDA receptor conductance alterations on multisensory integration. a-c**) Reduced NMDA conductance (60% reduction): **a**) Fusion probability as a function of spatial disparity for control (green dashed) and NMDA-reduced networks (purple solid). **b**) Fusion probability as a function of audio-visual onset asynchrony; negative values indicate visual-leading, positive indicate auditory-leading stimuli. **c**) Localization precision (1/σ) for auditory, visual, and bimodal conditions; coloured bars represent perturbed networks with control values shown as black dashed lines. **d-f**) Increased NMDA conductance (threefold increase): **d**) Spatial fusion probability, **e**) Temporal fusion probability, and **f**) Localization precision, following the same format as panels a-c. Vertical green dashed lines and shaded regions in (**a**, **b**, **d**, **e**) indicate where fusion probability exceeds 50% for control and perturbed networks, respectively; negative asynchronies in (**b**, **e**) indicate visual-leading stimuli. Error bars indicate ±SEM across ten network instantiations.

Increased NMDA conductance led to a different pattern of alterations that revealed comparable effects on spatial and temporal processing (**Fig. 5d**, **e**). The spatial binding window underwent minimal yet significant expansion going from ±26° to approximately ±29°, with fusion probability approaching unity across the central ±20° range, above the fusion probability observed in controls. This plateaued fusion profile suggests that enhanced NMDA currents could create overly permissive spatial

integration, potentially allowing misaligned inputs to drive fused percepts (Rhodes, 2006). Following a similar trend, the temporal binding window increased from -139 to +76 ms (215 ms total) in controls to -173 to +94 ms (267 ms total) following an increase in NMDA conductance, while maintaining the same asymmetric profile as control networks (Drotos et al., 2024). Localization sensitivity showed improvements across all stimulus conditions (1% enhancement across audio sensitivity, 25% increase across visual and 33% increase across bimodal stimuli), with the multisensory benefit in localization accuracy showing enhancements following manipulation (19% multisensory enhancement in controls compared to 41% enhancement following perturbation). The enhanced NMDA conductance likely improved localization accuracy by stabilizing synaptic integration and reducing location-dependent variability in neuronal responses (Li & Gulledge, 2021). This would effectively increase the fidelity of EPSP-spike coupling across spatial domains despite the more permissive binding window, thereby creating more reliable spatial representations even when fusion probability increased.

The bidirectional effects of NMDA manipulation suggest that these receptors play a complex role in multisensory processing. In our model, NMDA receptors appear to provide sustained depolarization that facilitates spatial integration across topographic maps, with reduced NMDA limiting effective spatial summation (Ewald et al., 2008; Monyer et al., 1994) and elevated NMDA potentially causing indiscriminate binding of spatially disparate inputs. The preservation of multisensory enhancement with increased NMDA contrasted with its elimination following NMDA reduction, suggests that while adequate NMDA function may be necessary for optimal integration, the system appears more tolerant of excess than deficiency in our network architecture.

## DISCUSSION

***Mechanistic heterogeneity in ASD multisensory processing.*** Here for the first time, a biologically constrained SNN model of the SC was deployed to investigate how particular synaptic and cellular perturbations give rise to deficits in multisensory integration in ASD. Our systematic manipulation of neuronal adaptation, E/I balance and NMDA receptor conductance showed that each perturbation produced alterations in spatiotemporal binding. Reduced adaptation yielded uniformly expanded binding windows (spatial: ±26° to ±34°; temporal: 215 ms to 416 ms), diminished feedforward inhibition generated dissociated effects (spatial contraction to ±20°; temporal expansion to 319 ms), and NMDA receptor alterations produced bidirectional, magnitude-dependent changes. Our findings show that the neural mechanisms tested here can lead to the enlarged temporal binding windows observed in ASD populations (Foss-Feig et al., 2010). They also produce distinct effects on spatial integration (Noel et al., 2022) and localization precision (Fujihira et al., 2022; Visser et al., 2013). This contrast in results may account for the variability in symptoms characteristic of autism (Lombardo et al., 2019).

The differences observed across our three perturbation conditions implies that a set of distinct mechanisms may give rise to the behavioural deficits seen in ASD. Reduction of adaptation allowed for long active times for the neurons, extending their temporal windows of integration by sustaining NMDA receptor activation. In contrast, decreased inhibition narrowed spatial binding while expanding temporal windows. Modifications of NMDA receptor had graded effects that scaled with the level of conductance, which bidirectionally impacted spatiotemporal processing. These mechanisms reflect a frequently reported clinical observation: individuals with ASD can show similar extended temporal binding deficits yet differ markedly in other aspects of sensory processing. Instead of viewing ASD as deviations along a single axis of dysfunction, our results suggest that different combinations of cellular or synaptic modifications could lead to the same behavioural responses, while varying in their computational pathologies. Understanding these differences in mechanistic terms requires an examination of how each perturbation alters the fundamental operations of the multisensory neurons.

***Perturbation-specific computational mechanisms***. A reduction in neural adaptation led to disruptions in multisensory integration, extending spatiotemporal windows by

significant margins. When we converted multisensory neurons from regular-spiking to near-tonic firing patterns, a reduction in spike frequency adaptation stopped the polarisation that normally followed stimulus driven activity, maintaining NMDA receptors in a partially unblocked state for extended periods (the average gate relief increased from 10% to 17%; Zhang-Hooks et al., 2016). This sustained depolarization created a computational state where neurons could no longer separate when one stimulus ended and another began, nor maintain precise spatial boundaries between adjacent inputs, explaining why both temporal and spatial windows expanded proportionally (Kwakye et al., 2011). The mechanism resembles the "sticky attention" phenomenon observed clinically (Dwyer et al., 2024; Zwaigenbaum et al., 2005), where individuals with ASD show difficulty disengaging from stimuli, suggesting that adaptation deficits might underlie the automatic orienting impairments characteristic of the condition (Gonçalves & Monteiro, 2023). A reduction in adaptation stands out in comparison to the other perturbations discussed here, because while they affect different aspects of integration in an asymmetric fashion, disrupting adaptation can compromise the basic ability of a neuron to reset between stimuli (Takarae & Sweeney, 2017). This intrinsic cellular mechanism contrasts with our E/I balance manipulations, which had differing effects on spatial and temporal integration.

While adaptation altered intrinsic reset, feed-forward disinhibition separates where and for how long inputs are bound. Weakening the unimodal-to-multisensory GABAergic projection led to contrasting changes in the network's response: spatial binding narrowed while temporal windows expanded (Kwakye et al., 2011; Lee et al., 2020; Robertson et al., 2013). This distinction arose through measurable circuit reorganization. With a decrease in the strength of early inhibitory gating, aligned audiovisual inputs generated stronger central responses that also led to an increase in the strength of lateral inhibition (the surround pathway charge increased by 19% while feedforward inhibition decreased by 45%), which doubled their ratio and sharpened spatial tuning in spite of a decrease in inhibition (Schallmo et al., 2020). This was evidenced by the finding that abolishing surround inhibition greatly reduced the deficits produced by such disinhibition (**Supplementary Fig. 4**). Simultaneously, loss of early GABA shunting allowed prolonged NMDA accumulation, with the NMDA/AMPA ratio rising 27% and extending temporal integration windows. The recurrent inhibitory loops remained stable throughout, as they were not directly affected by changes to feedforward inhibition. These findings reveal how the strength

and timing of inhibition determines if and how audiovisual inputs bind across space and time (Kwakye et al., 2011; Robertson et al., 2013). Such inhibition mediated effects may explain why some individuals with ASD show narrowed spatial attention alongside difficulty filtering stimuli separated in time.

By contrast, tuning NMDA currents acted as a molecular time-constant that bidirectionally regulated integration windows (Paoletti et al., 2013). Reducing NMDA conductance by 60% narrowed both spatial (±26° to ±17°) and temporal (215 to 199 ms) binding windows, while threefold enhancement expanded spatial (±26° to ±29°) and temporal (215 to 267 ms) windows with improved localization precision (Binns & Salt, 1996). This bidirectional relationship resembles the developmental GluN2B→GluN2A subunit switch, where early GluN2B-enriched receptors cause longer decay times and broader integration windows that narrow as GluN2A expression increases (Bellone & Nicoll, 2007; Brigman et al., 2010). Multiple GRIN2B variants identified in ASD cohorts alter receptor kinetics in opposing directions, some reducing channel open time while others enhance conductance (Fedele et al., 2018; Sabo et al., 2023). This could explain why the temporal binding window of some individuals with ASD is expanded, while for others it is contracted (de Boer-Schellekens, Keetels, et al., 2013; Kwakye et al., 2011). Our model suggests these opposing clinical observations may reflect a continuous spectrum of NMDA function rather than distinct pathophysiological mechanisms (Zoodsma et al., 2022). This model shows an increase in multisensory enhancement with increased NMDA but an elimination of enhancement upon lowering NMDA conductance, which goes on to imply that integration benefits require a minimum threshold of slow synaptic current, below which coincidence detection fails regardless of fast AMPA-mediated transmission (Binns & Salt, 1996).

The responses demonstrated by our model post NMDA manipulations did not consistently reproduce the extension in temporal binding metrics seen in behavioural studies of ASD. While we did observe a decrease in binding metrics following a decrease in NMDA and vice versa, observations from clinical studies have frequently reported broadened temporal integration, across various paradigms (Foss-Feig et al., 2010;Stevenson, Siemann, et al., 2014). This discrepancy likely reflects our simplified implementation of NMDA dynamics, which does not incorporate developmental changes in receptor subunit composition (Monyer et al., 1994), NMDA-reliant inhibitory pathways (Carlén et al., 2012), or interactions with synaptic scaffolding proteins

implicated in ASD (Coley & Gao, 2019; Duffney et al., 2013). Models incorporating these additional biological mechanisms may be better suited to capture the relationship between NMDA dysfunction and alterations in integration metrics, in neurodevelopmental disorders.

***Experimental predictions and translational implications***. The three perturbations explored here shed light on the distinct computational signatures that lead to disruptions in multisensory integration in autism. The findings from this study separate three different phenotypes: a uniform extension in both spatial and temporal windows, which resembles how neurons retain activity over time in Fragile-X models (He et al., 2017); a contrasting trend, where reduced inhibition narrows spatial while widening temporal integration, resembling PV-interneuron suppression experiments where receptive fields are sharper, alongside prolonged responses (Seybold et al., 2012); and a bidirectional trend reflecting NMDA conductance, which explains why some individuals show narrow temporal windows while others show broadened windows (prolonged GluN2B currents; Martí nez-Lázaro et al., 2025). This framework aligns with cross-model surveys that show distinct connectivity clusters. Brain-wide mapping across 16 ASD mutations segregates into hypo- and hyper-connectivity groups, while cortical recordings identify elevated E/I ratios in Fmr1, Cntnap2, and 16p11.2 deletion models against reduced ratios in MeCP2-null mice (Antoine et al., 2019; Banerjee et al., 2016; Zerbi et al., 2021). These mechanistic subtypes argue against treating ASD as monolithic (Just et al., 2012; Lawson et al., 2014; Rubenstein & Merzenich, 2003), instead supporting stratification by binding-window profiles and circuit biomarkers for targeted interventions.

The various perturbation phenotypes explored in this study help to connect divergent findings relating to multisensory processing. The temporal binding window expansion under reduced adaptation (going from 215 to 416 ms) and diminished feedforward inhibition (216 to 319 ms) aligns with behavioural studies showing autistic children perceive the sound-induced flash illusion at ~600 ms asynchronies, roughly double the ~300 ms neurotypical range (Foss-Feig et al., 2010). This temporal expansion also correlates with speech-in-noise difficulties, where autistic listeners struggle when consonants and vowels are temporally separated by background noise dips (Tsuji & Imaizumi, 2024). Our spatial findings offer a mechanistic account for conflicting peripersonal space reports: while most studies document expanded

interpersonal distance preferences in autism (Farkas et al., 2023), Cascio et al. (2008) found smaller, sharper tactile boundaries in adults with ASD. Our model suggests that such diminution could arise from disinhibition leading to a relative enhancement in centre-surround contrast. This disinhibition phenotype also matches the "tunnel vision" enhancement described by Robertson et al. (2013), where spatial attention shows steeper eccentricity fall-off despite broad temporal windows. On the other hand, reduced adaptation widens the spatial window in the model, which, if this generalized to peripersonal space coding, would bias comfortable (peripersonal) distances outward; together with the opposite spatial narrowing seen under feedforward disinhibition, such contrasting shifts could help account for the individual differences in interpersonal distances reported in ASD (Givon-Benjio et al., 2024). At cellular levels, adaptation-driven expansion mirrors Fragile-X data showing abolished spike-frequency adaptation from reduced K+ currents (Luque et al., 2024), while disinhibition manipulations parallel impaired multisensory gain in Shank3 mice with weakened GABAergic inhibition (Pagano et al., 2023). The remaining discrepancy, our symmetric spatial-temporal NMDA effects contrasting with predominantly temporal deficits in humans, suggests additional factors like developmental timing or top-down modulation selectively gate temporal binding in vivo. Nevertheless, the model's responses that do align with biological findings could be investigated further to argue for targeted therapeutic avenues.

Each perturbation mechanism generates specific differences in the responses that could be experimentally validated. Kv7 channels have been highlighted as critical mediators of neuronal adaptations in biological systems; after-hyperpolarisation currents mediated by Kv7 channels regulate excitability and produce early spike-frequency adaptation (Luque et al., 2024). The channel opener retigabine has been shown to restore adaptation via a reduction in spiking frequency and thus, acute or chronic retigabine may reverse the uniform spatial and temporal window enlargement we observed following adaptation reduction (Stas et al., 2016). With regard to feedforward perturbations, deletion of the SHANK3 gene in PV interneurons causes circuit hyper-excitability and abnormal behaviours that can be rescued by enhancing GABAergic signalling (Pagano et al., 2023). Our findings suggest that opto- or chemo-activation of PV cells in Shank3 mice will contract the model matched >300ms temporal binding window towards control values. A similar prediction has already been tested in Fragile-X mice, where boosting interneuron activity after the critical period

brought sensory thresholds back to baseline (Kourdougli et al., 2023). In line with such inhibition associated deficits, in vivo micro-iontophoresis of GABA in rat SC has been shown to reduce visual responses and tighten the inhibitory surround (Murthy & Humphrey, 1999; Razak & Pallas, 2007). Our simulations similarly predict a double dissociation: increasing GABAergic center surround strength will narrow spatial binding but lengthen the temporal window in a balanced SC, whereas the same manipulation applied to an SC with reduced inhibition would yield a different pattern. Lastly, recent findings have shown that the GlyT1 inhibitor PF-03463275 enhances neuroplasticity by augmenting NMDAR co-agonism in humans (D'Souza et al., 2018; Surti et al., 2023). The current findings therefore indicate that GlyT1 blockade (or other glycine-site agonists) in NMDA-hypofunction mouse lines will broaden the temporal-binding window into the optimal ~200 ms range.

***Model scope and architectural refinements***. While our spiking model captures core principles of collicular multisensory processing, it is also important to consider the simplifications made in this work that limit its validity. We simplified fine layering of superficial SC and excluded cortico-tectal feedback loops, even though visual and prefrontal projections to these strata have been shown to gate cross-modal responses and decision speed in behaving animals (Cuppini et al., 2010; Dash et al., 2018). These top-down signals reshape both spatial and temporal binding windows (Felch et al., 2016). For instance, anterior cingulate suppression lengthens localisation latencies while broadening temporal integration windows, potentially modulating the three phenotypes we modelled (Vázquez, Maulhardt, et al., 2024; Vázquez, Peña-Flores, et al., 2024). Beyond architectural constraints, each perturbation (adaptation reduction, feed-forward disinhibition, NMDA scaling) was tested in isolation, whereas experimental work shows that adaptation and inhibition interact, and multiple synaptic defects frequently co-occur in ASD models and clinical populations (Jiang et al., 2022; Monday et al., 2023; Natan et al., 2017). Moving past the network, the stimulus environment itself employed isolated Gaussian signals rather than the continuous, competing sensory streams that bombard the SC in natural scenes, where stimulus reliability and congruence fluctuate moment-to-moment (Choi et al., 2018). Additionally, we omitted specific neuromodulatory systems, such as endogenous serotonin which scales SC gain and can flip multisensory enhancement into

suppression (Tang & Trussell, 2017), and cholinergic input from the pedunculopontine nucleus which sharpens spatial tuning and accelerates saccades (Wolf et al., 2015).

These abstractions, however, represent deliberate methodological choices that enhance interpretability while establishing a validated foundation for systematic extension. By focusing on intermediate/deep SC layers, we isolated the canonical, bottom-up rule set (spatial coincidence, inverse-effectiveness) intrinsic to deep SC circuitry (Stein & Stanford, 2008), making perturbation effects unambiguous; top-down influences can later be incorporated as a separate attentional control layer, following computational frameworks advocated in recent SC modelling reviews. We simplified the stimulus paradigm to parallel psychophysics studies that use minimal stimuli like the sound-induced flash illusion to reveal key temporal-binding rules before adding naturalistic complexity (Shams et al., 2000). Once validated, competitive computations observed under dynamic scenes can be layered onto this base architecture. The isolation of individual perturbations follows factorial design principles in computational biology (Murphy & Miller, 2003), establishing single factor baselines necessary to quantify synergies, particularly relevant given that adaptation and inhibition interact multiplicatively in the cortex. This further suggests that our single factor results represent lower bound shifts that would amplify when combined, mirroring stronger clinical phenotypes (Girirajan et al., 2010). Similarly, excluding neuromodulatory inputs keeps the parameter space tractable while preserving the excitatory-inhibitory core; these signals act largely as multiplicative gates that can be added as a state dimension to capture learning effects without re-tuning the entire synaptic layout (Ferguson & Cardin, 2020; Martinez-Trujillo & Treue, 2004). Collectively, these choices create an interpretable and falsifiable framework while mapping a clear trajectory for incorporating cortico-tectal loops, compound perturbations, naturalistic stimuli, and state-dependent modulation in future iterations (Basso & May, 2017).

# DISCUSSION

THESIS

**Overview**

Biological constraints give computational models explanatory power. Without them, neural networks remain black boxes that match patterns but reveal little about underlying mechanisms. This thesis embedded physiological details directly into network architectures to expose how specific circuit operations produce perceptual phenomena, and two case studies demonstrate this approach. The first added adaptation to a motion processing network and discovered how metabolic constraints shape sensory coding, while the second built a spiking superior colliculus model to trace how synaptic alterations generate the sensory differences seen in autism. Together, they show that biological realism transforms models from descriptive tools into mechanistic instruments. Both investigations required different levels of biological detail to answer their respective questions about healthy function and dysfunction.

Motion processing offered an ideal starting point because decades of neurophysiology have mapped its computational hierarchy. To match the organisation seen in the primate visual cortex, I built a network with V1-like convolutional units feeding into MT-like recurrent layers. Trained on natural image sequences, tuning properties emerged within the network such as direction and speed selectivity. Utilizing plaid stimuli, it was possible to reproduce pooling behaviour in the V1 to MT pathway, by separating component from pattern motion. But these features appeared whether or not adaptation was included. The key difference emerged only upon cessation of motion. The adaptive network exhibited motion aftereffects, perceiving illusory movement opposite to the preceding stimulus, and population recordings revealed why. During sustained motion, neurons tuned to that direction fired continuously while opponent channels remained suppressed. When stimulation ceased, the adapted units recovered slowly. This temporary imbalance between opposing populations created the aftereffect, consistent with theoretical predictions from the 1960s (Barlow & Hill, 1963; Mather et al., 2008). Beyond reproducing this classic phenomenon, adaptation conferred measurable benefits. Neural activity dropped by sixty percent during sustained stimulation, reducing metabolic consumption. Parallelly, response latencies shortened after velocity changes, improving change detection. The trade-off was reduced accuracy for constant motion. While this study demonstrated how biological realism captures healthy computational principles, biologically grounded networks could equally illuminate what happens when neural circuits malfunction.

The second study investigated neural dysfunction, by means of validating and then perturbing a network model of multisensory integration in the superior colliculus. I began this second study with one key question: could similar mechanistic exploration be exploited to understand how imbalances in synaptic and network parameters would give way to altered behavioural metrics, like those found in conditions of disorder? A study of multisensory integration would come with its own set of challenges, given the brain's reliance on precise neurotransmitter clocks and localised learning mechanisms to accomplish this feat. But advances in computational power over the last few decades meant that a superior colliculus network could be modelled feasibly by prioritizing essential mechanisms and controlling computational costs. Looking at this problem in the context of energy utilization, the core mechanisms that were necessary, especially in the context of audiovisual integration and subsequent autism perturbations, were AMPA/NMDA dynamics, E/I balance, and localised Hebbian learning. The choice to implement spiking dynamics in the network made sense architecturally, given the reliance of a phenomenon like multisensory integration on temporal and charge dynamics, which are factors a rate-based network could not typically control or measure.

What followed next were the perturbation experiments that simulated states of dysfunction. After identifying, implementing, and validating the relevant mechanisms underlying the multisensory integration network, parametric dysfunction was then introduced into the network and the variances in response metrics were observed in relation to their deviation from baseline. Across multiple perturbations, an extension of the temporal binding window was observed, proportional to the scale of dysfunction. On the other hand, the spatial binding window varied in a non-intuitive fashion, with both extensions and diminutions being exhibited depending on the parameter being perturbed. A majority of the experiments were also accompanied by a drop in multisensory enhancement other than in the NMDA gain test, where an increase in enhancement was noted, albeit at the cost of extended spatial and temporal windows. These findings reflect what is often observed in individuals with ASD — extended temporal windows, altered (without a consistent direction of change) spatial windows, and reduced multisensory enhancement (Foss-Feig et al., 2010; Noel et al., 2022; Ross et al., 2024). Crucially, the validation of this network, along with the results of the network perturbation tests, demonstrated how biologically inspired architectures could

be utilized to derive useful insights about neural activity as well as behavioural responses, in both health and dysfunction.

Designing systems for effective neuroscientific inference calls for a shift in modelling perspective. One of the primary constraints that made such a detailed analysis of neural activity possible in this work, is the adherence to biologically grounded mechanisms. Most DNNs and other related artificial simulations used today are built with the purpose of comparison against human performance benchmarks (Saxe et al., 2021; Yamins & DiCarlo, 2016). But in adopting this scheme of validation, a higher priority is assigned to the final goal alone, rather than the caveats of the machinery employed to get there, unless it directly results in an improvement in benchmarking metrics (Geirhos et al., 2020). Models trained solely to optimize task loss can converge on solutions that are functionally adequate, but by using shortcuts or dynamics not available to biological circuits (Geirhos et al., 2020, 2022). Consequently, parameter changes *in silico* need not translate to perturbations *in vivo* (Jonas & Kording, 2017; Lillicrap et al., 2020). For example, motion processing could be performed via a simple algorithm that detects motion energy by subtracting pixel data between successive frames. The same task could also be undertaken utilizing a spiking neural network with detailed temporal and learning mechanics. Depending on the level of abstraction, the resemblance of the network to what is seen in biology, and hence the inferences that can be drawn from such a network, shall vary. Effective inference therefore requires choosing the appropriate level of mechanistic detail that matches the question at hand. To that extent, the guiding principle here is minimal realism — include only those physiological degrees of freedom that correspond to measurable quantities, like adaptation, NMDA/AMPA ratios, and E/I balance. This is the route from strong benchmarks to mechanistic comparisons, and it is the standard against which the analyses in this work are evaluated. In the first case study, the aim was to demonstrate how the addition of a simple biological mechanism could be used to investigate the effect of adaptation on both perception as well as the metabolism of information processing in a recurrent neural network.

Two things were made clear on embedding adaptation in a motion processing neural network: adaptive effects, even at the neuronal level, had the ability to alter a network's responses drastically, and that the mechanism conferred efficiency benefits into the network, even though it came at the price of sustained accuracy. To ensure that the differences in response of the modified network could truly be attributed to

adaptive mechanisms, the changes implemented were incremental in nature — first, a motion processing network inspired by recent work by Rideaux & Welchman (2020) was modified to include adaptive mechanisms in the V1- and MT-like units of the network. With adaptation enabled, illusory aftereffects could be observed in the network's responses, which upon further investigation were explained by the recovery of tuned populations at different rates, which temporarily unbalanced opponent neurons. Adaptation also resulted in a dramatic reduction of neural activity by about 60% during sustained stimulation, while resulting in slightly lower accuracy. In response to dynamically changing stimuli on the other hand, AdaptNet did slightly better than the baseline network. This computational trade-off between accuracy and energy utilized by the system has previously been theorized to be a functional benefit for adaptation, and the findings from this study support this hypothesis. The work here also matches recent computational findings, such as the modelling of the biophysical adaptation by Idrees et al. (2024), which enabled ANNs to capture retinal dynamics under natural statistics. A simple motion processing network trained on natural stimuli would fall short of capturing these adaptive dynamics, which would then make it harder to draw accurate inferences from such a network, across various stimulus paradigms. Adaptation as a phenomenon takes into account a time-varying prior that gradient learning alone does not guarantee. And these advantages in inference are even more pronounced in the second study, where similar biologically grounded mechanisms are employed to model multisensory integration.

A computational study of dysfunction would prove most useful if the computational model developed could either be used to support/challenge existing theories or to derive additional inferences about the condition that could not be measured using classical methods alone. A pre-requisite to be able to use any computational model for these purposes though, is to first be able to ensure the validity of that model by comparing it against measured characteristics of that biological system. In the case of the superior colliculus, the area's instantiation of multisensory integration as a computational task can be described via three key metrics: a temporal binding window, a spatial binding window, and a multisensory enhancement gain. Once I had validated the response of the model against these metrics, I perturbed the network into controlled states of dysfunction, from where I could both compare the responses of the network against those found in autism, as well as explore the network further to understand the causal neural pathways behind those altered responses. The

extension in temporal binding was attributable to an increase in NMDA currents and decreased inhibitive forces across perturbations, while the alterations in spatial binding had explanations that varied with the type of perturbation. While an increase in NMDA gain was the reason for an increase in the spatial binding window under reduced adaptation, the presence of a stronger surround inhibition was the determining factor leading to a reduced spatial window, when feedforward inhibition was reduced. An altered inhibitory balance followed every disruption, which aligns well with accounts of autism implicating disruptions in the E/I balance. The sections that follow take each result in turn and compare them with related findings from recent literature. In doing so, I provide further empirical support for these findings, as well as underline their translational implications. For example, when adaptation mechanisms would benefit ANNs that are optimized for a certain task, or how network parameters such as E/I balance could serve as targets for further therapeutic interventions.

The adaptive motion network described in this thesis highlights the role of adaptation as a tuneable prior signal, which manifests computationally as a lowering of response during sustained activity, while sharpening the sensitivity of the network to changes in input signals. With this model, I reproduced motion aftereffect phenomena and in doing so provided computational validity to classical accounts of the observation by Barlow & Hill (1963). The first step following model design was to ensure that the model of adaptation used in both V1- and MT-like layers was biologically rooted. After constructing an artificial network with an adaptive element, evaluation of the responses highlighted an adjustable trade-off between the accuracy of the network and the net activity of the units. The notion that adaptive codes maximize information transmission in the network has been previously explored, utilizing different computational methodologies than the one applied here. In the adaptive network that I implemented, this information transmission benefit manifested as reduced activity to sustained input, while enhancing sensitivity to changes in stimulus. While this result was expected in terms of network activity, it was surprising that to observe a reduction in the response latency of the adaptive network (while ANNs aren't typically utilized to derive temporal insights, the network activity when measured against the number of frames processed, showed a difference between networks).

**A computational study of adaptation**

AdaptNet's successful reproduction of motion adaptation phenomena adds to the mounting evidence which shows that incorporating biophysical mechanisms into computational networks leads to closer alignment of the network with biological data. Following a similar implementation strategy, where explicit modelling of biophysical mechanisms is prioritized, Idrees showed enhanced detection of dynamical retinal responses, in recent work. By adding photoreceptor and bipolar cell adaptation to deep networks, they improved the network's ability to predict retinal ganglion cell responses — a finding which loosely resembles the increase in sensitivity to change detection found in AdaptNet. Parallel work by Luczak et al. (2023) showed that Hebbian networks required 30-40% fewer computational steps to achieve comparable learning performance, upon implementation of bio-realistic neuronal adaptation mechanisms. By explicitly modelling adaptive pathways and then inferring from the results that follow, these works incorporate the idea of adaptation as a canonical computation that is seen across biological systems, rather than a dataset-specific implementation detail. An examination of related work in this area further highlights the need to incorporate adaptation into biological models simulating the visual cortex.

Over the last few decades, several groups have modelled motion processing, yet key aspects have been omitted. Modelling of the motion processing stream has progressed from Adelson and Bergen's (1985) spatiotemporal energy detectors through Simoncelli and Heeger's (1998) divisive normalization framework, all the way to modern DNNs like DorsalNet, which have captured increasingly sophisticated properties relating to area MT, which typically includes metrics like direction and speed selectivity. But because these models do not explicitly account for time dependent optimizations such as like adaptation, they cannot account for the optimization of information transmission, reduction in latency, or aftereffect phenomena that biological systems frequently exhibit. A more direct, interesting comparison of AdaptNet is with the work by Rideaux & Welchman (2020), where researchers designed a motion processing CNN utilizing motion energy estimates as linear computations. While they accounted for "static" illusions by exploiting variances in natural image statistics, the model could not account for time-varying aftereffect phenomena along with its underlying neural causation. More importantly, the models discussed here cannot account for strategies employed by the brain to reduce the metabolic burden of motion processing. This could have a more visible effect with the recent adoption of SNNs,

especially affecting studies comparing the energy burden attributed to the spiking dynamics of computational networks with the brain, or even with more fundamental concepts like the prioritization of initial spikes, during STDP based learning. Beyond computational inferences, incorporating mechanisms like adaptation could also lead to testable predictions that could then be verified using traditional experimentation.

Implementing adaptive mechanisms into computational simulations specifies how fast and by how much responses change, and as a result yields responses that are more suitable for comparison with psychophysical measurements. In a study of the auditory cortex, Rabinowitz et al. (2011) determined that neuronal gain would rescale with changes in spectro-temporal contrast, a result which generalized across stimuli. This time-varying gain rescaling was a testable prediction, which was then directly tested against ferret A1 recordings, which validated the responses. Computational work on object vision by Vinken et al. (2020) attributed a per-neuron adaptation state across a CNN, and resulted in predictions about suppression of activity in response to repeated stimuli, and also about an increase in adaptation strength along a feedforward hierarchy. Upon matching the findings from the model with the rat V1 to LI pathway, unexplored forecasts for MEG/EEG latencies could also be generated that traditional CNNs could not supply. In a similar implementation of a recurrent network of area V1 with short-timescale adaptation implemented, Quiroga et al. (2019) noted a sign reversal of the tilt aftereffect at sub-second timescales. They tested findings from the model in human subjects, including the recovery time course of the tilt aftereffect. Similarly, the work here in this thesis predicts opposing neural ensembles would have time-varying activity in response to the waterfall illusion, which would correlate with a stronger BOLD/EEG signal that would fluctuate over time. Reaction time benefits offered by adaptation would also be a testable finding, but one that might be difficult experimentally due to the widespread presence of adaptive mechanisms in biological neurons. While implementation of such adaptive principles proves useful as far as biological modelling is concerned, adaptation mechanisms could also confer benefits to computational fields such as artificial intelligence (AI).

**Applications of adaptation as a computational tool**

A key property that AdaptNet showed is a reduction in sustained neural activity while only taking marginal losses in the representational accuracy of sustained motion, which translates to an actionable mechanism for any computational system operating

under resource constraints. This realization has compelled several recent computational systems to implement a similar approach, with observable benefits. The popular approach seems to be direct adaptation of contrast in sensors or pixel data (Chane et al., 2016; Paul Moeys et al., 2018), along with innovative methods which extend of the concept to event suppression (Vanarse, 2016). With a recent rise in neuromorphic hardware systems that directly simulate spiking mechanics via hardware instead of relying to transistor-based processing, there has been a rise in the development of more biologically inspired computing. A widely adopted method of implementation is via use of spiking networks that utilize adaptive units, partly because of an increased availability of computational libraries available that incorporate them (Richter et al., 2024; Stradmann et al., 2022). More experimental work has focused on incorporating realistic forms of adaptation like stimulation specific adaptation, to uncover similar benefits like improved change detection while suppressing responses to repeat stimuli (Vanattou-Saïfoudine et al., 2021). Developments in material science have also led to advancements in the neuromorphic synapses themselves, inspired by synaptic adaptation (Wu et al., 2024). Apart from lowering the energy burden, adaptive mechanisms have also been shown to reduce the computational requirements of neural networks. A recent study by Baronig et al. (2025) implemented realistic adaptation mechanisms similar in design to the AdaptNet model, which resulted in less computational requirements in an SNN (a reduction in parameters needed by orders of magnitude). Since spike frequency adaptation suppresses firing, it also reduces the metabolic cost of signalling within adapted networks (Salaj et al., 2021). Inspired by these advances in adaptive computing, commercially available neuromorphic systems like Intel's Loihi-2 have also started to support the integration of adaptive neurons (Blouw et al., 2019). Following a similar computational approach, the second study explored in this thesis utilizes spiking networks to study states of dysfunction in a biological system.

**Validating the superior colliculus multisensory model: why "biological detail" matters**

Computational modelling in neuroscience has seen a progression in mechanistic detail over the years, hinging largely on advancements made in computational hardware. This move towards more realistic modelling has been motivated by the drive to draw inferences that are comparable with biology, which

traditional weight-only approaches do not typically converge on. Divisive normalisation is an information-maximizing computation that exemplifies this. While early CNN approaches could match average tuning across weights and produce responses that matched biology to an extent, they fell short of capturing fundamental interactions like cross orientation suppression and contrast dependent summation. This was mainly due to the lack of an explicitly implemented gain control mechanism. When implemented as a mechanism (rather than an extra weight) such as divisive normalisation based gain control, the network predicts those nonlinearities, among other interactions like attentional modulation and cue reliability (Carandini & Heeger, 2012). Similarly, when researchers tried to capture the responses of the early inferotemporal cortex with a deep feedforward network, they mispredicted later population states and backward masking effects (Kar et al., 2019). By implementing time-varying recurrence, they captured these late neural dynamics. Such time-dependent computations are typically out-of-reach without time-explicit mechanisms implemented. More in line with the current study, rate-based models of the SC reproduce key findings including inverse effectiveness, but fall short of illustrating the neural dynamics that make such phenomena possible. In addition, it isn't feasible to explore receptor kinetics or the effects of synaptic perturbations in rate-based models as they do not provide the appropriate level of resolution required. The need for biological realism directly motivated the design of the superior colliculus model used in the second study.

The model of the superior colliculus described in this thesis reproduced five different metrics commonly associated with multisensory integration, at both systems as well as circuit resolutions. This validation was largely made possible by the explicit modelling of biophysical mechanisms combined with a cross-modal training paradigm, rather than depending on these qualities to emerge from abstract connection weights as a result of training alone. The network more strongly weights reliable inputs while also selectively enhancing signals with low input intensities, both qualities documented across decades of superior colliculus research (Ohshiro et al., 2011; Stein & Stanford, 2008). Latency recordings from the model also show a multisensory benefit of about 19 ms for audiovisual stimuli compared to either modality alone, while spatial and binding windows fuse input signals within ±26° and -150 to +70 ms respectively. These metrics emerge primarily as a consequence of the design choices made — AMPA receptors providing 2.5 ms excitation for immediate responses, NMDA receptors

sustaining 40-120 ms depolarization over longer temporal gaps, and GABAergic inhibition that gates activity over longer timescales. Out of these choices, the voltage dependent Mg block serves a key role, activating only when multimodal inputs converge to depolarize the neuron beyond -35 mV. Beyond these measures of multisensory integration, the model also satisfied general neural constraints such as distance-dependent noise correlations and stimulus-evoked variability suppression. The trend of variance quenching in response to a stimulus displayed by the network matched Fano-factor readings taken from across the cortex (Churchland et al., 2010). Similarly, the correlation in noise between neurons in the multisensory layer was indicative of network topography, and matched trends seen in areas V1 and V4 of the macaque (Smith & Sommer, 2013). Additionally, these bounds restrict the operating regime of the network to a viable range, the boundaries of which would serve as starting points for subsequent perturbation experiments.

**Perturbation phenotype I: reduced adaptation**

A reduction in neuronal adaptation lead to significant alterations in key multisensory metrics, mirroring the responses of biological networks to this dysfunction. Both the spatial and temporal binding windows expanded by significant margins, accompanied by a drop in bimodal sensitivity. While adaptation as a mechanism has previously been shown to be attenuated in certain brain regions in autistic cohorts, these findings have largely been correlational in nature, without explicit causative linking (Lawson et al., 2015; Millin et al., 2018; Turi et al., 2015). One of the main goals of modelling the superior colliculus was to generate testable predictions about the precise effect of neural adaptation on the metrics of integration discussed here. To tackle that goal, the neural dynamics resulting from reduced adaptation were first explored, which revealed an increase in NMDA current accompanied by an increase in relief time for the $Mg^{2+}$ block. The prolonged depolarization ensuing from the increase in slow NMDA currents could explain the expansion in the temporal binding metrics, as well as the decrease in the activity valley between adjacent neural populations, which led the decrease in the spatial binding window. When considered alongside parallel investigations of neural adaptation in the context of ASD, these observations solidify pre-existing findings from biology and provide testable predictions for clinical researchers.

Research into adaptation defects in autism has shown that this dysfunction has distinct neurochemical signatures that differ from other modes of perturbations,

although direct tests of sensory adaptation in autism are sparse. Previous work has shown that auditory loudness adaptation is impaired in autism (Lawson et al., 2015), while a reduction in adaptive aftereffects was observed for numerosity (Turi et al., 2015). In line with the current study, fMRI investigations have shown reduced cortical adaptation to repeated audiovisual stimuli (Millin et al., 2018), as well as to biological motion (van Boxtel et al., 2016). While these studies have correlated disturbances in adaptive mechanics with ASD, the study described in this thesis directly links this perturbation to extended binding windows and defects in multisensory integration. Conversely, this finding predicts that restoring adaptive mechanisms could rescue observed alterations in integration metrics. In biology, spike frequency adaptation depends on slow potassium currents like those gated by Kv7/M-channels, whose opening stabilizes membrane potential and curbs uncontrolled firing (Luque et al., 2024). Interestingly, a recent finding has implicated the same Kv7/M-channels in ASD phenotypes; restoring these channels resulted in rescuing of ASD-related symptoms (Oh et al., 2023), supporting the idea that neural adaptation defects could be a causative factor contributing to autistic traits.

**Perturbation phenotype II: reduced feedforward inhibition**

In contrast to the uniform changes associated with decreased neural adaptation, alteration in E/I balance affected the multisensory integration metrics in a heterogenous fashion — broadening the temporal binding window by 32%, while narrowing the spatial window by 23% and significantly reducing bimodal integration benefits. The changes in spatial binding observed following this perturbation are due to the decrease in early inhibition leading to a larger engagement of surround inhibition, which in turn tightens spatial binding. A reduced early inhibitory drive also typically leads to an increase in temporal binding windows, which is observed in the networks' responses. Across human postmortem and animal studies, ASD is associated with reduced parvalbumin-expressing interneurons and altered GAD65/67 receptors — features that would weaken early inhibitory gating (Contractor et al., 2021; Fatemi et al., 2002; Hashemi et al., 2017; Pagano et al., 2023). Functionally, PV interneurons sharpen spike timing and their loss results in longer temporal windows of integration, which is in line with the current findings. By the same account, this superior colliculus model predicts that activation along the PV axis should contract temporal integration windows while broadening spatial binding, while PV suppression should

lead to the opposite. This is consistent with PV's role in spike timing control, with literature showing inhibitory forces tighten temporal integration windows. Designing PV targeted experiments in superior colliculus simultaneously measuring both the temporal and spatial binding windows would serve as a test for this prediction. An examination of related works highlights the effectiveness of this computational approach, in the context of inhibition.

While previous computational studies have revealed insights on the effects of inhibition on multisensory integration, it is not always straightforward to compare their findings with biology due to the level of abstraction implemented. Perhaps the most detailed model of collicular integration to date has been work by Cuppini et al (2010) where researchers designed a rate based superior colliculus model with excitatory and inhibitory pools, lateral competition, and cortical gating. While the model reproduced certain qualities of integration like inverse effectiveness, the abstraction in receptor design meant that inferences about NMDA/AMPA kinetics or feedforward inhibition timing could not be drawn. Furthermore, a lack of spiking mechanics restricted further inferences about spatial and temporal binding metrics. Moving on to more abstract models, pioneering work by Ohshiro et al (2011) implicated divisive normalisation as a central mechanism in multisensory integration, and accounted for inhibition with "shunting" terms incorporated in their mathematical description of integration, inverse effectiveness, and cue reliability weighting. While they reproduced key metrics like inverse effectiveness and spatial principle across cue reliabilities with a canonical mathematical operation, the level of abstraction in their work similarly led to restrictions in inference. For example, it wasn't possible to study the lengthening of temporal binding metrics or the specific effect of surround inhibition on integration by probing the mathematical description of their model. Parallel work by Rideaux et al (2021) explored integration using an ANN which developed congruent/opposite units when trained to perform causal inference . Because inhibition in the model was implicit in the weights/nonlinearities instead of an explicit E/I pathway, it wasn't possible to ask, for instance, how the timing of inhibition, surround inhibition, or NMDA time constants would selectively reshape temporal or spatial windows. While rate/normalization models have shown to be effective at summarising behavioural trends like inverse effectiveness and reliability weighting, circuit-explicit SC models could enable a more thorough analysis of the neural machinery behind multisensory integration.

**Perturbation phenotype III: NMDA bidirectionality**

NMDA manipulations to the network affect the temporal and spatial binding windows along a bidirectional axis of dysfunction. While previous work in cat superior colliculus has causally linked disruptions in collicular integration with NMDA hypofunction, no work has tested how temporal and spatial windows of integration are altered in response to variances in NMDA expression. Taking a computational approach, the model predicts that increases in NMDA conductance would lead to an enhancement of bimodal response enhancement (although with an extension in temporal and spatial binding windows), while hypo-function results in reduced bimodal enhancement along a narrowing in binding metrics. These observations are a direct reflection of NMDA's role in facilitating late-stage temporal integration, while also playing a role in tuning the spatial boundaries of neurons. Being a synaptic perturbation rather than a change in circuit dynamics, the effects of altering NMDA expression are more intuitive to analyse than other more complex network disruptions. An increase in NMDA conductance directly increases late-stage currents into the neurons, which thereby increases the temporal binding window. A rise in these currents also leads to a higher spread in activity in a topographic group, which translates to a broader spatial binding window. While no study has mechanistically linked alterations in NMDA functionality directly to temporal or spatial windows, findings from biology provide correlational support for the same. A shortening of NMDA time constant during development in humans also coincides with a narrowing of temporal binding window with age, showing that the receptor may contribute to the temporal aspects of integration. Interestingly, in our network, NMDA hyper-function also causes an increase in bimodal sensitivity, with a decrease in expression resulting in the opposite, which resembles the axis of dysfunction found in the Xenopus tectum. These findings along with the predictions put forward by this superior colliculus model support the idea of NMDA receptors being a key contributing factor to multisensory integration, maintaining a balance between bimodal enhancement and binding metrics in a bidirectional fashion.

**Limitations**

Given the computational resources available today, researchers must make a key trade-off between choosing the appropriate level of biological plausibility in network design and maintaining feasibility in computation. Respecting this constraint, I have

made abstractions in the networks presented in this thesis that do not compromise the validity of the findings but are nevertheless important to consider alongside the results. The adaptive network utilizes a functionally modified ANN to study the phenomenon, but learning in the network is still dependent on backpropagation, which leaves room for natural emergence of a solution, but undermines the importance of timing. In addition to this, energy measurements in the network are measured in terms of activity magnitudes and not estimated ATP cost or simulations of neurovascular demand. As a result, translations to biological measurements might not be directly possible. On the other hand, while the superior colliculus model does implement a spiking network with Hebbian learning mechanisms, specific neural pathways are omitted for computational simplicity, like the top-down pathway. In the human brain, the top-down collicular projection connects higher order cortical areas to the superior colliculus and is critical in the facilitation of multisensory integration, with analogous pathways tuning multisensory integration in the cat SC. Additionally, developmental dynamics aren't explored using this model, while developmental changes are typically implicated in ASD. But rather than just for purely computational simplifications, these design decisions were also made to maximize the inferences drawn from these models.

While these design decisions limit the biological validity of the models discussed here to an extent, the same decisions increase computational ease while maintaining the focus on the key mechanisms to be explored. In the case of AdaptNet, while the usage of backpropagation as the central learning mechanism renders any study of precise neural timing difficult, it still leaves room for a sequential analysis of the different stages of motion processing, based on the discrete activity in the network. By choosing to focus on ANN dynamics rather than custom built energy mechanisms, the efficiency inferences drawn from this network are also easily transferrable to other similar artificial systems used today. On the other hand, the omission of top-down influences to collicular neurons shifts the primary focus of the study to the fundamental mechanisms underlying multisensory integration. This enables an incremental study that centres around three basic mechanisms underlying integration, rather than complicating the validity of the results by incorporating higher additional pathways that haven't been fully explored in biological systems yet. The scope of the study involved model validation and perturbation experiments post training, but the same network could just as easily be extended to enable developmental analysis, which could serve as a goal for future studies utilizing this network. Both networks discussed in this thesis

have been designed to easily incorporate further extensions and mechanisms, to leave room for further exploration.

## Conclusion

The studies explored in this thesis advocate for the incorporation of biologically grounded mechanisms into network simulations of biological systems, which holds especially relevant against the backdrop of the recent increase in computational models that solely prioritize performance benchmarks. Adaptive mechanisms embedded in a motion processing network reproduced both aftereffect phenomena as well as the energy-efficiency trade-off long hypothesized to be a primary functional benefit of adaptation; a spiking model of the superior colliculus reproduced canonical multisensory benchmarks without explicitly training for them, while offering insights into how perturbations in the network could lead to disruptions in multisensory integration that have commonly been associated with neurodevelopmental conditions like ASD. These results substantiate the broader claim motivating the thesis, and future extensions that incorporate explicit metabolic costs or top-down cortical influences will further tighten the biological comparability while preserving economy of detail. In doing so, these networks advance a principled path from benchmarks to mechanisms and from mechanisms to translation.

# Appendix

## Chapter 2

- A motion processing neural network as is implemented in this thesis extracts ‘motion energy’ from motion sequences of images that move across a larger scene, typically with a step size of a few pixels.
- For example, motion sequences could be images created using a window of about 20x20, sliding across a larger scene image that is 100x100. Each stride or movement step of the window would result in a new image that could be appended to the original motion sequence set.
- Because subsequent images are derived from a larger scenic image, there shall be slight yet consistent shifts in the direction of pixels across the images, which could be viewed as a form of ‘motion energy’ that neural networks can learn to extrapolate.
- The neural network used in the first chapter of this work is trained via supervised backpropagation, where the prediction of the network is compared against expected value (motion direction and velocity vectors in this case), and then the errors are propagated back through the network to update the weights between the neurons. Once the network has been exposed to all the sequences in the dataset, it is trained again from the start, and each of these runs through the data is called an epoch. Such epoch run training is standard practice in machine learning.
- Networks utilizing this training regime could suffer from the vanishing gradient problem, where gradients become extremely small as they move back through a neural network. To remedy this, ReLU activation functions are used in between the layers of the neural network.

## Chapter 3

- In contrast to the standardized backpropagation done in ANNs, the network utilized in chapter 3 is a spiking neural system, designed to learn using Hebbian strategies and channelling mechanisms.
- Multisensory integration in the network is characterized using various methodologies, both neural and behavioural. Where possible, neural implementations of standard multisensory tests are implemented, as it provides for a direct observation of multisensory advantage.

- One such example is measurement of response latency. While several psychophysics investigations have utilized the RACE model of latency advantage to facilitate non-invasive ease of recording, the computational study done here enables and implementation of a delta latency time-to-first-spike measurement here that measures the multisensory advantage conferred to the network, at a membrane voltage level.

## Bibliography


Abbott, L. F. (1994). Decoding neuronal firing and modelling neural networks. *Quarterly Reviews of Biophysics*, *27*(3), 291–331. https://doi.org/10.1017/s0033583500003024

Abbott, L. F., & Nelson, S. B. (2000). Synaptic plasticity: Taming the beast. *Nature Neuroscience*, *3 Suppl*, 1178–1183. https://doi.org/10.1038/81453

Abbott, L. F., & Regehr, W. G. (2004). Synaptic computation. *Nature*, *431*(7010), 796–803. https://doi.org/10.1038/nature03010

Abbott, L. F., Varela, J. A., Sen, K., & Nelson, S. B. (1997). Synaptic depression and cortical gain control. *Science (New York, N.Y.)*, *275*(5297), 220–224. https://doi.org/10.1126/science.275.5297.221

Adams, R. A., Pinotsis, D., Tsirlis, K., Unruh, L., Mahajan, A., Horas, A. M., Convertino, L., Summerfelt, A., Sampath, H., Du, X. M., Kochunov, P., Ji, J. L., Repovs, G., Murray, J. D., Friston, K. J., Hong, L. E., & Anticevic, A. (2022). Computational Modeling of Electroencephalography and Functional Magnetic Resonance Imaging Paradigms Indicates a Consistent Loss of Pyramidal Cell Synaptic Gain in Schizophrenia. *Biological Psychiatry*, *91*(2), 202–215. https://doi.org/10.1016/j.biopsych.2021.07.024

Adibi, M., Clifford, C. W. G., & Arabzadeh, E. (2013). Informational basis of sensory adaptation: Entropy and single-spike efficiency in rat barrel cortex. *The Journal of Neuroscience: The Official Journal of the Society for Neuroscience*, *33*(37), 14921–14926. https://doi.org/10.1523/JNEUROSCI.1313-13.2013

Adibi, M., McDonald, J. S., Clifford, C. W. G., & Arabzadeh, E. (2013). Adaptation Improves Neural Coding Efficiency Despite Increasing Correlations in Variability. *The Journal of Neuroscience*, *33*(5), 2108–2120. https://doi.org/10.1523/JNEUROSCI.3449-12.2013

Agnes, E. J., & Vogels, T. P. (2024). Co-dependent excitatory and inhibitory plasticity accounts for quick, stable and long-lasting memories in biological networks. *Nature Neuroscience*, *27*(5), 964–974. https://doi.org/10.1038/s41593-024-01597-4

Alais, D., & Burr, D. (2004). The Ventriloquist Effect Results from Near-Optimal Bimodal Integration. *Current Biology*, *14*(3), 257–262. https://doi.org/10.1016/j.cub.2004.01.029

Albright, T. D. (1984). Direction and orientation selectivity of neurons in visual area MT of the macaque. *Journal of Neurophysiology*, *52*(6), 1106–1130. https://doi.org/10.1152/jn.1984.52.6.1106

Al-Fatly, B., Ewert, S., Kübler, D., Kroneberg, D., Horn, A., & Kühn, A. A. (2019). Connectivity profile of thalamic deep brain stimulation to effectively treat essential tremor. *Brain*, *142*(10), 3086–3098. https://doi.org/10.1093/brain/awz236

Alizadeh, A., & Van Opstal, A. J. (2022). A spiking neural network model of the Superior Colliculus that is robust to changes in the spatial–temporal input. *Scientific Reports*, *12*(1), 6916. https://doi.org/10.1038/s41598-022-10991-6

Allman, J., Miezin, F., & McGuinness, E. (1985). Direction- and Velocity-Specific Responses from beyond the Classical Receptive Field in the Middle Temporal Visual Area (MT). *Perception*, *14*(2), 105–126. https://doi.org/10.1068/p140105

Antoine, M. W., Langberg, T., Schnepel, P., & Feldman, D. E. (2019). Increased excitation-inhibition ratio stabilizes synapse and circuit excitability in four autism mouse models. *Neuron*, *101*(4), 648. https://doi.org/10.1016/j.neuron.2018.12.026

Antunes, F. M., Nelken, I., Covey, E., & Malmierca, M. S. (2010). Stimulus-Specific Adaptation in the Auditory Thalamus of the Anesthetized Rat. *PLOS ONE*, *5*(11), e14071. https://doi.org/10.1371/journal.pone.0014071

Atallah, B. V., Bruns, W., Carandini, M., & Scanziani, M. (2012). Parvalbumin-expressing interneurons linearly transform cortical responses to visual stimuli. *Neuron*, *73*(1), 159–170. https://doi.org/10.1016/j.neuron.2011.12.013

Attwell, D., & Laughlin, S. B. (2001). An Energy Budget for Signaling in the Grey Matter of the Brain. *Journal of Cerebral Blood Flow & Metabolism*, *21*(10), 1133–1145. https://doi.org/10.1097/00004647-200110000-00001

Avissar, M., Furman, A. C., Saunders, J. C., & Parsons, T. D. (2007). Adaptation Reduces Spike-Count Reliability, But Not Spike-Timing Precision, of Auditory Nerve Responses. *The Journal of Neuroscience*, *27*(24), 6461–6472. https://doi.org/10.1523/JNEUROSCI.5239-06.2007

Azevedo, F. A. C., Carvalho, L. R. B., Grinberg, L. T., Farfel, J. M., Ferretti, R. E. L., Leite, R. E. P., Jacob Filho, W., Lent, R., & Herculano-Houzel, S. (2009). Equal numbers of neuronal and nonneuronal cells make the human brain an isometrically scaled-up primate brain. *The Journal of Comparative Neurology*, *513*(5), 532–541. https://doi.org/10.1002/cne.21974

Baccus, S. A., & Meister, M. (2002). Fast and Slow Contrast Adaptation in Retinal Circuitry. *Neuron*, *36*(5), 909–919. https://doi.org/10.1016/S0896-6273(02)01050-4

Bahry, J. A., Fedder-Semmes, K. N., Sceniak, M. P., & Sabo, S. L. (2021). An Autism-Associated de novo Mutation in GluN2B Destabilizes Growing Dendrites by Promoting Retraction and Pruning. *Frontiers in Cellular Neuroscience*, *15*. https://doi.org/10.3389/fncel.2021.692232

Baillet, S. (2017). Magnetoencephalography for brain electrophysiology and imaging. *Nature Neuroscience*, *20*(3), 327–339. https://doi.org/10.1038/nn.4504

Bair, W., & Movshon, J. A. (2004). Adaptive Temporal Integration of Motion in Direction-Selective Neurons in Macaque Visual Cortex. *The Journal of Neuroscience*, *24*(33), 7305–7323. https://doi.org/10.1523/JNEUROSCI.0554-04.2004

Balasco, L., Provenzano, G., & Bozzi, Y. (2020). Sensory Abnormalities in Autism Spectrum Disorders: A Focus on the Tactile Domain, From Genetic Mouse Models to the Clinic. *Frontiers in Psychiatry*, *10*. https://doi.org/10.3389/fpsyt.2019.01016

Banerjee, A., Rikhye, R. V., Breton-Provencher, V., Tang, X., Li, C., Li, K., Runyan, C. A., Fu, Z., Jaenisch, R., & Sur, M. (2016). Jointly reduced inhibition and excitation underlies circuit-wide changes in cortical processing in Rett syndrome. *Proceedings of the National Academy of Sciences of the United States of America*, *113*(46), E7287–E7296. https://doi.org/10.1073/pnas.1615330113

Barlow, H. B. (2012). Possible Principles Underlying the Transformations of Sensory Messages. In W. A. Rosenblith (Ed.), *Sensory Communication* (pp. 216–234). The MIT Press. https://doi.org/10.7551/mitpress/9780262518420.003.0013

Barlow, H. B., & Hill, R. M. (1963). Evidence for a Physiological Explanation of the Waterfall Phenomenon and Figural After-effects. *Nature*, *200*(4913), 1345–1347. https://doi.org/10.1038/2001345a0

Barlow, H., & Földiàgk, P. (1989). *Adaptation and decorrelation in the cortex*.

Baronig, M., Ferrand, R., Sabathiel, S., & Legenstein, R. (2025). Advancing spatio-temporal processing through adaptation in spiking neural networks. *Nature Communications*, *16*(1), 5776. https://doi.org/10.1038/s41467-025-60878-z

Barri, A., Wiechert, M. T., Jazayeri, M., & DiGregorio, D. A. (2022). Synaptic basis of a sub-second representation of time in a neural circuit model. *Nature Communications*, *13*(1), 7902. https://doi.org/10.1038/s41467-022-35395-y

Basso, M. A., & May, P. J. (2017). Circuits for Action and Cognition: A View from the Superior Colliculus. *Annual Review of Vision Science*, *3*, 197–226. https://doi.org/10.1146/annurev-vision-102016-061234

Battaglia, P. W., Jacobs, R. A., & Aslin, R. N. (2003). Bayesian integration of visual and auditory signals for spatial localization. *Journal of the Optical Society of America. A, Optics, Image Science, and Vision*, *20*(7), 1391–1397. https://doi.org/10.1364/josaa.20.001391

Bean, B. P. (2007). The action potential in mammalian central neurons. *Nature Reviews. Neuroscience*, *8*(6), 451–465. https://doi.org/10.1038/nrn2148

Beker, S., Foxe, J. J., & Molholm, S. (2018). Ripe for solution: Delayed development of multisensory processing in autism and its remediation. *Neuroscience and Biobehavioral Reviews*, *84*, 182–192. https://doi.org/10.1016/j.neubiorev.2017.11.008

Bellec, G., Scherr, F., Subramoney, A., Hajek, E., Salaj, D., Legenstein, R., & Maass, W. (2020). A solution to the learning dilemma for recurrent networks of spiking neurons. *Nature Communications*, *11*(1), 3625. https://doi.org/10.1038/s41467-020-17236-y

Bellone, C., & Nicoll, R. A. (2007). Rapid bidirectional switching of synaptic NMDA receptors. *Neuron*, *55*(5), 779–785. https://doi.org/10.1016/j.neuron.2007.07.035

Benavidez, N. L., Bienkowski, M. S., Zhu, M., Garcia, L. H., Fayzullina, M., Gao, L., Bowman, I., Gou, L., Khanjani, N., Cotter, K. R., Korobkova, L., Becerra, M., Cao, C., Song, M. Y., Zhang, B., Yamashita, S., Tugangui, A. J., Zingg, B., Rose, K., … Dong, H.-W. (2021). Organization of the inputs and outputs of the mouse superior colliculus. *Nature Communications*, *12*(1), 4004. https://doi.org/10.1038/s41467-021-24241-2

Benda, J., & Herz, A. V. M. (2003). A universal model for spike-frequency adaptation. *Neural Computation*, *15*(11), 2523–2564. https://doi.org/10.1162/089976603322385063

Bhatia, A., Moza, S., & Bhalla, U. S. (2019). Precise excitation-inhibition balance controls gain and timing in the hippocampus. *eLife*, *8*, e43415. https://doi.org/10.7554/eLife.43415

Binda, P., Bruno, A., Burr, D. C., & Morrone, M. C. (2007). Fusion of Visual and Auditory Stimuli during Saccades: A Bayesian Explanation for Perisaccadic Distortions. *Journal of Neuroscience*, *27*(32), 8525–8532. https://doi.org/10.1523/JNEUROSCI.0737-07.2007

Binns, K. E., & Salt, T. E. (1994). Excitatory amino acid receptors participate in synaptic transmission of visual responses in the superficial layers of the cat superior colliculus. *The European Journal of Neuroscience*, *6*(1), 161–169. https://doi.org/10.1111/j.1460-9568.1994.tb00257.x

Binns, K. E., & Salt, T. E. (1996). Importance of NMDA receptors for multimodal integration in the deep layers of the cat superior colliculus. *Journal of Neurophysiology*, *75*(2), 920–930. https://doi.org/10.1152/jn.1996.75.2.920

Binns, K. E., & Salt, T. E. (1997). Different roles for GABAA and GABAB receptors in visual processing in the rat superior colliculus. *The Journal of Physiology*, *504*(Pt 3), 629. https://doi.org/10.1111/j.1469-7793.1997.629bd.x

Blouw, P., Choo, X., Hunsberger, E., & Eliasmith, C. (2019). *Benchmarking Keyword Spotting Efficiency on Neuromorphic Hardware* (No. arXiv:1812.01739). arXiv. https://doi.org/10.48550/arXiv.1812.01739

Born, R. T., & Bradley, D. C. (2005). STRUCTURE AND FUNCTION OF VISUAL AREA MT. *Annual Review of Neuroscience*, *28*(1), 157–189. https://doi.org/10.1146/annurev.neuro.26.041002.131052

Bouton, S., Delgado-Saa, J., Olasagasti, I., & Giraud, A.-L. (2020). Audio-visual combination of syllables involves time-sensitive dynamics following from fusion failure. *Scientific Reports*, *10*(1), 18009. https://doi.org/10.1038/s41598-020-75201-7

Brand, A., Behrend, O., Marquardt, T., McAlpine, D., & Grothe, B. (2002). Precise inhibition is essential for microsecond interaural time difference coding. *Nature*, *417*(6888), 543–547. https://doi.org/10.1038/417543a

Breakspear, M. (2017). Dynamic models of large-scale brain activity. *Nature Neuroscience*, *20*(3), 340–352. https://doi.org/10.1038/nn.4497

Brenner, N., Bialek, W., & De Ruyter Van Steveninck, R. (2000). Adaptive Rescaling Maximizes Information Transmission. *Neuron*, *26*(3), 695–702. https://doi.org/10.1016/S0896-6273(00)81205-2

Brette, R., & Gerstner, W. (2005). Adaptive exponential integrate-and-fire model as an effective description of neuronal activity. *Journal of Neurophysiology*, *94*(5), 3637–3642. https://doi.org/10.1152/jn.00686.2005

Brigman, J. L., Wright, T., Talani, G., Prasad-Mulcare, S., Jinde, S., Seabold, G. K., Mathur, P., Davis, M. I., Bock, R., Gustin, R. M., Colbran, R. J., Alvarez, V. A., Nakazawa, K., Delpire, E., Lovinger, D. M., & Holmes, A. (2010). Loss of GluN2B-Containing NMDA Receptors in CA1 Hippocampus and Cortex Impairs Long-Term Depression, Reduces Dendritic Spine Density, and Disrupts Learning. *The Journal of Neuroscience*, *30*(13), 4590. https://doi.org/10.1523/JNEUROSCI.0640-10.2010

Britten, K. H. (2008). Mechanisms of self-motion perception. *Annual Review of Neuroscience*, *31*, 389–410. https://doi.org/10.1146/annurev.neuro.29.051605.112953

Brunel, N. (2000). Dynamics of sparsely connected networks of excitatory and inhibitory spiking neurons. *Journal of Computational Neuroscience*, *8*(3), 183–208. https://doi.org/10.1023/a:1008925309027

Brunel, N., & Wang, X. J. (2001). Effects of neuromodulation in a cortical network model of object working memory dominated by recurrent inhibition. *Journal of Computational Neuroscience*, *11*(1), 63–85. https://doi.org/10.1023/a:1011204814320

Brunel, N., & Wang, X.-J. (2003). What determines the frequency of fast network oscillations with irregular neural discharges? I. Synaptic dynamics and excitation-inhibition balance. *Journal of Neurophysiology*, *90*(1), 415–430. https://doi.org/10.1152/jn.01095.2002

Burr, D., & Thompson, P. (2011). Motion psychophysics: 1985–2010. *Vision Research*, *51*(13), 1431–1456. https://doi.org/10.1016/j.visres.2011.02.008

Buzsáki, G., & Draguhn, A. (2004). Neuronal oscillations in cortical networks. *Science (New York, N.Y.)*, *304*(5679), 1926–1929. https://doi.org/10.1126/science.1099745

Buzsáki, G., & Wang, X.-J. (2012). Mechanisms of Gamma Oscillations. *Annual Review of Neuroscience*, *35*, 203. https://doi.org/10.1146/annurev-neuro-062111-150444

C, S. C., Sh, I., C, P., & Rb, B. (2016). Event-Based Tone Mapping for Asynchronous Time-Based Image Sensor. *PubMed*. https://pubmed.ncbi.nlm.nih.gov/27642275/

Cadieu, C. F., Hong, H., Yamins, D. L. K., Pinto, N., Ardila, D., Solomon, E. A., Majaj, N. J., & DiCarlo, J. J. (2014). Deep Neural Networks Rival the Representation of Primate IT Cortex for Core Visual Object Recognition. *PLoS Computational Biology*, *10*(12), e1003963. https://doi.org/10.1371/journal.pcbi.1003963

Calvert, G. A., Hansen, P. C., Iversen, S. D., & Brammer, M. J. (2001). Detection of audio-visual integration sites in humans by application of electrophysiological criteria to the BOLD effect. *NeuroImage*, *14*(2), 427–438. https://doi.org/10.1006/nimg.2001.0812

Cang, J., Chen, C., Li, C., & Liu, Y. (2024). Genetically defined neuron types underlying visuomotor transformation in the superior colliculus. *Nature Reviews Neuroscience*, *25*(11), 726–739. https://doi.org/10.1038/s41583-024-00856-4

Carandini, M., & Heeger, D. J. (2012). Normalization as a canonical neural computation. *Nature Reviews Neuroscience*, *13*(1), 51–62. https://doi.org/10.1038/nrn3136

Carandini, M., Heeger, D. J., & Anthony Movshon, J. (1999). Linearity and Gain Control in V1 Simple Cells. In P. S. Ulinski, E. G. Jones, & A. Peters (Eds.), *Cerebral Cortex* (Vol. 13, pp. 401–443). Springer US. https://doi.org/10.1007/978-1-4615-4903-1_7

Carlén, M., Meletis, K., Siegle, J. H., Cardin, J. A., Futai, K., Vierling-Claassen, D., Rühlmann, C., Jones, S. R., Deisseroth, K., Sheng, M., Moore, C. I., & Tsai, L.-H. (2012). A critical role for NMDA receptors in parvalbumin interneurons for gamma rhythm induction and behavior. *Molecular Psychiatry*, *17*(5), 537–548. https://doi.org/10.1038/mp.2011.31

Cascio, C., McGlone, F., Folger, S., Tannan, V., Baranek, G., Pelphrey, K. A., & Essick, G. (2008). Tactile perception in adults with autism: A multidimensional psychophysical study. *Journal of Autism and Developmental Disorders*, *38*(1), 127–137. https://doi.org/10.1007/s10803-007-0370-8

Cathala, L., Misra, C., & Cull-Candy, S. (2000). Developmental profile of the changing properties of NMDA receptors at cerebellar mossy fiber-granule cell synapses. *The Journal of Neuroscience: The Official Journal of the Society for Neuroscience*, *20*(16), 5899–5905. https://doi.org/10.1523/JNEUROSCI.20-16-05899.2000

Catterall, W. A., Raman, I. M., Robinson, H. P. C., Sejnowski, T. J., & Paulsen, O. (2012). The Hodgkin-Huxley Heritage: From Channels to Circuits. *The Journal of Neuroscience*, *32*(41), 14064. https://doi.org/10.1523/JNEUROSCI.3403-12.2012

Cha, J. H., Kim, J. M., Yun, H.-J., Chin, H., Kim, H. J., Kim, W., Kim, S. Y., Lim, B. C., Kim, K. J., Lee, S., & Chae, J.-H. (2025). Exploring gene-phenotype relationships in GRIN-related neurodevelopmental disorders. *Npj Genomic Medicine*, *10*(1), 40. https://doi.org/10.1038/s41525-025-00499-z

Chen, Q., Deister, C. A., Gao, X., Guo, B., Lynn-Jones, T., Chen, N., Wells, M. F., Liu, R., Goard, M. J., Dimidschstein, J., Feng, S., Shi, Y., Liao, W., Lu, Z., Fishell, G., Moore, C. I., & Feng, G. (2020). Dysfunction of cortical GABAergic neurons leads to sensory hyper-reactivity in a Shank3 mouse model of ASD. *Nature Neuroscience*, *23*(4), 520–532. https://doi.org/10.1038/s41593-020-0598-6

Choi, I., Lee, J.-Y., & Lee, S.-H. (2018). Bottom-up and top-down modulation of multisensory integration. *Current Opinion in Neurobiology*, *52*, 115–122. https://doi.org/10.1016/j.conb.2018.05.002

Churchland, M. M., & Lisberger, S. G. (2001). Shifts in the population response in the middle temporal visual area parallel perceptual and motor illusions produced by apparent motion. *The Journal of Neuroscience*, *21*(23), 9387–9402.

Churchland, M. M., Yu, B. M., Cunningham, J. P., Sugrue, L. P., Cohen, M. R., Corrado, G. S., Newsome, W. T., Clark, A. M., Hosseini, P., Scott, B. B., Bradley, D. C., Smith, M. A., Kohn, A., Movshon, J. A., Armstrong, K. M., Moore, T., Chang, S. W., Snyder, L. H., Lisberger, S. G., … Shenoy, K. V. (2010). Stimulus onset quenches neural variability: A widespread cortical phenomenon. *Nature Neuroscience*, *13*(3), 369–378. https://doi.org/10.1038/nn.2501

Clifford, C. W. G., Webster, M. A., Stanley, G. B., Stocker, A. A., Kohn, A., Sharpee, T. O., & Schwartz, O. (2007). Visual adaptation: Neural, psychological and computational aspects. *Vision Research*, *47*(25), 3125–3131. https://doi.org/10.1016/j.visres.2007.08.023

Clifford, C. W. G., & Wenderoth, P. (1999). Adaptation to temporal modulation can enhance differential speed sensitivity. *Vision Research*, *39*(26), 4324–4331. https://doi.org/10.1016/S0042-6989(99)00151-0

Clopath, C., Büsing, L., Vasilaki, E., & Gerstner, W. (2010). Connectivity reflects coding: A model of voltage-based STDP with homeostasis. *Nature Neuroscience*, *13*(3), 344–352. https://doi.org/10.1038/nn.2479

Coley, A. A., & Gao, W.-J. (2019). PSD-95 deficiency disrupts PFC-associated function and behavior during neurodevelopment. *Scientific Reports*, *9*(1), 9486. https://doi.org/10.1038/s41598-019-45971-w

Contractor, A., Ethell, I. M., & Portera-Cailliau, C. (2021). Cortical interneurons in autism. *Nature Neuroscience*, *24*(12), 1648–1659. https://doi.org/10.1038/s41593-021-00967-6

Cooke, S. F., & Bliss, T. V. P. (2006). Plasticity in the human central nervous system. *Brain*, *129*(7), 1659–1673. https://doi.org/10.1093/brain/awl082

Cox, D. D., & Dean, T. (2014). Neural Networks and Neuroscience-Inspired Computer Vision. *Current Biology*, *24*(18), R921–R929. https://doi.org/10.1016/j.cub.2014.08.026

Crosse, M. J., Foxe, J. J., Tarrit, K., Freedman, E. G., & Molholm, S. (2022). Resolution of impaired multisensory processing in autism and the cost of switching sensory modality. *Communications Biology*, *5*(1), 601. https://doi.org/10.1038/s42003-022-03519-1

Cuppini, C., Stein, B. E., Rowland, B. A., Magosso, E., & Ursino, M. (2011). A computational study of multisensory maturation in the superior colliculus (SC). *Experimental Brain Research*, *213*(2–3), 341–349. https://doi.org/10.1007/s00221-011-2714-z

Cuppini, C., Ursino, M., Magosso, E., Rowland, B. A., & Stein, B. E. (2010). An Emergent Model of Multisensory Integration in Superior Colliculus Neurons. *Frontiers in Integrative Neuroscience*, *4*, 6. https://doi.org/10.3389/fnint.2010.00006

Cuturi, L. F., & MacNeilage, P. R. (2014). Optic flow induces nonvisual self-motion aftereffects. *Current Biology: CB*, *24*(23), 2817–2821. https://doi.org/10.1016/j.cub.2014.10.015

Danks, D., & Davis, I. (2023). Causal inference in cognitive neuroscience. *Wiley Interdisciplinary Reviews. Cognitive Science*, *14*(5), e1650. https://doi.org/10.1002/wcs.1650

Daoudal, G., & Debanne, D. (2003). Long-term plasticity of intrinsic excitability: Learning rules and mechanisms. *Learning & Memory (Cold Spring Harbor, N.Y.)*, *10*(6), 456–465. https://doi.org/10.1101/lm.64103

Dash, S., Peel, T. R., Lomber, S. G., & Corneil, B. D. (2018). Frontal Eye Field Inactivation Reduces Saccade Preparation in the Superior Colliculus but Does Not Alter How Preparatory Activity Relates to Saccades of a Given Latency. *eNeuro*, *5*(2). https://doi.org/10.1523/ENEURO.0024-18.2018

de Boer-Schellekens, L., Eussen, M., & Vroomen, J. (2013). Diminished sensitivity of audiovisual temporal order in autism spectrum disorder. *Frontiers in Integrative Neuroscience*, *7*, 8. https://doi.org/10.3389/fnint.2013.00008

de Boer-Schellekens, L., Keetels, M., Eussen, M., & Vroomen, J. (2013). No evidence for impaired multisensory integration of low-level audiovisual stimuli in adolescents and

young adults with autism spectrum disorders. *Neuropsychologia*, *51*(14), 3004–3013. https://doi.org/10.1016/j.neuropsychologia.2013.10.005

De Gelder, B., & Bertelson, P. (2003). Multisensory integration, perception and ecological validity. *Trends in Cognitive Sciences*, *7*(10), 460–467. https://doi.org/10.1016/j.tics.2003.08.014

De Rubeis, S., He, X., Goldberg, A. P., Poultney, C. S., Samocha, K., Ercument Cicek, A., Kou, Y., Liu, L., Fromer, M., Walker, S., Singh, T., Klei, L., Kosmicki, J., Fu, S.-C., Aleksic, B., Biscaldi, M., Bolton, P. F., Brownfeld, J. M., Cai, J., … Buxbaum, J. D. (2014). Synaptic, transcriptional and chromatin genes disrupted in autism. *Nature*, *515*(7526), 209–215. https://doi.org/10.1038/nature13772

De Valois, R. L., Albrecht, D. G., & Thorell, L. G. (1982). Spatial frequency selectivity of cells in macaque visual cortex. *Vision Research*, *22*(5), 545–559. https://doi.org/10.1016/0042-6989(82)90113-4

DeAngelis, G. C., Ghose, G. M., Ohzawa, I., & Freeman, R. D. (1999). Functional Micro-Organization of Primary Visual Cortex: Receptive Field Analysis of Nearby Neurons. *Journal of Neuroscience*, *19*(10), 4046–4064. https://doi.org/10.1523/JNEUROSCI.19-10-04046.1999

Deisseroth, K. (2015). Optogenetics: 10 years of microbial opsins in neuroscience. *Nature Neuroscience*, *18*(9), 1213. https://doi.org/10.1038/nn.4091

Delmas, P., & Brown, D. A. (2005). Pathways modulating neural KCNQ/M (Kv7) potassium channels. *Nature Reviews. Neuroscience*, *6*(11), 850–862. https://doi.org/10.1038/nrn1785

Denève, S., & Machens, C. K. (2016). Efficient codes and balanced networks. *Nature Neuroscience*, *19*(3), 375–382. https://doi.org/10.1038/nn.4243

Dinstein, I., Heeger, D. J., Lorenzi, L., Minshew, N. J., Malach, R., & Behrmann, M. (2012). Unreliable evoked responses in autism. *Neuron*, *75*(6), 981. https://doi.org/10.1016/j.neuron.2012.07.026

Dobler, Z., Suresh, A., Chari, T., Mula, S., Tran, A., Buonomano, D. V., & Portera-Cailliau, C. (2024). Adapting and facilitating responses in mouse somatosensory cortex are dynamic and shaped by experience. *Current Biology : CB*, *34*(15), 3506-3521.e5. https://doi.org/10.1016/j.cub.2024.06.070

Dp, M., F, C., C, L., Sa, B., L, L., Ff, V., S, B., G, T., F, H., & T, D. (n.d.). A Sensitive Dynamic and Active Pixel Vision Sensor for Color or Neural Imaging Applications. *PubMed*. Retrieved September 15, 2025, from https://pubmed.ncbi.nlm.nih.gov/29377801/

Drotos, A. C., Zarb, R. L., Booth, V., & Roberts, M. T. (2024). GluN2C/D-containing NMDA receptors enhance temporal summation and increase sound-evoked and spontaneous

firing in the inferior colliculus. *bioRxiv*, 2023.04.27.538607. https://doi.org/10.1101/2023.04.27.538607

D'Souza, D. C., Carson, R. E., Driesen, N., Johannesen, J., Ranganathan, M., & Krystal, J. H. (2018). Dose-related target occupancy and effects on circuitry, behavior, and neuroplasticity of the glycine transporter-1 inhibitor, PF-03463275, in healthy and schizophrenia subjects. *Biological Psychiatry*, *84*(6), 413. https://doi.org/10.1016/j.biopsych.2017.12.019

Duffney, L. J., Wei, J., Cheng, J., Liu, W., Smith, K. R., Kittler, J. T., & Yan, Z. (2013). Shank3 Deficiency Induces NMDA Receptor Hypofunction via an Actin-Dependent Mechanism. *The Journal of Neuroscience*, *33*(40), 15767. https://doi.org/10.1523/JNEUROSCI.1175-13.2013

Duong, L. R., Bredenberg, C., Heeger, D. J., & Simoncelli, E. P. (2023). *Adaptive coding efficiency in recurrent cortical circuits via gain control* (No. arXiv:2305.19869). arXiv. https://doi.org/10.48550/arXiv.2305.19869

Dwyer, P., Sillas, A., Prieto, M., Camp, E., Nordahl, C. W., & Rivera, S. M. (2024). Hyper-focus, sticky attention, and springy attention in young autistic children: Associations with sensory behaviors and cognitive ability. *Autism Research: Official Journal of the International Society for Autism Research*, *17*(8), 1677–1695. https://doi.org/10.1002/aur.3174

Edwards, M., & Rideaux, R. (2013). How many motion signals can be simultaneously perceived? *Vision Research*, *76*, 11–16. https://doi.org/10.1016/j.visres.2012.10.004

Ernst, M. O., & Banks, M. S. (2002). Humans integrate visual and haptic information in a statistically optimal fashion. *Nature*, *415*(6870), 429–433. https://doi.org/10.1038/415429a

Esser, S. K., Merolla, P. A., Arthur, J. V., Cassidy, A. S., Appuswamy, R., Andreopoulos, A., Berg, D. J., McKinstry, J. L., Melano, T., Barch, D. R., Nolfo, C. di, Datta, P., Amir, A., Taba, B., Flickner, M. D., & Modha, D. S. (2016). Convolutional networks for fast, energy-efficient neuromorphic computing. *Proceedings of the National Academy of Sciences of the United States of America*, *113*(41), 11441. https://doi.org/10.1073/pnas.1604850113

Essig, J., Hunt, J. B., & Felsen, G. (2021). Inhibitory neurons in the superior colliculus mediate selection of spatially-directed movements. *Communications Biology*, *4*(1), 719. https://doi.org/10.1038/s42003-021-02248-1

Ewald, R. C., Keuren-Jensen, K. R. V., Aizenman, C. D., & Cline, H. T. (2008). Roles of NR2A and NR2B in the Development of Dendritic Arbor Morphology In Vivo. *The Journal of Neuroscience*, *28*(4), 850. https://doi.org/10.1523/JNEUROSCI.5078-07.2008

F, M., & Rb, B. (2013). Adaptation of cerebral oxygen metabolism and blood flow and modulation of neurovascular coupling with prolonged stimulation in human visual cortex. *NeuroImage*, *82*. https://doi.org/10.1016/j.neuroimage.2013.05.110

Faber, E. L., & Sah, P. (2007). Functions of Sk Channels in Central Neurons. *Clinical and Experimental Pharmacology and Physiology*, *34*(10), 1077–1083. https://doi.org/10.1111/j.1440-1681.2007.04725.x

Fairhall, A. L., Lewen, G. D., Bialek, W., & De Ruyter Van Steveninck, R. R. (2001). Efficiency and ambiguity in an adaptive neural code. *Nature*, *412*(6849), 787–792. https://doi.org/10.1038/35090500

Faisal, A. A., Selen, L. P. J., & Wolpert, D. M. (2008). Noise in the nervous system. *Nature Reviews Neuroscience*, *9*(4), 292–303. https://doi.org/10.1038/nrn2258

Farkas, K., Pesthy, O., Guttengéber, A., Weigl, A. S., Veres, A., Szekely, A., Komoróczy, E., Szuromi, B., Janacsek, K., Réthelyi, J. M., & Németh, D. (2023). Altered interpersonal distance regulation in autism spectrum disorder. *PLOS ONE*, *18*(3), e0283761. https://doi.org/10.1371/journal.pone.0283761

Fatemi, S. H., Halt, A. R., Stary, J. M., Kanodia, R., Schulz, S. C., & Realmuto, G. R. (2002). Glutamic acid decarboxylase 65 and 67 kDa proteins are reduced in autistic parietal and cerebellar cortices. *Biological Psychiatry*, *52*(8), 805–810. https://doi.org/10.1016/S0006-3223(02)01430-0

Fedele, L., Newcombe, J., Topf, M., Gibb, A., Harvey, R. J., & Smart, T. G. (2018). Disease-associated missense mutations in GluN2B subunit alter NMDA receptor ligand binding and ion channel properties. *Nature Communications*, *9*(1), 957. https://doi.org/10.1038/s41467-018-02927-4

Felch, D. L., Khakhalin, A. S., & Aizenman, C. D. (2016). Multisensory integration in the developing tectum is constrained by the balance of excitation and inhibition. *eLife*, *5*, e15600. https://doi.org/10.7554/eLife.15600

Feldman, D. E. (2012). The spike timing dependence of plasticity. *Neuron*, *75*(4), 556. https://doi.org/10.1016/j.neuron.2012.08.001

Feldman, J. I., Dunham, K., Cassidy, M., Wallace, M. T., Liu, Y., & Woynaroski, T. G. (2018). Audiovisual multisensory integration in individuals with autism spectrum disorder: A systematic review and meta-analysis. *Neuroscience & Biobehavioral Reviews*, *95*, 220–234. https://doi.org/10.1016/j.neubiorev.2018.09.020

Feldmeyer, D. (2012). Excitatory neuronal connectivity in the barrel cortex. *Frontiers in Neuroanatomy*, *6*, 24. https://doi.org/10.3389/fnana.2012.00024

Ferguson, K. A., & Cardin, J. A. (2020). Mechanisms underlying gain modulation in the cortex. *Nature Reviews. Neuroscience*, *21*(2), 80–92. https://doi.org/10.1038/s41583-019-0253-y

Fiorillo, C. D., Kim, J. K., & Hong, S. Z. (2014). The meaning of spikes from the neuron's point of view: Predictive homeostasis generates the appearance of randomness. *Frontiers in Computational Neuroscience*, *8*, 49. https://doi.org/10.3389/fncom.2014.00049

Fortune, E. S., & Rose, G. J. (2001). Short-term synaptic plasticity as a temporal filter. *Trends in Neurosciences*, *24*(7), 381–385. https://doi.org/10.1016/s0166-2236(00)01835-x

Foss-Feig, J. H., Kwakye, L. D., Cascio, C. J., Burnette, C. P., Kadivar, H., Stone, W. L., & Wallace, M. T. (2010). An extended multisensory temporal binding window in autism spectrum disorders. *Experimental Brain Research*, *203*(2), 381–389. https://doi.org/10.1007/s00221-010-2240-4

Foxe, J. J., Molholm, S., Del Bene, V. A., Frey, H.-P., Russo, N. N., Blanco, D., Saint-Amour, D., & Ross, L. A. (2015). Severe multisensory speech integration deficits in high-functioning school-aged children with Autism Spectrum Disorder (ASD) and their resolution during early adolescence. *Cerebral Cortex (New York, N.Y.: 1991)*, *25*(2), 298–312. https://doi.org/10.1093/cercor/bht213

Franken, T. P., Roberts, M. T., Wei, L., Golding, N. L., & Joris, P. X. (2015). In vivo coincidence detection in mammalian sound localization generates phase delays. *Nature Neuroscience*, *18*(3), 444–452. https://doi.org/10.1038/nn.3948

Friston, K. J., Harrison, L., & Penny, W. (2003). Dynamic causal modelling. *NeuroImage*, *19*(4), 1273–1302. https://doi.org/10.1016/S1053-8119(03)00202-7

Fujihira, H., Itoi, C., Furukawa, S., Kato, N., & Kashino, M. (2022). Sensitivity to interaural level and time differences in individuals with autism spectrum disorder. *Scientific Reports*, *12*(1), 19142. https://doi.org/10.1038/s41598-022-23346-y

Gabernet, L., Jadhav, S. P., Feldman, D. E., Carandini, M., & Scanziani, M. (2005). Somatosensory integration controlled by dynamic thalamocortical feed-forward inhibition. *Neuron*, *48*(2), 315–327. https://doi.org/10.1016/j.neuron.2005.09.022

Gandal, M. J., Anderson, R. L., Billingslea, E. N., Carlson, G. C., Roberts, T. P. L., & Siegel, S. J. (2012). Mice with reduced NMDA receptor expression: More consistent with autism than schizophrenia? *Genes, Brain, and Behavior*, *11*(6), 740–750. https://doi.org/10.1111/j.1601-183X.2012.00816.x

Ganguli, D., & Simoncelli, E. P. (2014). Efficient Sensory Encoding and Bayesian Inference with Heterogeneous Neural Populations. *Neural Computation*, *26*(10), 2103. https://doi.org/10.1162/NECO_a_00638

Ganguly, C., Bezugam, S. S., Abs, E., Payvand, M., Dey, S., & Suri, M. (2024). Spike frequency adaptation: Bridging neural models and neuromorphic applications. *Communications Engineering*, *3*(1), 1–13. https://doi.org/10.1038/s44172-024-00165-9

Gehr, C., Sibille, J., & Kremkow, J. (2023). Retinal input integration in excitatory and inhibitory neurons in the mouse superior colliculus in vivo. *eLife*, *12*, RP88289. https://doi.org/10.7554/eLife.88289

Geirhos, R., Jacobsen, J.-H., Michaelis, C., Zemel, R., Brendel, W., Bethge, M., & Wichmann, F. A. (2020). Shortcut learning in deep neural networks. *Nature Machine Intelligence*, *2*(11), 665–673. https://doi.org/10.1038/s42256-020-00257-z

Geirhos, R., Rubisch, P., Michaelis, C., Bethge, M., Wichmann, F. A., & Brendel, W. (2022). *ImageNet-trained CNNs are biased towards texture; increasing shape bias improves accuracy and robustness* (No. arXiv:1811.12231). arXiv. https://doi.org/10.48550/arXiv.1811.12231

Georgieva, S. S., Todd, J. T., Peeters, R., & Orban, G. A. (2008). The extraction of 3D shape from texture and shading in the human brain. *Cerebral Cortex (New York, N.Y.: 1991)*, *18*(10), 2416–2438. https://doi.org/10.1093/cercor/bhn002

Gerstner, W., & Naud, R. (2009). How Good Are Neuron Models? *Science*, *326*(5951), 379–380. https://doi.org/10.1126/science.1181936

Ghodrati, M., Zavitz, E., Rosa, M. G. P., & Price, N. S. C. (2019). Contrast and luminance adaptation alter neuronal coding and perception of stimulus orientation. *Nature Communications*, *10*(1), 941. https://doi.org/10.1038/s41467-019-08894-8

Gingras, G., Rowland, B. A., & Stein, B. E. (2009). The Differing Impact of Multisensory and Unisensory Integration on Behavior. *The Journal of Neuroscience*, *29*(15), 4897. https://doi.org/10.1523/JNEUROSCI.4120-08.2009

Girirajan, S., Rosenfeld, J. A., Cooper, G. M., Antonacci, F., Siswara, P., Itsara, A., Vives, L., Walsh, T., McCarthy, S. E., Baker, C., Mefford, H. C., Kidd, J. M., Browning, S. R., Browning, B. L., Dickel, D. E., Levy, D. L., Ballif, B. C., Platky, K., Farber, D. M., … Eichler, E. E. (2010). A recurrent 16p12.1 microdeletion supports a two-hit model for severe developmental delay. *Nature Genetics*, *42*(3), 203–209. https://doi.org/10.1038/ng.534

Givon-Benjio, N., Marx, T., Hartston, M., Aderka, I. M., Hadad, B.-S., & Okon-Singer, H. (2024). The relationship between interpersonal distance preference and estimation accuracy in autism. *PLOS ONE*, *19*(9), e0306536. https://doi.org/10.1371/journal.pone.0306536

Gjorgjieva, J., Drion, G., & Marder, E. (2016). Computational implications of biophysical diversity and multiple timescales in neurons and synapses for circuit performance. *Current Opinion in Neurobiology*, *37*, 44–52. https://doi.org/10.1016/j.conb.2015.12.008

Glasser, D. M., Tsui, J. M. G., Pack, C. C., & Tadin, D. (2011). Perceptual and neural consequences of rapid motion adaptation. *Proceedings of the National Academy of Sciences*, *108*(45). https://doi.org/10.1073/pnas.1101141108

Gollisch, T., & Meister, M. (2008). Rapid neural coding in the retina with relative spike latencies. *Science (New York, N.Y.)*, *319*(5866), 1108–1111. https://doi.org/10.1126/science.1149639

Gonçalves, A. M., & Monteiro, P. (2023). Autism Spectrum Disorder and auditory sensory alterations: A systematic review on the integrity of cognitive and neuronal functions related to auditory processing. *Journal of Neural Transmission*, *130*(3), 325. https://doi.org/10.1007/s00702-023-02595-9

Grunewald, A., & Lankheet, M. J. M. (1996). The Orthogonal Motion Aftereffect. *Perception*, *25*(1_suppl), 65–65. https://doi.org/10.1068/v96l0805

Guclu, U., & Van Gerven, M. A. J. (2015). Deep Neural Networks Reveal a Gradient in the Complexity of Neural Representations across the Ventral Stream. *Journal of Neuroscience*, *35*(27), 10005–10014. https://doi.org/10.1523/JNEUROSCI.5023-14.2015

Gundavarapu, A., Chakravarthy, V. S., & Soman, K. (2019). A Model of Motion Processing in the Visual Cortex Using Neural Field With Asymmetric Hebbian Learning. *Frontiers in Neuroscience*, *13*, 67. https://doi.org/10.3389/fnins.2019.00067

Ha, G. E., Lee, J., Kwak, H., Song, K., Kwon, J., Jung, S.-Y., Hong, J., Chang, G.-E., Hwang, E. M., Shin, H.-S., Lee, C. J., & Cheong, E. (2016). The Ca2+-activated chloride channel anoctamin-2 mediates spike-frequency adaptation and regulates sensory transmission in thalamocortical neurons. *Nature Communications*, *7*(1), 13791. https://doi.org/10.1038/ncomms13791

Hagmann, C. E., & Russo, N. (2016). Multisensory integration of redundant trisensory stimulation. *Attention, Perception & Psychophysics*, *78*(8), 2558–2568. https://doi.org/10.3758/s13414-016-1192-6

Hahamy, A., Behrmann, M., & Malach, R. (2015). The idiosyncratic brain: Distortion of spontaneous connectivity patterns in autism spectrum disorder. *Nature Neuroscience*, *18*(2), 302–309. https://doi.org/10.1038/nn.3919

Hallermann, S., de Kock, C. P. J., Stuart, G. J., & Kole, M. H. P. (2012). State and location dependence of action potential metabolic cost in cortical pyramidal neurons. *Nature Neuroscience*, *15*(7), 1007–1014. https://doi.org/10.1038/nn.3132

Harris, J. J., Jolivet, R., & Attwell, D. (2012). Synaptic energy use and supply. *Neuron*, *75*(5), 762–777. https://doi.org/10.1016/j.neuron.2012.08.019

Hashemi, E., Ariza, J., Rogers, H., Noctor, S. C., & Martínez-Cerdeño, V. (2017). The Number of Parvalbumin-Expressing Interneurons Is Decreased in the Prefrontal Cortex in Autism. *Cerebral Cortex (New York, NY)*, *27*(3), 1931–1943. https://doi.org/10.1093/cercor/bhw021

Hasinoff, S. W. (2014). Photon, Poisson Noise. In *Computer Vision* (pp. 608–610). Springer, Boston, MA. https://doi.org/10.1007/978-0-387-31439-6_482

He, C. X., Cantu, D. A., Mantri, S. S., Zeiger, W. A., Goel, A., & Portera-Cailliau, C. (2017). Tactile Defensiveness and Impaired Adaptation of Neuronal Activity in the Fmr1 Knock-Out Mouse Model of Autism. *The Journal of Neuroscience: The Official Journal of the Society for Neuroscience*, *37*(27), 6475–6487. https://doi.org/10.1523/JNEUROSCI.0651-17.2017

Heeger, D. J., Boynton, G. M., Demb, J. B., Seidemann, E., & Newsome, W. T. (1999). Motion Opponency in Visual Cortex. *The Journal of Neuroscience*, *19*(16), 7162. https://doi.org/10.1523/JNEUROSCI.19-16-07162.1999

Herculano-Houzel, S. (2009). The human brain in numbers: A linearly scaled-up primate brain. *Frontiers in Human Neuroscience*, *3*. https://doi.org/10.3389/neuro.09.031.2009

Hietanen, M. A., Crowder, N. A., Price, N. S. C., & Ibbotson, M. R. (2007). Influence of adapting speed on speed and contrast coding in the primary visual cortex of the cat. *The Journal of Physiology*, *584*(Pt 2), 451–462. https://doi.org/10.1113/jphysiol.2007.131631

Hopfield, J. J. (1982). Neural networks and physical systems with emergent collective computational abilities. *Proceedings of the National Academy of Sciences of the United States of America*, *79*(8), 2554. https://doi.org/10.1073/pnas.79.8.2554

Hu, B., Garrett, M. E., Groblewski, P. A., Ollerenshaw, D. R., Shang, J., Roll, K., Manavi, S., Koch, C., Olsen, S. R., & Mihalas, S. (2021). Adaptation supports short-term memory in a visual change detection task. *PLOS Computational Biology*, *17*(9), e1009246. https://doi.org/10.1371/journal.pcbi.1009246

Hubel, D. H., & Wiesel, T. N. (1962). Receptive fields, binocular interaction and functional architecture in the cat's visual cortex. *The Journal of Physiology*, *160*(1), 106-154.2.

Huda, R., Sipe, G. O., Breton-Provencher, V., Cruz, K. G., Pho, G. N., Adam, E., Gunter, L. M., Sullins, A., Wickersham, I. R., & Sur, M. (2020). Distinct prefrontal top-down circuits differentially modulate sensorimotor behavior. *Nature Communications*, *11*(1), 6007. https://doi.org/10.1038/s41467-020-19772-z

Huys, Q. J. M., Maia, T. V., & Frank, M. J. (2016). Computational psychiatry as a bridge from neuroscience to clinical applications. *Nature Neuroscience*, *19*(3), 404–413. https://doi.org/10.1038/nn.4238

Idrees, S., Manookin, M. B., Rieke, F., Field, G. D., & Zylberberg, J. (2024). Biophysical neural adaptation mechanisms enable artificial neural networks to capture dynamic retinal computation. *Nature Communications*, *15*(1), 5957. https://doi.org/10.1038/s41467-024-50114-5

Isaacson, J. S., & Scanziani, M. (2011). How inhibition shapes cortical activity. *Neuron*, *72*(2), 231–243. https://doi.org/10.1016/j.neuron.2011.09.027

Ito, S., & Feldheim, D. A. (2018). The Mouse Superior Colliculus: An Emerging Model for Studying Circuit Formation and Function. *Frontiers in Neural Circuits*, *12*. https://doi.org/10.3389/fncir.2018.00010

Izhikevich, E. M. (2003). Simple model of spiking neurons. *IEEE Transactions on Neural Networks*, *14*(6), 1569–1572. IEEE Transactions on Neural Networks. https://doi.org/10.1109/TNN.2003.820440

Jalali-Yazdi, F., Chowdhury, S., Yoshioka, C., & Gouaux, E. (2018). Mechanisms for Zinc and Proton Inhibition of the GluN1/GluN2A NMDA Receptor. *Cell*, *175*(6), 1520-1532.e15. https://doi.org/10.1016/j.cell.2018.10.043

Jazayeri, M., & Afraz, A. (2017). Navigating the Neural Space in Search of the Neural Code. *Neuron*, *93*(5), 1003–1014. https://doi.org/10.1016/j.neuron.2017.02.019

Jiang, C.-C., Lin, L.-S., Long, S., Ke, X.-Y., Fukunaga, K., Lu, Y.-M., & Han, F. (2022). Signalling pathways in autism spectrum disorder: Mechanisms and therapeutic implications. *Signal Transduction and Targeted Therapy*, *7*(1), 229. https://doi.org/10.1038/s41392-022-01081-0

Jiang, W., Wallace, M. T., Jiang, H., Vaughan, J. W., & Stein, B. E. (2001). Two cortical areas mediate multisensory integration in superior colliculus neurons. *Journal of Neurophysiology*, *85*(2), 506–522. https://doi.org/10.1152/jn.2001.85.2.506

Jj, van B., M, D., & H, L. (n.d.). Intact recognition, but attenuated adaptation, for biological motion in youth with autism spectrum disorder. *PubMed*. Retrieved September 16, 2025, from https://pubmed.ncbi.nlm.nih.gov/26808343/

Johansson, R. S., & Birznieks, I. (2004). First spikes in ensembles of human tactile afferents code complex spatial fingertip events. *Nature Neuroscience*, *7*(2), 170–177. https://doi.org/10.1038/nn1177

Johnston, A., Arnold, D. H., & Nishida, S. (2006). Spatially localized distortions of event time. *Current Biology: CB*, *16*(5), 472–479. https://doi.org/10.1016/j.cub.2006.01.032

Jonas, E., & Kording, K. P. (2017). Could a Neuroscientist Understand a Microprocessor? *PLoS Computational Biology*, *13*(1), e1005268. https://doi.org/10.1371/journal.pcbi.1005268

Jun, E. J., Bautista, A. R., Nunez, M. D., Allen, D. C., Tak, J. H., Alvarez, E., & Basso, M. A. (2021). Causal role for the primate superior colliculus in the computation of evidence for perceptual decisions. *Nature Neuroscience*, *24*(8), 1121–1131. https://doi.org/10.1038/s41593-021-00878-6

Jure, R. (2019). Autism Pathogenesis: The Superior Colliculus. *Frontiers in Neuroscience*, *12*, 1029. https://doi.org/10.3389/fnins.2018.01029

Just, M. A., Keller, T. A., Malave, V. L., Kana, R. K., & Varma, S. (2012). Autism as a neural systems disorder: A theory of frontal-posterior underconnectivity. *Neuroscience & Biobehavioral Reviews*, *36*(4), 1292–1313. https://doi.org/10.1016/j.neubiorev.2012.02.007

K, V., X, B., & G, K. (2020). Incorporating intrinsic suppression in deep neural networks captures dynamics of adaptation in neurophysiology and perception. *PubMed*. https://pubmed.ncbi.nlm.nih.gov/33055170/

Kar, K., Kubilius, J., Schmidt, K., Issa, E. B., & DiCarlo, J. J. (2019). Evidence that recurrent circuits are critical to the ventral stream's execution of core object recognition behavior. *Nature Neuroscience*, *22*(6), 974–983. https://doi.org/10.1038/s41593-019-0392-5

Kardamakis, A. A., Pérez-Fernández, J., & Grillner, S. (2016). Spatiotemporal interplay between multisensory excitation and recruited inhibition in the lamprey optic tectum. *eLife*, *5*, e16472. https://doi.org/10.7554/eLife.16472

Kawakami, S., & Otsuka, S. (2021). Multisensory Processing in Autism Spectrum Disorders. In A. M. Grabrucker (Ed.), *Autism Spectrum Disorders*. Exon Publications. http://www.ncbi.nlm.nih.gov/books/NBK573614/

Kawakami, S., Uono, S., Otsuka, S., Yoshimura, S., Zhao, S., & Toichi, M. (2020). Atypical Multisensory Integration and the Temporal Binding Window in Autism Spectrum Disorder. *Journal of Autism and Developmental Disorders*, *50*(11), 3944–3956. https://doi.org/10.1007/s10803-020-04452-0

Kay, K. N., Naselaris, T., Prenger, R. J., & Gallant, J. L. (2008). Identifying natural images from human brain activity. *Nature*, *452*(7185), 352–355. https://doi.org/10.1038/nature06713

Keetels, M., & Vroomen, J. (2012). Perception of Synchrony between the Senses. In M. M. Murray & M. T. Wallace (Eds.), *The Neural Bases of Multisensory Processes*. CRC Press/Taylor & Francis. http://www.ncbi.nlm.nih.gov/books/NBK92837/

Kell, A. J. E., Yamins, D. L. K., Shook, E. N., Norman-Haignere, S. V., & McDermott, J. H. (2018). A Task-Optimized Neural Network Replicates Human Auditory Behavior, Predicts Brain Responses, and Reveals a Cortical Processing Hierarchy. *Neuron*, *98*(3), 630-644.e16. https://doi.org/10.1016/j.neuron.2018.03.044

Khaligh-Razavi, S.-M., & Kriegeskorte, N. (2014). Deep Supervised, but Not Unsupervised, Models May Explain IT Cortical Representation. *PLoS Computational Biology*, *10*(11), e1003915. https://doi.org/10.1371/journal.pcbi.1003915

Khan, S., Gramfort, A., Shetty, N. R., Kitzbichler, M. G., Ganesan, S., Moran, J. M., Lee, S. M., Gabrieli, J. D. E., Tager-Flusberg, H. B., Joseph, R. M., Herbert, M. R., Hämäläinen, M. S., & Kenet, T. (2013). Local and long-range functional connectivity is reduced in concert in autism spectrum disorders. *Proceedings of the National Academy of Sciences*, *110*(8), 3107–3112. https://doi.org/10.1073/pnas.1214533110

King, A. J. (2004). The superior colliculus. *Current Biology: CB*, *14*(9), R335-338. https://doi.org/10.1016/j.cub.2004.04.018

King, A. J., Hutchings, M. E., Moore, D. R., & Blakemore, C. (1988). Developmental plasticity in the visual and auditory representations in the mammalian superior colliculus. *Nature*, *332*(6159), 73–76. https://doi.org/10.1038/332073a0

King, A. J., Jiang, Z. D., & Moore, D. R. (1998). Auditory brainstem projections to the ferret superior colliculus: Anatomical contribution to the neural coding of sound azimuth. *The Journal of Comparative Neurology*, *390*(3), 342–365.

Kingma, D. P., & Ba, J. (2017). *Adam: A Method for Stochastic Optimization* (No. arXiv:1412.6980). arXiv. https://doi.org/10.48550/arXiv.1412.6980

Kohn, A. (2007). Visual Adaptation: Physiology, Mechanisms, and Functional Benefits. *Journal of Neurophysiology*, *97*(5), 3155–3164. https://doi.org/10.1152/jn.00086.2007

Kohn, A., & Movshon, J. A. (2003). Neuronal adaptation to visual motion in area MT of the macaque. *Neuron*, *39*(4), 681–691. https://doi.org/10.1016/s0896-6273(03)00438-0

Kohn, A., & Movshon, J. A. (2004). Adaptation changes the direction tuning of macaque MT neurons. *Nature Neuroscience*, *7*(7), 764–772. https://doi.org/10.1038/nn1267

Kourdougli, N., Suresh, A., Liu, B., Juarez, P., Lin, A., Chung, D. T., Graven Sams, A., Gandal, M. J., Martínez-Cerdeño, V., Buonomano, D. V., Hall, B. J., Mombereau, C., & Portera-Cailliau, C. (2023). Improvement of sensory deficits in fragile X mice by increasing cortical interneuron activity after the critical period. *Neuron*, *111*(18), 2863-2880.e6. https://doi.org/10.1016/j.neuron.2023.06.009

Krakauer, J. W., Ghazanfar, A. A., Gomez-Marin, A., MacIver, M. A., & Poeppel, D. (2017). Neuroscience Needs Behavior: Correcting a Reductionist Bias. *Neuron*, *93*(3), 480–490. https://doi.org/10.1016/j.neuron.2016.12.041

Krekelberg, B., Boynton, G. M., & Van Wezel, R. J. A. (2006). Adaptation: From single cells to BOLD signals. *Trends in Neurosciences*, *29*(5), 250–256. https://doi.org/10.1016/j.tins.2006.02.008

Kriegeskorte, N., & Douglas, P. K. (2018). Cognitive computational neuroscience. *Nature Neuroscience*, *21*(9), 1148–1160. https://doi.org/10.1038/s41593-018-0210-5

Kwakye, L. D., Foss-Feig, J. H., Cascio, C. J., Stone, W. L., & Wallace, M. T. (2011). Altered auditory and multisensory temporal processing in autism spectrum disorders. *Frontiers in Integrative Neuroscience*, *4*, 129. https://doi.org/10.3389/fnint.2010.00129

Latimer, K. W., Barbera, D., Sokoletsky, M., Awwad, B., Katz, Y., Nelken, I., Lampl, I., Fairhall, A. L., & Priebe, N. J. (2019). Multiple Timescales Account for Adaptive Responses across Sensory Cortices. *Journal of Neuroscience*, *39*(50), 10019–10033. https://doi.org/10.1523/JNEUROSCI.1642-19.2019

Laughlin, S. (2001). Energy as a constraint on the coding and processing of sensory information. *Current Opinion in Neurobiology*, *11*(4), 475–480. https://doi.org/10.1016/S0959-4388(00)00237-3

Lawson, R. P., Aylward, J., White, S., & Rees, G. (2015). A striking reduction of simple loudness adaptation in autism. *Scientific Reports*, *5*(1), 16157. https://doi.org/10.1038/srep16157

Lawson, R. P., Rees, G., & Friston, K. J. (2014). An aberrant precision account of autism. *Frontiers in Human Neuroscience*, *8*. https://doi.org/10.3389/fnhum.2014.00302

Lebedeva, J., Zakharov, A., Burkhanova, G., Chernova, K., & Khazipov, R. (2019). The Effects of NMDA Receptor Blockade on Sensory-Evoked Responses in Superficial Layers of the Rat Barrel Cortex. *Frontiers in Cellular Neuroscience*, *13*, 259. https://doi.org/10.3389/fncel.2019.00259

Lee, A. L. F. (2018). The contribution of local and global motion adaptation in the repulsive direction aftereffect. *Journal of Vision*, *18*(12), 2. https://doi.org/10.1167/18.12.2

Lee, J., Choi, J. H., & Rah, J.-C. (2020). Frequency-dependent gating of feedforward inhibition in thalamofrontal synapses. *Molecular Brain*, *13*(1), 68. https://doi.org/10.1186/s13041-020-00608-2

Lee, K. H., Tran, A., Turan, Z., & Meister, M. (2020). The sifting of visual information in the superior colliculus. *eLife*, *9*, e50678. https://doi.org/10.7554/eLife.50678

Lee, S., Jung, W. B., Moon, H., Im, G. H., Noh, Y. W., Shin, W., Kim, Y. G., Yi, J. H., Hong, S. J., Jung, Y., Ahn, S., Kim, S.-G., & Kim, E. (2024). Anterior cingulate cortex-related functional hyperconnectivity underlies sensory hypersensitivity in Grin2b-mutant mice. *Molecular Psychiatry*, *29*(10), 3195–3207. https://doi.org/10.1038/s41380-024-02572-y

Lengyel, M. (2024). Marr's three levels of analysis are useful as a framework for neuroscience. *The Journal of Physiology*, *602*(9), 1911–1914. https://doi.org/10.1113/JP279549

Lennie, P. (2003). The cost of cortical computation. *Current Biology: CB*, *13*(6), 493–497. https://doi.org/10.1016/s0960-9822(03)00135-0

Li, C., & Gulledge, A. T. (2021). NMDA Receptors Enhance the Fidelity of Synaptic Integration. *eNeuro*, *8*(2), ENEURO.0396-20.2020. https://doi.org/10.1523/ENEURO.0396-20.2020

Li, L., Ji, X., Liang, F., Li, Y., Xiao, Z., Tao, H. W., & Zhang, L. I. (2014). A Feedforward Inhibitory Circuit Mediates Lateral Refinement of Sensory Representation in Upper Layer 2/3 of Mouse Primary Auditory Cortex. *Journal of Neuroscience*, *34*(41), 13670–13683. https://doi.org/10.1523/JNEUROSCI.1516-14.2014

Lillicrap, T. P., Santoro, A., Marris, L., Akerman, C. J., & Hinton, G. (2020). Backpropagation and the brain. *Nature Reviews. Neuroscience*, *21*(6), 335–346. https://doi.org/10.1038/s41583-020-0277-3

Lindsay, G. W. (2021). Convolutional Neural Networks as a Model of the Visual System: Past, Present, and Future. *Journal of Cognitive Neuroscience*, *33*(10), 2017–2031. https://doi.org/10.1162/jocn_a_01544

Lohse, M., Bajo, V. M., King, A. J., & Willmore, B. D. B. (2020). Neural circuits underlying auditory contrast gain control and their perceptual implications. *Nature Communications*, *11*(1), 324. https://doi.org/10.1038/s41467-019-14163-5

Lombardo, M. V., Lai, M.-C., & Baron-Cohen, S. (2019). Big data approaches to decomposing heterogeneity across the autism spectrum. *Molecular Psychiatry*, *24*(10), 1435–1450. https://doi.org/10.1038/s41380-018-0321-0

Loosen, A. M., Kato, A., & Gu, X. (2025). Revisiting the role of computational neuroimaging in the era of integrative neuroscience. *Neuropsychopharmacology*, *50*(1), 103–113. https://doi.org/10.1038/s41386-024-01946-8

Lotter, W., Kreiman, G., & Cox, D. (2020). A neural network trained for prediction mimics diverse features of biological neurons and perception. *Nature Machine Intelligence*, *2*(4), 210. https://doi.org/10.1038/s42256-020-0170-9

Luczak, A., & Kubo, Y. (2022). Predictive Neuronal Adaptation as a Basis for Consciousness. *Frontiers in Systems Neuroscience*, *15*. https://doi.org/10.3389/fnsys.2021.767461

Luque, M. A., Morcuende, S., Torres, B., & Herrero, L. (2024). Kv7/M channel dysfunction produces hyperexcitability in hippocampal CA1 pyramidal cells of Fmr1 knockout mice. *The Journal of Physiology*, *602*(15), 3769–3791. https://doi.org/10.1113/JP285244

Maass, W. (1997). Networks of spiking neurons: The third generation of neural network models. *Neural Networks*, *10*(9), 1659–1671. https://doi.org/10.1016/S0893-6080(97)00011-7

Maass, W., Natschläger, T., & Markram, H. (2002). A Model for Real-Time Computation in Generic Neural Microcircuits. *Advances in Neural Information Processing Systems*, *15*. https://papers.nips.cc/paper_files/paper/2002/hash/6211080fa89981f66b1a0c9d55c61d0f-Abstract.html

Mahajan, N. R., & Mysore, S. P. (2022). Donut-like organization of inhibition underlies categorical neural responses in the midbrain. *Nature Communications*, *13*(1), 1680. https://doi.org/10.1038/s41467-022-29318-0

Mainen, Z. F., & Sejnowski, T. J. (1995). Reliability of spike timing in neocortical neurons. *Science (New York, N.Y.)*, *268*(5216), 1503–1506. https://doi.org/10.1126/science.7770778

Manyukhina, V. O., Prokofyev, A. O., Galuta, I. A., Goiaeva, D. E., Obukhova, T. S., Schneiderman, J. F., Altukhov, D. I., Stroganova, T. A., & Orekhova, E. V. (2022). Globally elevated excitation–inhibition ratio in children with autism spectrum disorder and below-average intelligence. *Molecular Autism*, *13*(1), 20. https://doi.org/10.1186/s13229-022-00498-2

Mao, J., Rothkopf, C. A., & Stocker, A. A. (2025). Adaptation optimizes sensory encoding for future stimuli. *PLOS Computational Biology*, *21*(1), e1012746. https://doi.org/10.1371/journal.pcbi.1012746

Marder, E., & Bucher, D. (2007). Understanding circuit dynamics using the stomatogastric nervous system of lobsters and crabs. *Annual Review of Physiology*, *69*, 291–316. https://doi.org/10.1146/annurev.physiol.69.031905.161516

Markram, H., Lübke, J., Frotscher, M., & Sakmann, B. (1997). Regulation of synaptic efficacy by coincidence of postsynaptic APs and EPSPs. *Science (New York, N.Y.)*, *275*(5297), 213–215. https://doi.org/10.1126/science.275.5297.213

Marotta, R., Risoleo, M. C., Messina, G., Parisi, L., Carotenuto, M., Vetri, L., & Roccella, M. (2020). The Neurochemistry of Autism. *Brain Sciences*, *10*(3), 163. https://doi.org/10.3390/brainsci10030163

Marreiros, A. C., Cagnan, H., Moran, R. J., Friston, K. J., & Brown, P. (2013). Basal ganglia-cortical interactions in Parkinsonian patients. *NeuroImage*, *66*, 301–310. https://doi.org/10.1016/j.neuroimage.2012.10.088

Marsicano, G., Cerpelloni, F., Melcher, D., & Ronconi, L. (2022). Lower multisensory temporal acuity in individuals with high schizotypal traits: A web-based study. *Scientific Reports*, *12*(1), 2782. https://doi.org/10.1038/s41598-022-06503-1

Martin, D., Fowlkes, C., Tal, D., & Malik, J. (2001). A database of human segmented natural images and its application to evaluating segmentation algorithms and measuring ecological statistics. *Proceedings Eighth IEEE International Conference on Computer Vision. ICCV 2001*, *2*, 416–423 vol.2. https://doi.org/10.1109/ICCV.2001.937655

Martínez-Lázaro, R., Minguez-Viñas, T., Reyes-Carrión, A., Gómez, R., Rosa, D. A. de la, Bartolomé-Martín, D., & Giraldez, T. (2025). GRIN2B disease-associated mutations disrupt the function of BK channels and NMDA receptor signaling nanodomains. *The Journal of General Physiology*, *157*(5), e202513799. https://doi.org/10.1085/jgp.202513799

Martinez-Trujillo, J. C., & Treue, S. (2004). Feature-Based Attention Increases the Selectivity of Population Responses in Primate Visual Cortex. *Current Biology*, *14*(9), 744–751. https://doi.org/10.1016/j.cub.2004.04.028

Masquelier, T., Guyonneau, R., & Thorpe, S. J. (2008). Spike Timing Dependent Plasticity Finds the Start of Repeating Patterns in Continuous Spike Trains. *PLOS ONE*, *3*(1), e1377. https://doi.org/10.1371/journal.pone.0001377

Mather, G., & Harris, J. (1998). Theoretical Models of the Motion Aftereffect. In G. Mather, F. Verstraten, & S. Anstis (Eds.), *The Motion Aftereffect* (pp. 153–181). The MIT Press. https://doi.org/10.7551/mitpress/4779.003.0008

Mather, G., Pavan, A., Campana, G., & Casco, C. (2008). The motion after-effect reloaded. *Trends in Cognitive Sciences*, *12*(12), 481. https://doi.org/10.1016/j.tics.2008.09.002

Mather, G., Verstraten, F., & Anstis, S. (Eds.). (1998). *The Motion Aftereffect: A Modern Perspective*. The MIT Press. https://doi.org/10.7551/mitpress/4779.001.0001

Maunsell, J., & Van Essen, D. (1983). The connections of the middle temporal visual area (MT) and their relationship to a cortical hierarchy in the macaque monkey. *The Journal of Neuroscience*, *3*(12), 2563–2586. https://doi.org/10.1523/JNEUROSCI.03-12-02563.1983

May, P. J. (2006). The mammalian superior colliculus: Laminar structure and connections. *Progress in Brain Research*, *151*, 321–378. https://doi.org/10.1016/S0079-6123(05)51011-2

Mayer, M. L., Westbrook, G. L., & Guthrie, P. B. (1984). Voltage-dependent block by Mg2+ of NMDA responses in spinal cord neurones. *Nature*, *309*(5965), 261–263. https://doi.org/10.1038/309261a0

Md, J., & Cc, M. (2008). Quantifying the neural elements activated and inhibited by globus pallidus deep brain stimulation. *Journal of Neurophysiology*, *100*(5). https://doi.org/10.1152/jn.90372.2008

Mdm, Q., Ap, M., & B, K. (2019). Short-Term Attractive Tilt Aftereffects Predicted by a Recurrent Network Model of Primary Visual Cortex. *PubMed*. https://pubmed.ncbi.nlm.nih.gov/31780906/

Meredith, M. A., Nemitz, J. W., & Stein, B. E. (1987). Determinants of multisensory integration in superior colliculus neurons. I. Temporal factors. *The Journal of Neuroscience: The Official Journal of the Society for Neuroscience*, *7*(10), 3215–3229. https://doi.org/10.1523/JNEUROSCI.07-10-03215.1987

Meredith, M. A., & Stein, B. E. (1983). Interactions among converging sensory inputs in the superior colliculus. *Science (New York, N.Y.)*, *221*(4608), 389–391. https://doi.org/10.1126/science.6867718

Meredith, M. A., & Stein, B. E. (1986). Visual, auditory, and somatosensory convergence on cells in superior colliculus results in multisensory integration. *Journal of Neurophysiology*, *56*(3), 640–662. https://doi.org/10.1152/jn.1986.56.3.640

Merolla, P. A., Arthur, J. V., Alvarez-Icaza, R., Cassidy, A. S., Sawada, J., Akopyan, F., Jackson, B. L., Imam, N., Guo, C., Nakamura, Y., Brezzo, B., Vo, I., Esser, S. K., Appuswamy, R., Taba, B., Amir, A., Flickner, M. D., Risk, W. P., Manohar, R., & Modha, D. S. (2014). Artificial brains. A million spiking-neuron integrated circuit with a scalable communication network and interface. *Science (New York, N.Y.)*, *345*(6197), 668–673. https://doi.org/10.1126/science.1254642

Mienye, I. D., Swart, T. G., & Obaido, G. (2024). Recurrent Neural Networks: A Comprehensive Review of Architectures, Variants, and Applications. *Information*, *15*(9), 517. https://doi.org/10.3390/info15090517

Millin, R., Kolodny, T., Flevaris, A. V., Kale, A. M., Schallmo, M.-P., Gerdts, J., Bernier, R. A., & Murray, S. (2018). Reduced auditory cortical adaptation in autism spectrum disorder. *eLife*, *7*, e36493. https://doi.org/10.7554/eLife.36493

Monday, H. R., Wang, H. C., & Feldman, D. E. (2023). Circuit-level theories for sensory dysfunction in autism: Convergence across mouse models. *Frontiers in Neurology*, *14*, 1254297. https://doi.org/10.3389/fneur.2023.1254297

Monyer, H., Burnashev, N., Laurie, D. J., Sakmann, B., & Seeburg, P. H. (1994). Developmental and regional expression in the rat brain and functional properties of four NMDA receptors. *Neuron*, *12*(3), 529–540. https://doi.org/10.1016/0896-6273(94)90210-0

Movshon, J. A., & Newsome, W. T. (1996). Visual Response Properties of Striate Cortical Neurons Projecting to Area MT in Macaque Monkeys. *The Journal of Neuroscience*, *16*(23), 7733–7741. https://doi.org/10.1523/JNEUROSCI.16-23-07733.1996

Movshon, J., Adelson, E. H., Gizzi, M. S., & Newsome, W. T. (1985). The analysis of moving visual patterns. In C. Chagas, R. Gattass, & C. Gross (Eds.), *Pattern recognition mechanisms* (pp. 117–151). Vatican Press.

Murphy, B. K., & Miller, K. D. (2003). Multiplicative Gain Changes Are Induced by Excitation or Inhibition Alone. *Journal of Neuroscience*, *23*(31), 10040–10051. https://doi.org/10.1523/JNEUROSCI.23-31-10040.2003

Murthy, A., & Humphrey, A. L. (1999). Inhibitory Contributions to Spatiotemporal Receptive-Field Structure and Direction Selectivity in Simple Cells of Cat Area 17. *Journal of Neurophysiology*, *81*(3), 1212–1224. https://doi.org/10.1152/jn.1999.81.3.1212

Naselaris, T., Kay, K. N., Nishimoto, S., & Gallant, J. L. (2010). Encoding and decoding in fMRI. *NeuroImage*, *56*(2), 400. https://doi.org/10.1016/j.neuroimage.2010.07.073

Natan, R. G., Rao, W., & Geffen, M. N. (2017). Cortical Interneurons Differentially Shape Frequency Tuning following Adaptation. *Cell Reports*, *21*(4), 878–890. https://doi.org/10.1016/j.celrep.2017.10.012

Nishida, S. (2011). Advancement of motion psychophysics: Review 2001-2010. *Journal of Vision*, *11*(5), 11–11. https://doi.org/10.1167/11.5.11

Niven, J. E. (2016). Neuronal energy consumption: Biophysics, efficiency and evolution. *Current Opinion in Neurobiology*, *41*, 129–135. https://doi.org/10.1016/j.conb.2016.09.004

Noel, J.-P., Shivkumar, S., Dokka, K., Haefner, R. M., & Angelaki, D. E. (2022). Aberrant causal inference and presence of a compensatory mechanism in autism spectrum disorder. *eLife*, *11*, e71866. https://doi.org/10.7554/eLife.71866

Norman, H. F., Norman, J. F., Clayton, A. M., Lianekhammy, J., & Zielke, G. (2003). The visual and haptic perception of natural object shape. *Journal of Vision*, *3*(9), 778. https://doi.org/10.1167/3.9.778

Nowak, L., Bregestovski, P., Ascher, P., Herbet, A., & Prochiantz, A. (1984). Magnesium gates glutamate-activated channels in mouse central neurones. *Nature*, *307*(5950), 462–465. https://doi.org/10.1038/307462a0

Oh, H., Lee, S., Oh, Y., Kim, S., Kim, Y. S., Yang, Y., Choi, W., Yoo, Y.-E., Cho, H., Lee, S., Yang, E., Koh, W., Won, W., Kim, R., Lee, C. J., Kim, H., Kang, H., Kim, J. Y., Ku, T., … Kim, E. (2023). Kv7/KCNQ potassium channels in cortical hyperexcitability and juvenile

seizure-related death in Ank2-mutant mice. *Nature Communications*, *14*(1), 3547. https://doi.org/10.1038/s41467-023-39203-z

Ohshiro, T., Angelaki, D. E., & DeAngelis, G. C. (2011). A normalization model of multisensory integration. *Nature Neuroscience*, *14*(6), 775–782. https://doi.org/10.1038/nn.2815

Oldenburg, I. A., Hendricks, W. D., Handy, G., Shamardani, K., Bounds, H. A., Doiron, B., & Adesnik, H. (2024). The logic of recurrent circuits in the primary visual cortex. *Nature Neuroscience*, *27*(1), 137–147. https://doi.org/10.1038/s41593-023-01510-5

Olshausen, B. A., & Field, D. J. (1996). Emergence of simple-cell receptive field properties by learning a sparse code for natural images. *Nature*, *381*(6583), 607–609. https://doi.org/10.1038/381607a0

O'Roak, B. J., Deriziotis, P., Lee, C., Vives, L., Schwartz, J. J., Girirajan, S., Karakoc, E., Mackenzie, A. P., Ng, S. B., Baker, C., Rieder, M. J., Nickerson, D. A., Bernier, R., Fisher, S. E., Shendure, J., & Eichler, E. E. (2011). Exome sequencing in sporadic autism spectrum disorders identifies severe de novo mutations. *Nature Genetics*, *43*(6), 585–589. https://doi.org/10.1038/ng.835

Ortone, A., Vergani, A. A., Ahmadipour, M., Mannella, R., & Mazzoni, A. (2023). Dopamine depletion leads to pathological synchronization of distinct basal ganglia loops in the beta band. *PLoS Computational Biology*, *19*(4), e1010645. https://doi.org/10.1371/journal.pcbi.1010645

Ostrolenk, A., Bao, V. A., Mottron, L., Collignon, O., & Bertone, A. (2019). Reduced multisensory facilitation in adolescents and adults on the Autism Spectrum. *Scientific Reports*, *9*(1), 11965. https://doi.org/10.1038/s41598-019-48413-9

Otchy, T. M., Wolff, S. B. E., Rhee, J. Y., Pehlevan, C., Kawai, R., Kempf, A., Gobes, S. M. H., & Ölveczky, B. P. (2015). Acute off-target effects of neural circuit manipulations. *Nature*, *528*(7582), 358–363. https://doi.org/10.1038/nature16442

Ottes, F. P., Van Gisbergen, J. A., & Eggermont, J. J. (1986). Visuomotor fields of the superior colliculus: A quantitative model. *Vision Research*, *26*(6), 857–873. https://doi.org/10.1016/0042-6989(86)90144-6

Padamsey, Z., Katsanevaki, D., Dupuy, N., & Rochefort, N. L. (2022). Neocortex saves energy by reducing coding precision during food scarcity. *Neuron*, *110*(2), 280-296.e10. https://doi.org/10.1016/j.neuron.2021.10.024

Pagano, J., Landi, S., Stefanoni, A., Nardi, G., Albanesi, M., Bauer, H. F., Pracucci, E., Schön, M., Ratto, G. M., Boeckers, T. M., Sala, C., & Verpelli, C. (2023). Shank3 deletion in PV neurons is associated with abnormal behaviors and neuronal functions that are

rescued by increasing GABAergic signaling. *Molecular Autism*, *14*(1), 28. https://doi.org/10.1186/s13229-023-00557-2

Paoletti, P., Bellone, C., & Zhou, Q. (2013). NMDA receptor subunit diversity: Impact on receptor properties, synaptic plasticity and disease. *Nature Reviews. Neuroscience*, *14*(6), 383–400. https://doi.org/10.1038/nrn3504

Patterson, C. A., Duijnhouwer, J., Wissig, S. C., Krekelberg, B., & Kohn, A. (2014). Similar adaptation effects in primary visual cortex and area MT of the macaque monkey under matched stimulus conditions. *Journal of Neurophysiology*, *111*(6), 1203–1213. https://doi.org/10.1152/jn.00030.2013

Patterson, C. A., Wissig, S. C., & Kohn, A. (2013). Distinct Effects of Brief and Prolonged Adaptation on Orientation Tuning in Primary Visual Cortex. *The Journal of Neuroscience*, *33*(2), 532–543. https://doi.org/10.1523/JNEUROSCI.3345-12.2013

Paus, T. (2005). Inferring causality in brain images: A perturbation approach. *Philosophical Transactions of the Royal Society B: Biological Sciences*, *360*(1457), 1109. https://doi.org/10.1098/rstb.2005.1652

Peel, T. R., Dash, S., Lomber, S. G., & Corneil, B. D. (2017). Frontal Eye Field Inactivation Diminishes Superior Colliculus Activity, But Delayed Saccadic Accumulation Governs Reaction Time Increases. *The Journal of Neuroscience: The Official Journal of the Society for Neuroscience*, *37*(48), 11715–11730. https://doi.org/10.1523/JNEUROSCI.2664-17.2017

Perrone, J. A., & Thiele, A. (2001). Speed skills: Measuring the visual speed analyzing properties of primate MT neurons. *Nature Neuroscience*, *4*(5), 526–532. https://doi.org/10.1038/87480

Pesnot Lerousseau, J., Parise, C. V., Ernst, M. O., & van Wassenhove, V. (2022). Multisensory correlation computations in the human brain identified by a time-resolved encoding model. *Nature Communications*, *13*(1), 2489. https://doi.org/10.1038/s41467-022-29687-6

Pouget, A., Beck, J. M., Ma, W. J., & Latham, P. E. (2013). Probabilistic brains: Knowns and unknowns. *Nature Neuroscience*, *16*(9), 1170. https://doi.org/10.1038/nn.3495

Pouille, F., & Scanziani, M. (2001). Enforcement of temporal fidelity in pyramidal cells by somatic feed-forward inhibition. *Science (New York, N.Y.)*, *293*(5532), 1159–1163. https://doi.org/10.1126/science.1060342

Powers, A. R., Hillock, A. R., & Wallace, M. T. (2009). Perceptual Training Narrows the Temporal Window of Multisensory Binding. *The Journal of Neuroscience*, *29*(39), 12265–12274. https://doi.org/10.1523/JNEUROSCI.3501-09.2009

Pozzorini, C., Naud, R., Mensi, S., & Gerstner, W. (2013). Temporal whitening by power-law adaptation in neocortical neurons. *Nature Neuroscience*, *16*(7), 942–948. https://doi.org/10.1038/nn.3431

Priebe, N. J., Churchland, M. M., & Lisberger, S. G. (2002). Constraints on the Source of Short-Term Motion Adaptation in Macaque Area MT. I. The Role of Input and Intrinsic Mechanisms. *Journal of Neurophysiology*, *88*(1), 354–369. https://doi.org/10.1152/jn.00852.2001

Priebe, N. J., Lisberger, S. G., & Movshon, J. A. (2006). Tuning for Spatiotemporal Frequency and Speed in Directionally Selective Neurons of Macaque Striate Cortex. *Journal of Neuroscience*, *26*(11), 2941–2950. https://doi.org/10.1523/JNEUROSCI.3936-05.2006

Prinz, A. A., Bucher, D., & Marder, E. (2004). Similar network activity from disparate circuit parameters. *Nature Neuroscience*, *7*(12), 1345–1352. https://doi.org/10.1038/nn1352

Pulliam, G., Feldman, J. I., & Woynaroski, T. G. (2023). Audiovisual multisensory integration in individuals with reading and language impairments: A systematic review and meta-analysis. *Neuroscience & Biobehavioral Reviews*, *149*, 105130. https://doi.org/10.1016/j.neubiorev.2023.105130

Qian, N., & Andersen, R. (1994). Transparent motion perception as detection of unbalanced motion signals. II. Physiology. *The Journal of Neuroscience*, *14*(12), 7367–7380. https://doi.org/10.1523/JNEUROSCI.14-12-07367.1994

Qiao, L., & Shen, Q. (2021). Human Action Recognition Technology in Dance Video Image. *Scientific Programming*, *2021*(1), 6144762. https://doi.org/10.1155/2021/6144762

Rabinowitz, N. C., Willmore, B. D. B., Schnupp, J. W. H., & King, A. J. (n.d.). *Contrast Gain Control in Auditory Cortex*. Retrieved September 15, 2025, from https://www.cell.com/neuron/abstract/S0896-6273(11)00435-1

Rall, W. (2011). Core Conductor Theory and Cable Properties of Neurons. In *Comprehensive Physiology* (pp. 39–97). John Wiley & Sons, Ltd. https://doi.org/10.1002/cphy.cp010103

Razak, K. A., & Pallas, S. L. (2007). Inhibitory Plasticity Facilitates Recovery of Stimulus Velocity Tuning in the Superior Colliculus after Chronic NMDA Receptor Blockade. *Journal of Neuroscience*, *27*(27), 7275–7283. https://doi.org/10.1523/JNEUROSCI.1143-07.2007

Reid, A. T., Headley, D. B., Mill, R. D., Sanchez-Romero, R., Uddin, L. Q., Marinazzo, D., Lurie, D. J., Valdés-Sosa, P. A., Hanson, S. J., Biswal, B. B., Calhoun, V., Poldrack, R. A., &

Cole, M. W. (2019). Advancing functional connectivity research from association to causation. *Nature Neuroscience*, *22*(11), 1751–1760. https://doi.org/10.1038/s41593-019-0510-4

Rhodes, P. (2006). The Properties and Implications of NMDA Spikes in Neocortical Pyramidal Cells. *The Journal of Neuroscience*, *26*(25), 6704. https://doi.org/10.1523/JNEUROSCI.3791-05.2006

Richards, B. A., Lillicrap, T. P., Beaudoin, P., Bengio, Y., Bogacz, R., Christensen, A., Clopath, C., Costa, R. P., de Berker, A., Ganguli, S., Gillon, C. J., Hafner, D., Kepecs, A., Kriegeskorte, N., Latham, P., Lindsay, G. W., Miller, K. D., Naud, R., Pack, C. C., … Kording, K. P. (2019). A deep learning framework for neuroscience. *Nature Neuroscience*, *22*(11), 1761–1770. https://doi.org/10.1038/s41593-019-0520-2

Richter, O., Wu, C., Whatley, A. M., Köstinger, G., Nielsen, C., Qiao, N., & Indiveri, G. (2024). DYNAP-SE2: A scalable multi-core dynamic neuromorphic asynchronous spiking neural network processor. *Neuromorphic Computing and Engineering*, *4*(1), 014003. https://doi.org/10.1088/2634-4386/ad1cd7

Rideaux, R., & Edwards, M. (2014). Information extraction during simultaneous motion processing. *Vision Research*, *95*, 1–10. https://doi.org/10.1016/j.visres.2013.11.007

Rideaux, R., & Harrison, W. J. (2019). Border ownership-dependent tilt aftereffect for shape defined by binocular disparity and motion parallax. *Journal of Neurophysiology*, *121*(5), 1917. https://doi.org/10.1152/jn.00111.2019

Rideaux, R., Storrs, K. R., Maiello, G., & Welchman, A. E. (2021). How multisensory neurons solve causal inference. *Proceedings of the National Academy of Sciences*, *118*(32), e2106235118. https://doi.org/10.1073/pnas.2106235118

Rideaux, R., & Welchman, A. E. (2020). But Still It Moves: Static Image Statistics Underlie How We See Motion. *Journal of Neuroscience*, *40*(12), 2538–2552. https://doi.org/10.1523/JNEUROSCI.2760-19.2020

Rideaux, R., & Welchman, A. E. (2021). Exploring and explaining properties of motion processing in biological brains using a neural network. *Journal of Vision*, *21*(2), 11. https://doi.org/10.1167/jov.21.2.11

Rideaux, R., West, R. K., Rangelov, D., & Mattingley, J. B. (2023). Distinct early and late neural mechanisms regulate feature-specific sensory adaptation in the human visual system. *Proceedings of the National Academy of Sciences*, *120*(6), e2216192120. https://doi.org/10.1073/pnas.2216192120

Robertson, C. E., & Baron-Cohen, S. (2017). Sensory perception in autism. *Nature Reviews. Neuroscience*, *18*(11), 671–684. https://doi.org/10.1038/nrn.2017.112

Robertson, C. E., Kravitz, D. J., Freyberg, J., Baron-Cohen, S., & Baker, C. I. (2013). Tunnel vision: Sharper gradient of spatial attention in autism. *The Journal of Neuroscience: The Official Journal of the Society for Neuroscience*, *33*(16), 6776–6781. https://doi.org/10.1523/JNEUROSCI.5120-12.2013

Roelfsema, P. R., & Holtmaat, A. (2018). Control of synaptic plasticity in deep cortical networks. *Nature Reviews. Neuroscience*, *19*(3), 166–180. https://doi.org/10.1038/nrn.2018.6

Rohe, T., & Noppeney, U. (2015). Cortical Hierarchies Perform Bayesian Causal Inference in Multisensory Perception. *PLOS Biology*, *13*(2), e1002073. https://doi.org/10.1371/journal.pbio.1002073

Ross, L. A., Molholm, S., Butler, J. S., Del Bene, V. A., Brima, T., & Foxe, J. J. (2024). Neural correlates of audiovisual narrative speech perception in children and adults on the autism spectrum: A functional magnetic resonance imaging study. *Autism Research: Official Journal of the International Society for Autism Research*, *17*(2), 280–310. https://doi.org/10.1002/aur.3104

Ross, L. N., & Bassett, D. S. (2024). Causation in neuroscience: Keeping mechanism meaningful. *Nature Reviews Neuroscience*, *25*(2), 81–90. https://doi.org/10.1038/s41583-023-00778-7

Rowland, B. A., & Stein, B. E. (2007). Multisensory Integration Produces an Initial Response Enhancement. *Frontiers in Integrative Neuroscience*, *1*, 4. https://doi.org/10.3389/neuro.07.004.2007

Rubenstein, J. L. R., & Merzenich, M. M. (2003). Model of autism: Increased ratio of excitation/inhibition in key neural systems. *Genes, Brain, and Behavior*, *2*(5), 255–267. https://doi.org/10.1034/j.1601-183x.2003.00037.x

Rust, N. C., Mante, V., Simoncelli, E. P., & Movshon, J. A. (2006). How MT cells analyze the motion of visual patterns. *Nature Neuroscience*, *9*(11), 1421–1431. https://doi.org/10.1038/nn1786

S, M., M, P., Cr, B., Pj, H., Gs, R., Jl, V., & Cc, M. (2006). Computational analysis of subthalamic nucleus and lenticular fasciculus activation during therapeutic deep brain stimulation. *Journal of Neurophysiology*, *96*(3). https://doi.org/10.1152/jn.00305.2006

Sabo, S. L., Lahr, J. M., Offer, M., Weekes, A. L., & Sceniak, M. P. (2023). GRIN2B-related neurodevelopmental disorder: Current understanding of pathophysiological mechanisms. *Frontiers in Synaptic Neuroscience*, *14*, 1090865. https://doi.org/10.3389/fnsyn.2022.1090865

Sakano, Y., & Allison, R. S. (2014). Aftereffect of motion-in-depth based on binocular cues: Effects of adaptation duration, interocular correlation, and temporal correlation. *Journal of Vision*, *14*(8), 21. https://doi.org/10.1167/14.8.21

Salaj, D., Subramoney, A., Kraisnikovic, C., Bellec, G., Legenstein, R., & Maass, W. (n.d.). *Spike frequency adaptation supports network computations on temporally dispersed information*. Retrieved September 15, 2025, from https://pmc.ncbi.nlm.nih.gov/articles/PMC8313230/

Sapey-Triomphe, L.-A., Pattyn, L., Weilnhammer, V., Sterzer, P., & Wagemans, J. (2023). Neural correlates of hierarchical predictive processes in autistic adults. *Nature Communications*, *14*(1), 3640. https://doi.org/10.1038/s41467-023-38580-9

Saponati, M., & Vinck, M. (2023). Sequence anticipation and spike-timing-dependent plasticity emerge from a predictive learning rule. *Nature Communications*, *14*(1), 4985. https://doi.org/10.1038/s41467-023-40651-w

Saxe, A., Nelli, S., & Summerfield, C. (2021). If deep learning is the answer, what is the question? *Nature Reviews. Neuroscience*, *22*(1), 55–67. https://doi.org/10.1038/s41583-020-00395-8

Schallmo, M.-P., Kolodny, T., Kale, A. M., Millin, R., Flevaris, A. V., Edden, R. A. E., Gerdts, J., Bernier, R. A., & Murray, S. O. (2020). Weaker neural suppression in autism. *Nature Communications*, *11*(1), 2675. https://doi.org/10.1038/s41467-020-16495-z

Schneider-Mizell, C. M., Bodor, A. L., Brittain, D., Buchanan, J., Bumbarger, D. J., Elabbady, L., Gamlin, C., Kapner, D., Kinn, S., Mahalingam, G., Seshamani, S., Suckow, S., Takeno, M., Torres, R., Yin, W., Dorkenwald, S., Bae, J. A., Castro, M. A., Halageri, A., … da Costa, N. M. (2025). Inhibitory specificity from a connectomic census of mouse visual cortex. *Nature*, *640*(8058), 448–458. https://doi.org/10.1038/s41586-024-07780-8

Schrimpf, M., Kubilius, J., Lee, M. J., Ratan Murty, N. A., Ajemian, R., & DiCarlo, J. J. (2020). Integrative Benchmarking to Advance Neurally Mechanistic Models of Human Intelligence. *Neuron*, *108*(3), 413–423. https://doi.org/10.1016/j.neuron.2020.07.040

Seybold, B. A., Stanco, A., Cho, K. K. A., Potter, G. B., Kim, C., Sohal, V. S., Rubenstein, J. L. R., & Schreiner, C. E. (2012). Chronic reduction in inhibition reduces receptive field size in mouse auditory cortex. *Proceedings of the National Academy of Sciences*, *109*(34), 13829–13834. https://doi.org/10.1073/pnas.1205909109

Shams, L., Kamitani, Y., & Shimojo, S. (2000). What you see is what you hear. *Nature*, *408*(6814), 788–788. https://doi.org/10.1038/35048669

Shiu, P. K., Sterne, G. R., Spiller, N., Franconville, R., Sandoval, A., Zhou, J., Simha, N., Kang, C. H., Yu, S., Kim, J. S., Dorkenwald, S., Matsliah, A., Schlegel, P., Yu, S., McKellar, C. E., Sterling, A., Costa, M., Eichler, K., Bates, A. S., … Scott, K. (2024). A Drosophila

computational brain model reveals sensorimotor processing. *Nature*, *634*(8032), 210–219. https://doi.org/10.1038/s41586-024-07763-9

Shouval, H. Z., Wang, S. S.-H., & Wittenberg, G. M. (2010). Spike Timing Dependent Plasticity: A Consequence of More Fundamental Learning Rules. *Frontiers in Computational Neuroscience*, *4*. https://doi.org/10.3389/fncom.2010.00019

Siddiqi, S. H., Kording, K. P., Parvizi, J., & Fox, M. D. (2022). Causal mapping of human brain function. *Nature Reviews Neuroscience*, *23*(6), 361–375. https://doi.org/10.1038/s41583-022-00583-8

Siemann, J. K., Muller, C. L., Forsberg, C. G., Blakely, R. D., Veenstra-VanderWeele, J., & Wallace, M. T. (2017). An autism-associated serotonin transporter variant disrupts multisensory processing. *Translational Psychiatry*, *7*(3), e1067. https://doi.org/10.1038/tp.2017.17

Siemann, J. K., Veenstra-VanderWeele, J., & Wallace, M. T. (2020). Approaches to Understanding Multisensory Dysfunction in Autism Spectrum Disorder. *Autism Research : Official Journal of the International Society for Autism Research*, *13*(9), 1430–1449. https://doi.org/10.1002/aur.2375

Silver, R. A. (2010). Neuronal arithmetic. *Nature Reviews. Neuroscience*, *11*(7), 474–489. https://doi.org/10.1038/nrn2864

Simoncelli, E. P., & Olshausen, B. A. (2001). Natural Image Statistics and Neural Representation. *Annual Review of Neuroscience*, *24*(1), 1193–1216. https://doi.org/10.1146/annurev.neuro.24.1.1193

Smith, M. A., & Sommer, M. A. (2013). Spatial and temporal scales of neuronal correlation in visual area V4. *The Journal of Neuroscience: The Official Journal of the Society for Neuroscience*, *33*(12), 5422–5432. https://doi.org/10.1523/JNEUROSCI.4782-12.2013

Snowden, R. J., Treue, S., & Andersen, R. A. (1992). The response of neurons in areas V1 and MT of the alert rhesus monkey to moving random dot patterns. *Experimental Brain Research*, *88*(2), 389–400. https://doi.org/10.1007/BF02259114

Sohal, V. S., & Rubenstein, J. L. R. (2019). Excitation-inhibition balance as a framework for investigating mechanisms in neuropsychiatric disorders. *Molecular Psychiatry*, *24*(9), 1248. https://doi.org/10.1038/s41380-019-0426-0

Solomon, S. G., & Kohn, A. (2014). Moving Sensory Adaptation beyond Suppressive Effects in Single Neurons. *Current Biology : CB*, *24*(20), R1012–R1022. https://doi.org/10.1016/j.cub.2014.09.001

Srivastava, K. H., Holmes, C. M., Vellema, M., Pack, A. R., Elemans, C. P. H., Nemenman, I., & Sober, S. J. (2017). Motor control by precisely timed spike patterns.

*Proceedings of the National Academy of Sciences of the United States of America*, *114*(5), 1171–1176. https://doi.org/10.1073/pnas.1611734114

Srivastava, N., Hinton, G., Krizhevsky, A., Sutskever, I., & Salakhutdinov, R. (2014). Dropout: A Simple Way to Prevent Neural Networks from Overfitting. *Journal of Machine Learning Research*, *15*(56), 1929–1958.

Stanford, T. R., Quessy, S., & Stein, B. E. (2005). Evaluating the Operations Underlying Multisensory Integration in the Cat Superior Colliculus. *Journal of Neuroscience*, *25*(28), 6499–6508. https://doi.org/10.1523/JNEUROSCI.5095-04.2005

Stanojevic, A., Woźniak, S., Bellec, G., Cherubini, G., Pantazi, A., & Gerstner, W. (2024). High-performance deep spiking neural networks with 0.3 spikes per neuron. *Nature Communications*, *15*, 6793. https://doi.org/10.1038/s41467-024-51110-5

Stas, J. I., Bocksteins, E., Jensen, C. S., Schmitt, N., & Snyders, D. J. (2016). The anticonvulsant retigabine suppresses neuronal KV2-mediated currents. *Scientific Reports*, *6*(1), 35080. https://doi.org/10.1038/srep35080

Stein, B. E., & Rowland, B. A. (2020). Using superior colliculus principles of multisensory integration to reverse hemianopia. *Neuropsychologia*, *141*, 107413. https://doi.org/10.1016/j.neuropsychologia.2020.107413

Stein, B. E., & Stanford, T. R. (2008). Multisensory integration: Current issues from the perspective of the single neuron. *Nature Reviews. Neuroscience*, *9*(4), 255–266. https://doi.org/10.1038/nrn2331

Stein, B. E., Stanford, T. R., & Rowland, B. A. (2014). Development of multisensory integration from the perspective of the individual neuron. *Nature Reviews. Neuroscience*, *15*(8), 520–535. https://doi.org/10.1038/nrn3742

Stevenson, I. H., & Kording, K. P. (2011). How advances in neural recording affect data analysis. *Nature Neuroscience*, *14*(2), 139. https://doi.org/10.1038/nn.2731

Stevenson, R. A., Ghose, D., Fister, J. K., Sarko, D. K., Altieri, N. A., Nidiffer, A. R., Kurela, L. R., Siemann, J. K., James, T. W., & Wallace, M. T. (2014). Identifying and Quantifying Multisensory Integration: A Tutorial Review. *Brain Topography*, *27*(6), 707–730. https://doi.org/10.1007/s10548-014-0365-7

Stevenson, R. A., Siemann, J. K., Schneider, B. C., Eberly, H. E., Woynaroski, T. G., Camarata, S. M., & Wallace, M. T. (2014). Multisensory temporal integration in autism spectrum disorders. *The Journal of Neuroscience: The Official Journal of the Society for Neuroscience*, *34*(3), 691–697. https://doi.org/10.1523/JNEUROSCI.3615-13.2014

Stöckl, C., & Maass, W. (2021). Optimized spiking neurons can classify images with high accuracy through temporal coding with two spikes. *Nature Machine Intelligence*, *3*(3), 230–238. https://doi.org/10.1038/s42256-021-00311-4

Stradmann, Y., Billaudelle, S., Breitwieser, O., Ebert, F. L., Emmel, A., Husmann, D., Ilmberger, J., Müller, E., Spilger, P., Weis, J., & Schemmel, J. (2022). Demonstrating Analog Inference on the BrainScaleS-2 Mobile System. *IEEE Open Journal of Circuits and Systems*, *3*, 252–262. https://doi.org/10.1109/OJCAS.2022.3208413

Subbulakshmi Radhakrishnan, S., Sebastian, A., Oberoi, A., Das, S., & Das, S. (2021). A biomimetic neural encoder for spiking neural network. *Nature Communications*, *12*(1), 2143. https://doi.org/10.1038/s41467-021-22332-8

Surti, T. S., Ranganathan, M., Johannesen, J. K., Gueorguieva, R., Deaso, E., Kenney, J. G., Krystal, J. H., & D'Souza, D. C. (2023). Randomized controlled trial of the glycine transporter 1 inhibitor PF-03463275 to enhance cognitive training and neuroplasticity in schizophrenia. *Schizophrenia Research*, *256*, 36–43. https://doi.org/10.1016/j.schres.2023.04.010

Taaseh, N., Yaron, A., & Nelken, I. (2011). Stimulus-specific adaptation and deviance detection in the rat auditory cortex. *PloS One*, *6*(8), e23369. https://doi.org/10.1371/journal.pone.0023369

Takarae, Y., & Sweeney, J. (2017). Neural Hyperexcitability in Autism Spectrum Disorders. *Brain Sciences*, *7*(10), 129. https://doi.org/10.3390/brainsci7100129

Tan, A. Y. Y., Brown, B. D., Scholl, B., Mohanty, D., & Priebe, N. J. (2011). Orientation Selectivity of Synaptic Input to Neurons in Mouse and Cat Primary Visual Cortex. *Journal of Neuroscience*, *31*(34), 12339–12350. https://doi.org/10.1523/JNEUROSCI.2039-11.2011

Tan, H., & van Dijken, S. (2023). Dynamic machine vision with retinomorphic photomemristor-reservoir computing. *Nature Communications*, *14*(1), 2169. https://doi.org/10.1038/s41467-023-37886-y

Tang, Z.-Q., & Trussell, L. O. (2017). Serotonergic Modulation of Sensory Representation in a Central Multisensory Circuit Is Pathway Specific. *Cell Reports*, *20*(8), 1844. https://doi.org/10.1016/j.celrep.2017.07.079

Tesileanu, T., Piasini, E., & Balasubramanian, V. (2022). Efficient processing of natural scenes in visual cortex. *Frontiers in Cellular Neuroscience*, *16*. https://doi.org/10.3389/fncel.2022.1006703

Theusner, S., De Lussanet, M. H. E., & Lappe, M. (2011). Adaptation to biological motion leads to a motion and a form aftereffect. *Attention, Perception, & Psychophysics*, *73*(6), 1843–1855. https://doi.org/10.3758/s13414-011-0133-7

Thieu, T., & Melnik, R. (2025). Spike Timing-Dependent Plasticity and Random Inputs Shape Interspike Interval Regularity of Model STN Neurons. *Biomedicines*, *13*(7), 1718. https://doi.org/10.3390/biomedicines13071718

Thye, M. D., Bednarz, H. M., Herringshaw, A. J., Sartin, E. B., & Kana, R. K. (2018). The impact of atypical sensory processing on social impairments in autism spectrum disorder. *Developmental Cognitive Neuroscience*, *29*, 151–167. https://doi.org/10.1016/j.dcn.2017.04.010

Tollin, D. J., Koka, K., & Tsai, J. J. (2008). Interaural Level Difference Discrimination Thresholds for Single Neurons in the Lateral Superior Olive. *Journal of Neuroscience*, *28*(19), 4848–4860. https://doi.org/10.1523/JNEUROSCI.5421-07.2008

Trpevski, D., Khodadadi, Z., Carannante, I., & Hellgren Kotaleski, J. (2023). Glutamate spillover drives robust all-or-none dendritic plateau potentials—An in silico investigation using models of striatal projection neurons. *Frontiers in Cellular Neuroscience*, *17*. https://doi.org/10.3389/fncel.2023.1196182

Tsuji, Y., & Imaizumi, S. (2024). Autistic traits and speech perception in social and non-social noises. *Scientific Reports*, *14*, 1414. https://doi.org/10.1038/s41598-024-52050-2

Turi, M., Burr, D. C., Igliozzi, R., Aagten-Murphy, D., Muratori, F., & Pellicano, E. (2015). Children with autism spectrum disorder show reduced adaptation to number. *Proceedings of the National Academy of Sciences*, *112*(25), 7868–7872. https://doi.org/10.1073/pnas.1504099112

Turi, M., Karaminis, T., Pellicano, E., & Burr, D. (2016). No rapid audiovisual recalibration in adults on the autism spectrum. *Scientific Reports*, *6*(1), 21756. https://doi.org/10.1038/srep21756

Turrigiano, G. (2012). Homeostatic synaptic plasticity: Local and global mechanisms for stabilizing neuronal function. *Cold Spring Harbor Perspectives in Biology*, *4*(1), a005736. https://doi.org/10.1101/cshperspect.a005736

Turrigiano, G. G., & Nelson, S. B. (2004). Homeostatic plasticity in the developing nervous system. *Nature Reviews. Neuroscience*, *5*(2), 97–107. https://doi.org/10.1038/nrn1327

Uhlhaas, P. J., Pipa, G., Lima, B., Melloni, L., Neuenschwander, S., Nikolić, D., & Singer, W. (2009). Neural synchrony in cortical networks: History, concept and current status. *Frontiers in Integrative Neuroscience*, *3*, 17. https://doi.org/10.3389/neuro.07.017.2009

Urbanczik, R., & Senn, W. (2014). Learning by the dendritic prediction of somatic spiking. *Neuron*, *81*(3), 521–528. https://doi.org/10.1016/j.neuron.2013.11.030

van Vreeswijk, C., & Sompolinsky, H. (1996). Chaos in neuronal networks with balanced excitatory and inhibitory activity. *Science (New York, N.Y.)*, *274*(5293), 1724–1726. https://doi.org/10.1126/science.274.5293.1724

Vanarse, A. (2016). Interfacing of neuromorphic vision, auditory and olfactory sensors with digital neuromorphic circuits. *Theses: Doctorates and Masters*. https://ro.ecu.edu.au/theses/1802

Vanattou-Saïfoudine, N., Han, C., Krause, R., Vasilaki, E., von der Behrens, W., & Indiveri, G. (2021). A robust model of Stimulus-Specific Adaptation validated on neuromorphic hardware. *Scientific Reports*, *11*(1), 17904. https://doi.org/10.1038/s41598-021-97217-3

Vázquez, D., Maulhardt, S. R., Stalnaker, T. A., Solway, A., Charpentier, C. J., & Roesch, M. R. (2024). Optogenetic Inhibition of Rat Anterior Cingulate Cortex Impairs the Ability to Initiate and Stay on Task. *Journal of Neuroscience*, *44*(20). https://doi.org/10.1523/JNEUROSCI.1850-23.2024

Vázquez, D., Peña-Flores, N., Maulhardt, S. R., Solway, A., Charpentier, C. J., & Roesch, M. R. (2024). Anterior cingulate cortex lesions impair multiple facets of task engagement not mediated by dorsomedial striatum neuron firing. *Cerebral Cortex*, *34*(8), bhae332. https://doi.org/10.1093/cercor/bhae332

Vinje, W. E., & Gallant, J. L. (2000). Sparse coding and decorrelation in primary visual cortex during natural vision. *Science (New York, N.Y.)*, *287*(5456), 1273–1276. https://doi.org/10.1126/science.287.5456.1273

Vinken, K., Boix, X., & Kreiman, G. (2020). Incorporating intrinsic suppression in deep neural networks captures dynamics of adaptation in neurophysiology and perception. *Science Advances*, *6*(42), eabd4205. https://doi.org/10.1126/sciadv.abd4205

Visser, E., Zwiers, M. P., Kan, C. C., Hoekstra, L., Opstal, A. J. van, & Buitelaar, J. K. (2013). Atypical vertical sound localization and sound-onset sensitivity in people with autism spectrum disorders. *Journal of Psychiatry & Neuroscience : JPN*, *38*(6), 398. https://doi.org/10.1503/jpn.120177

Vogel, D. H. V., Jording, M., Esser, C., Conrad, A., Weiss, P. H., & Vogeley, K. (2022). Temporal binding of social events less pronounced in individuals with Autism Spectrum Disorder. *Scientific Reports*, *12*(1), 14853. https://doi.org/10.1038/s41598-022-19309-y

Vogels, T. P., Froemke, R. C., Doyon, N., Gilson, M., Haas, J. S., Liu, R., Maffei, A., Miller, P., Wierenga, C. J., Woodin, M. A., Zenke, F., & Sprekeler, H. (2013). Inhibitory synaptic plasticity: Spike timing-dependence and putative network function. *Frontiers in Neural Circuits*, *7*, 119. https://doi.org/10.3389/fncir.2013.00119

Vogels, T. P., Sprekeler, H., Zenke, F., Clopath, C., & Gerstner, W. (2011). Inhibitory Plasticity Balances Excitation and Inhibition in Sensory Pathways and Memory Networks. *Science*, *334*(6062), 1569–1573. https://doi.org/10.1126/science.1211095

Wainwright, M. J. (1999). Visual adaptation as optimal information transmission. *Vision Research*, *39*(23), 3960–3974. https://doi.org/10.1016/S0042-6989(99)00101-7

Wallace, M. T., & Stein, B. E. (1997). Development of multisensory neurons and multisensory integration in cat superior colliculus. *The Journal of Neuroscience: The Official Journal of the Society for Neuroscience*, *17*(7), 2429–2444. https://doi.org/10.1523/JNEUROSCI.17-07-02429.1997

Wallace, M. T., & Stevenson, R. A. (2014). The construct of the multisensory temporal binding window and its dysregulation in developmental disabilities. *Neuropsychologia*, *64*, 105–123. https://doi.org/10.1016/j.neuropsychologia.2014.08.005

Wallace, M. T., Woynaroski, T. G., & Stevenson, R. A. (2020). Multisensory Integration as a Window into Orderly and Disrupted Cognition and Communication. *Annual Review of Psychology*, *71*, 193–219. https://doi.org/10.1146/annurev-psych-010419-051112

Wang, E. Y., Fahey, P. G., Ding, Z., Papadopoulos, S., Ponder, K., Weis, M. A., Chang, A., Muhammad, T., Patel, S., Ding, Z., Tran, D., Fu, J., Schneider-Mizell, C. M., da Costa, N. M., Reid, R. C., Collman, F., da Costa, N. M., Franke, K., Ecker, A. S., … Tolias, A. S. (2025). Foundation model of neural activity predicts response to new stimulus types. *Nature*, *640*(8058), 470–477. https://doi.org/10.1038/s41586-025-08829-y

Wang, H. E., Woodman, M., Triebkorn, P., Lemarechal, J.-D., Jha, J., Dollomaja, B., Vattikonda, A. N., Sip, V., Medina Villalon, S., Hashemi, M., Guye, M., Makhalova, J., Bartolomei, F., & Jirsa, V. (2023). Delineating epileptogenic networks using brain imaging data and personalized modeling in drug-resistant epilepsy. *Science Translational Medicine*, *15*(680), eabp8982. https://doi.org/10.1126/scitranslmed.abp8982

Wang, L., McAlonan, K., Goldstein, S., Gerfen, C. R., & Krauzlis, R. J. (2020). A Causal Role for Mouse Superior Colliculus in Visual Perceptual Decision-Making. *The Journal of Neuroscience: The Official Journal of the Society for Neuroscience*, *40*(19), 3768–3782. https://doi.org/10.1523/JNEUROSCI.2642-19.2020

Wang, X. J. (2001). Synaptic reverberation underlying mnemonic persistent activity. *Trends in Neurosciences*, *24*(8), 455–463. https://doi.org/10.1016/s0166-2236(00)01868-3

Wang, X.-J. (1999). Synaptic Basis of Cortical Persistent Activity: The Importance of NMDA Receptors to Working Memory. *Journal of Neuroscience*, *19*(21), 9587–9603. https://doi.org/10.1523/JNEUROSCI.19-21-09587.1999

Wark, B., Lundstrom, B. N., & Fairhall, A. (2007). Sensory adaptation. *Current Opinion in Neurobiology*, *17*(4), 423–429. https://doi.org/10.1016/j.conb.2007.07.001

Wehr, M., & Zador, A. M. (2003). Balanced inhibition underlies tuning and sharpens spike timing in auditory cortex. *Nature*, *426*(6965), 442–446. https://doi.org/10.1038/nature02116

Weiland, R. F., Polderman, T. J., Smit, D. J., Begeer, S., & Van der Burg, E. (2023). No differences between adults with and without autism in audiovisual synchrony perception. *Autism: The International Journal of Research and Practice*, *27*(4), 927–937. https://doi.org/10.1177/13623613221121414

Wiemann, P. F. V., Kneib, T., & Hambuckers, J. (2024). Using the softplus function to construct alternative link functions in generalized linear models and beyond. *Statistical Papers*, *65*(5), 3155–3180. https://doi.org/10.1007/s00362-023-01509-x

Wilson, N. R., Runyan, C. A., Wang, F. L., & Sur, M. (2012). Division and subtraction by distinct cortical inhibitory networks in vivo. *Nature*, *488*(7411), 343–348. https://doi.org/10.1038/nature11347

Wissig, S. C., & Kohn, A. (2012). The influence of surround suppression on adaptation effects in primary visual cortex. *Journal of Neurophysiology*, *107*(12), 3370–3384. https://doi.org/10.1152/jn.00739.2011

Witten, I. B., Knudsen, E. I., & Sompolinsky, H. (2008). A Hebbian Learning Rule Mediates Asymmetric Plasticity in Aligning Sensory Representations. *Journal of Neurophysiology*, *100*(2), 1067. https://doi.org/10.1152/jn.00013.2008

Wolf, A. B., Lintz, M. J., Costabile, J. D., Thompson, J. A., Stubblefield, E. A., & Felsen, G. (2015). An integrative role for the superior colliculus in selecting targets for movements. *Journal of Neurophysiology*, *114*(4), 2118. https://doi.org/10.1152/jn.00262.2015

Wolff, S. B. E., & Ölveczky, B. P. (2018). The promise and perils of causal circuit manipulations. *Current Opinion in Neurobiology*, *49*, 84–94. https://doi.org/10.1016/j.conb.2018.01.004

Won, H., Lee, H.-R., Gee, H. Y., Mah, W., Kim, J.-I., Lee, J., Ha, S., Chung, C., Jung, E. S., Cho, Y. S., Park, S.-G., Lee, J.-S., Lee, K., Kim, D., Bae, Y. C., Kaang, B.-K., Lee, M. G., & Kim, E. (2012). Autistic-like social behaviour in Shank2-mutant mice improved by restoring NMDA receptor function. *Nature*, *486*(7402), 261–265. https://doi.org/10.1038/nature11208

Wong, K.-F., & Wang, X.-J. (2006). A recurrent network mechanism of time integration in perceptual decisions. *The Journal of Neuroscience: The Official Journal of the Society for Neuroscience*, *26*(4), 1314–1328. https://doi.org/10.1523/JNEUROSCI.3733-05.2006

Wu, J., d'Hollande, A., Du, H., & Rozenberg, M. (2025). Dynamics of neural motifs realized with a minimal memristive neurosynaptic unit. *Physical Review Applied*, *23*(3), 034030. https://doi.org/10.1103/PhysRevApplied.23.034030

Wu, X., Shi, S., Liang, B., Dong, Y., Yang, R., Ji, R., Wang, Z., & Huang, W. (2024). Ultralow-power optoelectronic synaptic transistors based on polyzwitterion dielectrics for in-sensor reservoir computing. *Science Advances*, *10*(16), eadn4524. https://doi.org/10.1126/sciadv.adn4524

Wu, Y. K., Hengen, K. B., Turrigiano, G. G., & Gjorgjieva, J. (2020). Homeostatic mechanisms regulate distinct aspects of cortical circuit dynamics. *Proceedings of the National Academy of Sciences of the United States of America*, *117*(39), 24514. https://doi.org/10.1073/pnas.1918368117

Yamins, D. L. K., & DiCarlo, J. J. (2016). Using goal-driven deep learning models to understand sensory cortex. *Nature Neuroscience*, *19*(3), 356–365. https://doi.org/10.1038/nn.4244

Yamins, D. L. K., Hong, H., Cadieu, C. F., Solomon, E. A., Seibert, D., & DiCarlo, J. J. (2014). Performance-optimized hierarchical models predict neural responses in higher visual cortex. *Proceedings of the National Academy of Sciences*, *111*(23), 8619–8624. https://doi.org/10.1073/pnas.1403112111

Yi, G., & Grill, W. M. (2019). Average firing rate rather than temporal pattern determines metabolic cost of activity in thalamocortical relay neurons. *Scientific Reports*, *9*(1), 6940. https://doi.org/10.1038/s41598-019-43460-8

Yu, L., Rowland, B. A., & Stein, B. E. (2010). Initiating the development of multisensory integration by manipulating sensory experience. *The Journal of Neuroscience: The Official Journal of the Society for Neuroscience*, *30*(14), 4904–4913. https://doi.org/10.1523/JNEUROSCI.5575-09.2010

Zaharia, A. D., Goris, R. L. T., Movshon, J. A., & Simoncelli, E. P. (2019). Compound Stimuli Reveal the Structure of Visual Motion Selectivity in Macaque MT Neurons. *eNeuro*, *6*(6). https://doi.org/10.1523/ENEURO.0258-19.2019

Zamboni, E., Kemper, V. G., Goncalves, N. R., Jia, K., Karlaftis, V. M., Bell, S. J., Giorgio, J., Rideaux, R., Goebel, R., & Kourtzi, Z. (2020). Fine-scale computations for adaptive processing in the human brain. *eLife*, *9*, e57637. https://doi.org/10.7554/eLife.57637

Zannone, S., Brzosko, Z., Paulsen, O., & Clopath, C. (2018). Acetylcholine-modulated plasticity in reward-driven navigation: A computational study. *Scientific Reports*, *8*, 9486. https://doi.org/10.1038/s41598-018-27393-2

Zeiler, M. D., & Fergus, R. (2013). *Visualizing and Understanding Convolutional Networks* (No. arXiv:1311.2901). arXiv. https://doi.org/10.48550/arXiv.1311.2901

Zenke, F., & Gerstner, W. (2014). Limits to high-speed simulations of spiking neural networks using general-purpose computers. *Frontiers in Neuroinformatics*, *8*. https://doi.org/10.3389/fninf.2014.00076

Zenke, F., Gerstner, W., & Ganguli, S. (2017). The temporal paradox of Hebbian learning and homeostatic plasticity. *Current Opinion in Neurobiology*, *43*, 166–176. https://doi.org/10.1016/j.conb.2017.03.015

Zerbi, V., Pagani, M., Markicevic, M., Matteoli, M., Pozzi, D., Fagiolini, M., Bozzi, Y., Galbusera, A., Scattoni, M. L., Provenzano, G., Banerjee, A., Helmchen, F., Basson, M. A., Ellegood, J., Lerch, J. P., Rudin, M., Gozzi, A., & Wenderoth, N. (2021). Brain mapping across 16 autism mouse models reveals a spectrum of functional connectivity subtypes. *Molecular Psychiatry*, *26*(12), 7610–7620. https://doi.org/10.1038/s41380-021-01245-4

Zhang-Hooks, Y., Agarwal, A., Mishina, M., & Bergles, D. E. (2016). NMDA Receptors Enhance Spontaneous Activity and Promote Neuronal Survival in the Developing Cochlea. *Neuron*, *89*(2), 337–350. https://doi.org/10.1016/j.neuron.2015.12.016

Zhao, H., Peters, J. H., Zhu, M., Page, S. J., Ritter, R. C., & Appleyard, S. M. (2014). Frequency-dependent facilitation of synaptic throughput via postsynaptic NMDA receptors in the nucleus of the solitary tract. *The Journal of Physiology*, *593*(Pt 1), 111. https://doi.org/10.1113/jphysiol.2013.258103

Zhou, H., Cai, X., Weigl, M., Bang, P., Cheung, E. F. C., & Chan, R. C. K. (2018). Multisensory temporal binding window in autism spectrum disorders and schizophrenia spectrum disorders: A systematic review and meta-analysis. *Neuroscience & Biobehavioral Reviews*, *86*, 66–76. https://doi.org/10.1016/j.neubiorev.2017.12.013

Zhou, S., & Yu, Y. (2018). Synaptic Excitatory-Inhibitory Balance Underlying Efficient Neural Coding. *Advances in Neurobiology*, *21*, 85–100. https://doi.org/10.1007/978-3-319-94593-4_5

Zoicas, I., & Kornhuber, J. (2019). The Role of the N-Methyl-D-Aspartate Receptors in Social Behavior in Rodents. *International Journal of Molecular Sciences*, *20*(22), 5599. https://doi.org/10.3390/ijms20225599

Zoodsma, J. D., Keegan, E. J., Moody, G. R., Bhandiwad, A. A., Napoli, A. J., Burgess, H. A., Wollmuth, L. P., & Sirotkin, H. I. (2022). Disruption of grin2B, an ASD-associated gene, produces social deficits in zebrafish. *Molecular Autism*, *13*(1), 38. https://doi.org/10.1186/s13229-022-00516-3

Zucker, R. S., & Regehr, W. G. (2002). Short-term synaptic plasticity. *Annual Review of Physiology*, *64*, 355–405. https://doi.org/10.1146/annurev.physiol.64.092501.114547

Zwaigenbaum, L., Bryson, S., Rogers, T., Roberts, W., Brian, J., & Szatmari, P. (2005). Behavioral manifestations of autism in the first year of life. *International Journal of Developmental Neuroscience: The Official Journal of the International Society for Developmental Neuroscience*, *23*(2–3), 143–152. https://doi.org/10.1016/j.ijdevneu.2004.05.001

## Supplementary Figures

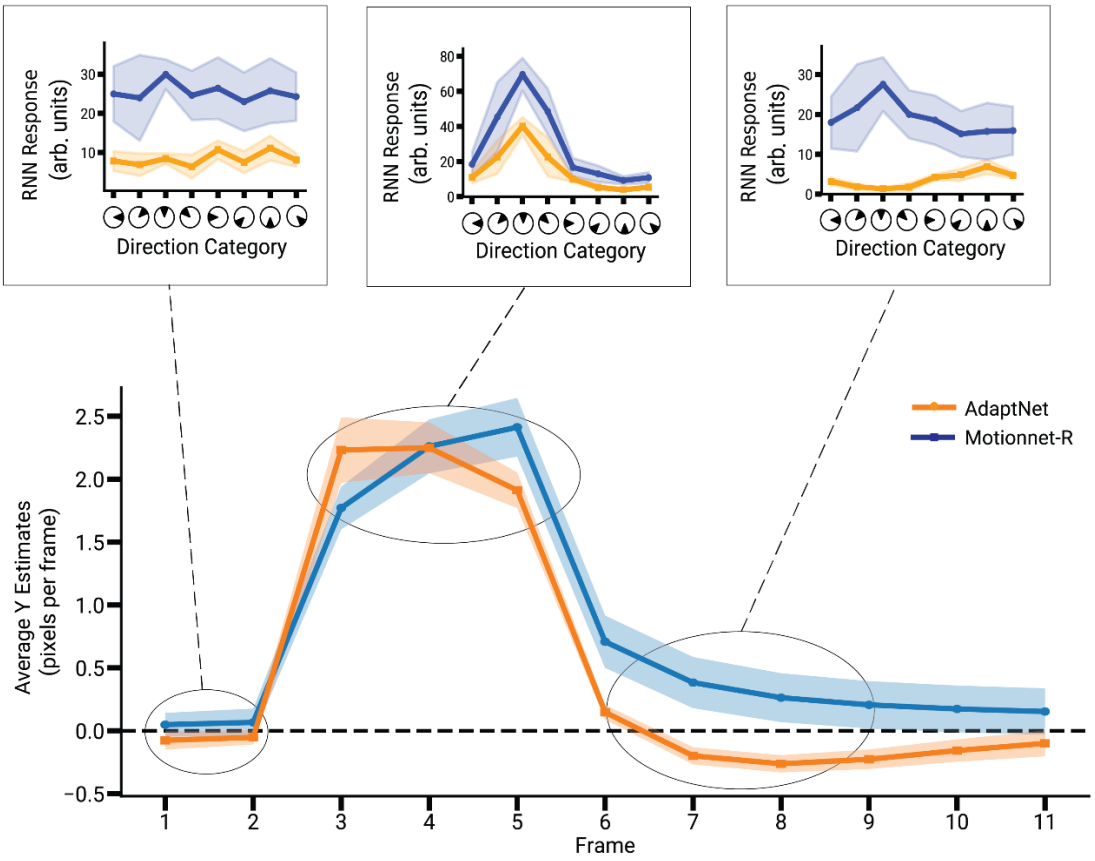


**Supplementary Figure 1. Motion Aftereffect in AdaptNet (Y component).** Time course of the networks' Y responses to an image sequence consisting of a stationary stage (2 frames), followed by a moving stage (3 frames), and then a return to stationary (5 frames). The lower plot shows MotionNet-R and AdaptNet's motion estimation over time. The upper insets (showing RNN responses during frames 2, 4 and 8 representing the stationary, moving and final phases of the sequence respectively) show the average activity of MT units, binned according to their directional tuning, during different stages of the sequence. Shaded regions indicate ±SD across multiple networks.

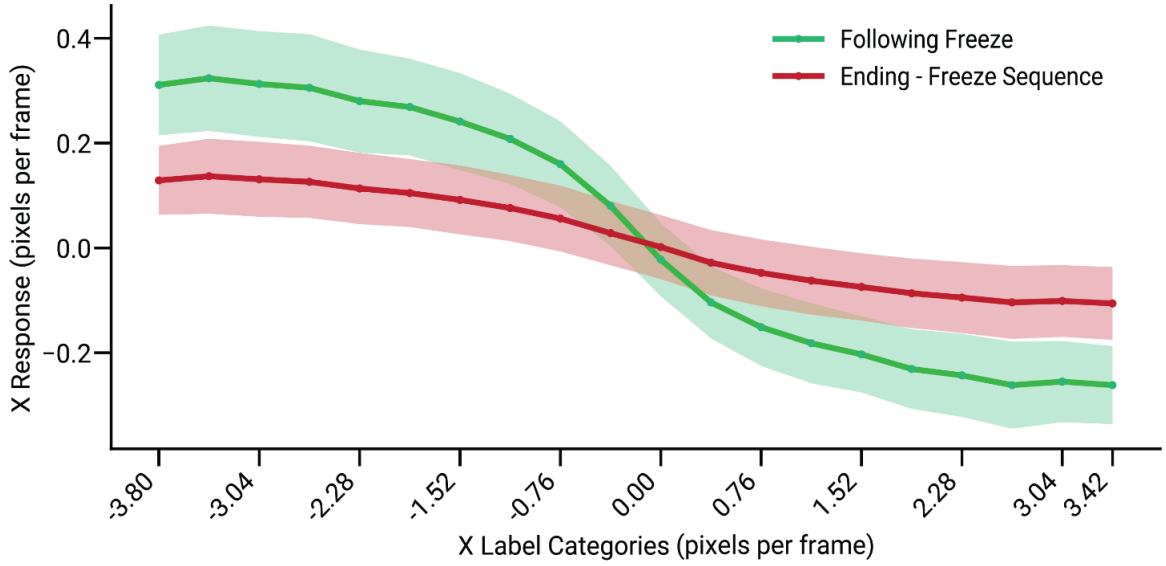


**Supplementary Figure 2. Motion Aftereffect observed across a range of sequence velocities** Response magnitudes of the X component of AdaptNet are plotted immediately after the motion sequence has been stopped (green) along with the response magnitudes of AdaptNet towards the end of the sequence (red). The graphs show how across a variety of input sequence velocities, AdaptNet first overshoots to make the opposite prediction and then corrects itself towards the end. Shaded regions indicate ±SD across multiple networks.

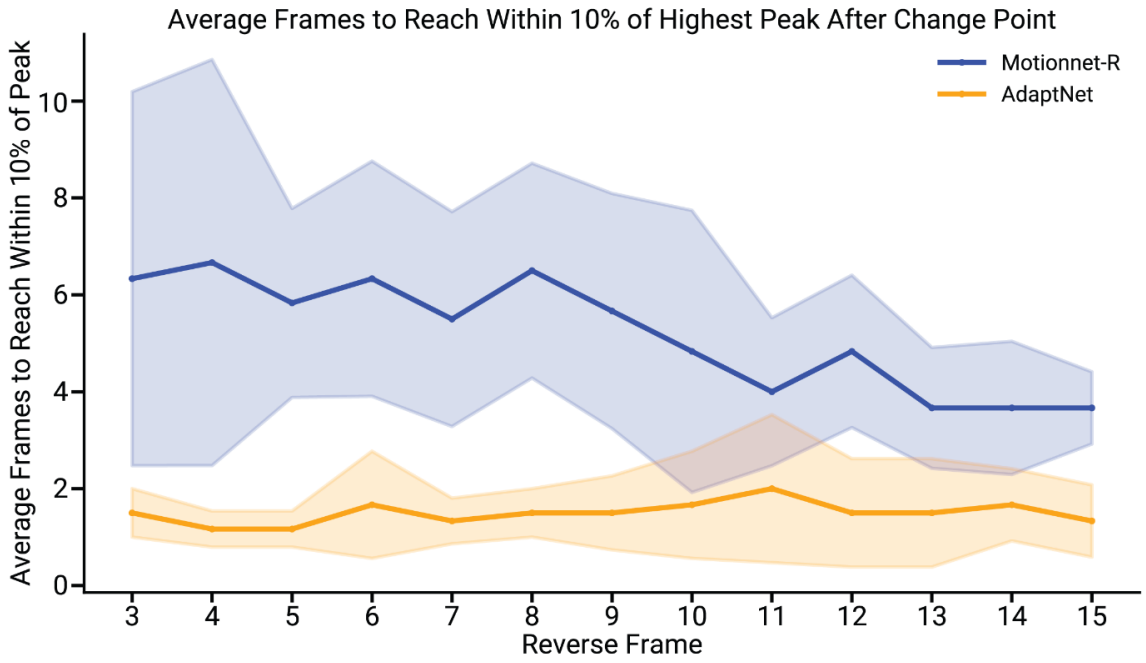


**Supplementary Figure 3. AdaptNet shows lower response latency** Graphs showing the average number of frames taken by the networks to reach within 10% of their maximum response value, following a change in the velocity of the input sequence. AdaptNet reaches this range within 1-2 frames on average regardless of how adapted the state of the network is, just before the change in velocity while MotionNet-R trails behind in terms of its response. Shaded regions indicate ±SD across multiple networks.

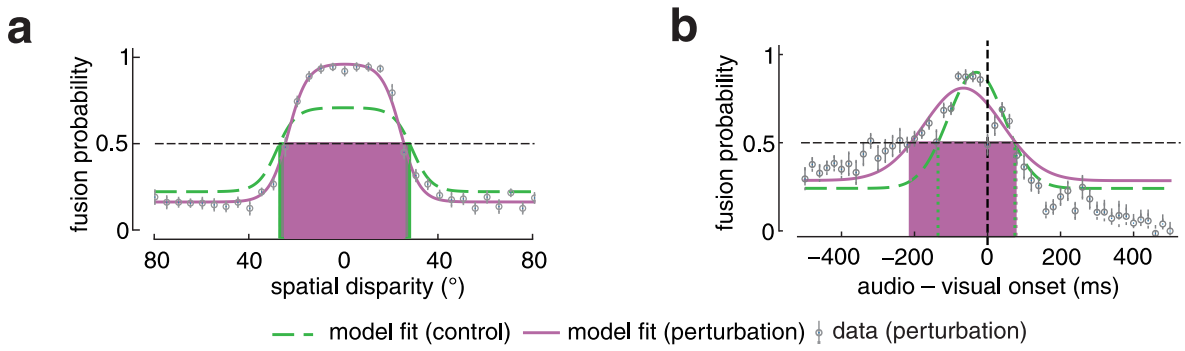


**Supplementary Figure 4. Decrease in effects of perturbation following removal of surround inhibition a**) Fusion probability as a function of spatial disparity for control (green dashed line) and reduced feedforward inhibition (magenta solid line) networks. **b**) Fusion probability as a function of audio-visual onset asynchrony for control and perturbed networks. Vertical green dashed lines and shaded regions in (**a**, **b**) indicate where fusion probability exceeds 50% for control and perturbed networks, respectively; negative asynchronies in (**b**) indicate visual-leading stimuli. The extent of response alterations here contrasts with that of disinhibition alone (no centre surround removal). Error bars indicate ±SEM across ten network instantiations.